RECENT DEVELOPMENTS IN THE STUDIES OF MOLECULAR OXYGEN ADDUCTS OF COBALT (II) COMPOUNDS AND RELATED SYSTEMS

THOMAS D. SMITH*

Chemistry Department, Monash University, Clayton, Victoria 3168 (Australia)

JOHN R. PILBROW

Physics Department, Monash University, Clayton, Victoria 3168 (Australia)

(Received 16 February 1981)

CONTENTS

* Correspondence to: T.D. Smith, Chemistry Department, Monash University, Clayton, Victoria 3168, Australia.

A. INTRODUCTION

An exceptional feature of the Earth's atmosphere, when compared to those of other celestial bodies, is the presence of significant amounts of oxygen. The presence of oxygen provides for the protective ozone layer in the upper atmosphere, and at lower altitudes is part of the extremely specialized environment which makes possible the existence of intelligent life [1]. Possible connections between the various stages in the evolution of life forms and the levels of oxygen in the atmosphere have been outlined [2]. The presence of oxygen in the Earth's atmosphere is due to the evolution of plant life which, by photosynthetic processes, keeps the level of carbon dioxide, which is consumed, and oxygen, which is produced, in balance [3]. The present level of oxygen in the atmosphere was achieved in about 2000 years, a period extremely short on the geological time-scale.

One way or another, in a variety of roles, there is an intimate connection between the chemical reactivity of molecular oxygen and its ability to interact with metal ion centres contained in diverse states of chemical environments. The reaction centre which gives rise to the formation of molecular oxygen in the photosynthetic process is thought to contain manganese [4]. In addition molecular oxygen reacts with a number of iron proteins involved in the physiological transport of molecular oxygen, in the oxidative metabolism of a wide variety of compounds and in the hydroxylation of a number of metabolites. As outlined in Table 1, a further range of oxidase properties, and molecular oxygen transport is shown by certain copper proteins. In addition to taking part in molecular biological roles involving respiration and oxidative metabolism, molecular oxygen possesses the ability to form, often reversibly, adducts with a wide variety of metal chelates, some recent examples being outlined in Table 2. The reversible formation of molecular oxygen adducts by metal chelates is at its most prolific when high-spin or low-spin cobalt(II) chelates or complexes in aqueous or non-aqueous media are involved. The occurrence of these compounds has been utilized in homogenous and heterogenous catalysis of oxidation of inorganic and organic substrates by molecular oxygen, in air fuel cell electrode assemblies, and to provide electronic and structural information by substitution for iron in the prosthetic group in certain iron proteins involved in molecular oxygen transport and storage. The formation,

TABLE 1

Roles of molecular oxygen in biological systems involving metalloproteins

Metalloprotein	Occurrence and function
Copper proteins [a]	
1. Hemocyanins	Oxygen carrying protein in the hemolymph of many molluscans, arthropod and arachnid species
2. Amine oxidases	Wide distribution in animal, bacterial and plant material; accomplish the catalytic aerobic oxidation of certain amines
3. Dopamin-β-hydroxylase	Occurs in the adrenal medulla; catalyzes the side chain hydroxylation of many analogues of phenylethylamine
4. Tyrosinase	Wide distribution in bacteria, plants, marine animals and mammals where it catalyzes the orthohydroxylation of monophenols
5. Laccases	Widely distributed in plants and micro-organisms where it catalyzes the oxidation of p-diphenols by molecular oxygen
6. Ascorbate oxidase	The protein occurs in various vegetable sources and catalyzes the oxidation of L-ascorbic acid
7. Galactose oxidase	Isolated from fungal plants; the enzyme takes in the catalytic conversion of galactose and in the presence of oxygen
Iron proteins [b]	
(a) Heme proteins	
1. Hemoglobin	The oxygen transporter in the mammalian blood stream
2. Myoglobin	Found in skeletal muscle, thought to act as oxygen reservoir
3. Leghemoglobin	Occurs in root nodules of legumes where it functions as an oxygen carrier
4. Cytochrome C-oxidase	Found in the mitochondrial inner membrane of cells and in the cytoplasmic membrane. An iron–copper protein which is the terminal member of the respiratory chain
5. Cytochromes P-450	The enzyme is of ubiquitous occurrence in plant and animal physiology and is involved in oxidative metabolism of a wide variety of endogenous compounds and xenobiotics
6. L-Tryptophan-2,3-dioxygenase and related compounds	Isolated from *Pseudomonad*, the enzyme catalyzes the insertion of two atoms of molecular oxygen into the pyrrole ring of L-tryptophan
(b) Non-heme proteins	
1. Hemerythrin	Oxygen-transporting protein of *Sipunculids, Priapulids* and some *Brachipods* and *Annelids*
2. Protocatechuate 3,4-dioxygenase and related enzymes	Obtained from *Pseudomonas aeruginosa*; catalyzes the cleavage of the benzene ring of protocatechuic acid with insertion of two atoms of oxygen

[a] J.F. Boas, J.R. Pilbrow and T.D. Smith in L.J. Berliner and J. Reuben (Eds.), Biological Magnetic Resonance. Plenum Press, New York and London, Volume 1, 1978, p. 277.
[b] T.D. Smith and J.R. Pilbrow in L.J. Berliner and J. Reuben (Eds.), Biological Magnetic Resonance Plenum Press, New York and London, Volume 2, 1980, p. 87.

TABLE 2

Molecular oxygen adducts of metal chelates

Metal	Type of compound	Ref.
1. (a)Titanium(III)	Porphyrin chelate	a(1), a(2)
(b)Titanium(IV)	Pyridine-2,6-dicarboxylate chelate	a(3), a(4)
2. Rhodium(II)	1. Porphyrin chelate	b
	2. Hydrido-amine complexes	c
3. Ruthenium(II)	Porphyrin chelate	d
5. Chromium(II)	Porphyrin chelate	e
6. Manganese(II)	Porphyrin chelate	f–i
7. Manganese(III)	bis(3,5-di-tert-butyl) chelate	j(1),j(2)
8. Manganese(II)	Phthalocyanine chelate	k
9. Vanadium(IV)	bis(3,5-di-tert-butyl)	l(1)
Vanadium(IV)	Pyridine-2,6-dicarboxylato chelate	l(2)
10. Copper(II)	Binuclear copper(II) chelate of a macrocyclic ligand	m,n
11. Cobalt(II) molybdenum	A heterobimetallic complex	o(1),o(2)
Molybdenum	Oxo-molybdenum fluoride	p
12. Rhodium(0)	Well-defined rhodium clusters	q
13. Manganese and cobalt	Manganese and cobalt carbonyl radicals	r,s
14. Palladium(0) sterically hindered phosphine complex	$Pd(O_2)[PPh(tBu)_2]_2$	t
15. Manganese(II)	Manganese halide or pseudohalide in complex of dimethylphenylphosphine in tetrahydrofuran	u(1),u(2)
16. Copper(I) chelate	Chelate formed by condensation of 2,6-diacetylpyridine and histamine	v(1),v(2)
17. Rhodium(I)	Rhodium cyclic olefin complexes	w
18. Vanadium(III)	Vanadium(III) chloride in the presence of pyridine	x

[a] (1) J.-M. Latour, J.-C. Marchow and M. Nakajima, J. Am. Chem. Soc., 101 (1979) 3974. (2) R. Ginlard, M. Fontense, P. Fourneri, C. Leromte and J. Protas, J. Chem. Soc., Chem. Commun., (1976) 161. (3) M.-M. Rohmer, M. Barry, A. Dedieu and A. Veillard, Internat. J. Quantum Chem., 4 (1977) 637. (4) D. Schwarzanbach, Helv. Chim. Acta, 55 (1972) 2990.

[b] B.B. Wayland and A.R. Newman, J. Am. Chem. Soc., 101 (1979) 6472.

[c] J.E. Endicott, C.L. Wong, T. Inoue and P. Matarajan, Inorg. Chem., 18 (1979) 450.

[d] N. Farrell, D.H. Dolphin and B.R. James, J. Am. Chem. Soc., 100 (1978) 324.

[e] S.K. Cheung, C.J. Grimes, J. Wong and C.A. Ard, J. Am. Chem. Soc., 98 (1976) 5028.

[f] R.D. Jones, D.A. Summerville and F.Basolo, J. Am. Chem. Soc., 100 (1978) 4416.

[g] C.J. Weschler, B.M. Hoffman and F. Basolo, J. Am. Chem. Soc., 97 (1975) 5278.

[h] B. Gonsalez, J. Rouba, S. Yee, C.A. Reed, J.E. Kirner and W.R. Sheidt, J. Am. Chem. Soc., 97 (1975) 3247.

[i] B.M. Hoffman, C.J. Weschler and F. Basolo, J. Am. Chem. Soc., 98 (1976) 5473.

[j] (1) K.D. Magers, C.G. Smith and D.T. Sawyer, J. Am. Chem. Soc., 100 (1978) 989; (2) Inorg. Chem., 19 (1980) 492.

TABLE 2 (continued)

---

[k] A.B.P. Lever, J.P. Wilshire and S.K. Quan, J. Am. Chem. Soc., 101 (1979) 3668; ibid., Inorg. Chem., 20 (1981) 761.

[l](1) J.P. Wilshire and D.T. Sawyer, J. Am. Chem. Soc., 100 (1978) 3972. (2) R.E. Drew and F.W.B. Einstein, Inorg. Chem., 12 (1973) 2990.

[m] A.H. Alberts, R. Annunziata and J.M. Lehn, J. Am. Chem. Soc., 99(1977) 8502.

[n] R. Louis, Y. Agnus and R. Weiss, J. Am. Chem. Soc., 100 (1978) 3604.

[o] (1) H. Arzoumanian, R.L. Alwarez, A.D. Kovalak and J. Metzger, J. Am. Chem. Soc., 99 (1977) 5175. (2) H. Arzoumenian, R. Lai, R.F. Alvarez, J.-F. Petrignani, J. Metzger and J. Fuhrhop, J. Am. Chem. Soc., 102 (1980) 845.

[p] D. Grandjean and R. Weiss, Bull. Soc. Chim. Fr., (1967), 3044.

[q] A.J.L. Hanlan and G.A. Ozin, Inorg. Chem., 16 (1977) 7857.

[r] S.A. Fieldhouse, B.W. Fulham, G.W. Neilson and M.C.R. Symons, J. Chem. Soc., Dalton Trans., (1974) 567.

[s] A.S. Haffadine, B.M. Peake, B.H. Robinson, J. Simpson and P.A. Dawson, J. Organomet. Chem., 121 (1976) 391.

[t] T. Yoshida, K. Tatsumi, M. Matsuomoto, N. Nakatsu, A. Nakamura, T. Fueno and S. Otsuka, Nouv. J. Chim., 3 (1979) 761.

[u](1) A. Hosseiny, C.A. McAuliffe, K. Minten, M.J. Parrott, R. Pritchard and J. Tames, Inorg. Chim. Acta, 39 (1980) 227. (2) C.A. McAuliffe, A.Al-Khateet, M.A. Jones, W. Levason, K. Minten and F.P. McCullough, J. Chem. Soc., Chem. Commun., (1979) 736.

[v](1) M.G. Simmons and L.J. Wilson, J. Chem. Soc., Chem. Commun., (1978) 634. (2) M.G. Simmons, C.L. Merrill, L.J. Wilson, L.A. Bottomley and K.M. Kadish, J. Chem. Soc., Dalton Trans., (1980) 1827.

[w] F. Sakurai, H. Suzuki, Y. Moro-oka and T. Ikawa, J. Am. Chem. Soc., 102 (1980) 1749.

[x] D.J. Halko and J.H. Swinehart, J. Inorg. Nucl. Chem., 41 (1979) 1589.

characterization, and chemical properties of the adducts of molecular oxygen with cobalt(II) compounds have been widely studied while the significance of these investigations has not exactly passed without notice. Thus the structure, electronic configuration and molecular orbital description of the paramagnetic 1:1 ($Co:O_2$) adducts and the diamagnetic 2:1 ($2Co:O_2$) complexes and their role in providing information about the oxygenation of oxygen transport and storage proteins and other aspects have been reviewed extensively [5–32].

It is the purpose of the present review to draw attention to the more recent advances made in the study of molecular oxygen adducts of cobalt(II) compounds. In a number of aspects of the description of the cobalt compounds it is relevant to compare their behaviour with corresponding iron compounds. Therefore, where this comparison is particularly profitable, assessment of the data available for both metal compounds will be made.

A wide range of cobalt(II) compounds form molecular oxygen complexes. Such compounds differ widely in chemical composition, spin state of

cobalt(II), solvent media and temperature conditions. To illustrate the diversity of cobalt(II) compounds, recent reports describe molecular oxygen complexes of five coordinate cobalt(II) triphosphine compounds, [32], the cobalt(II) chelate of N,N'-bis(2-thioformyl-2-phenylvinyl)trimethylene-diamine [33], cobalt(II) amino acid-imidazole complexes [34], the cobalt(II) chelate of dipyruvamide bleomycin [35], and binuclear chelate system $Co_2LL_2^1$ in which L is the bisterdentate ligand, 1,4-bis(bis(2-aminoethyl)aminoethyl)-benzene, and L^1 is either glycine or ethylenediamine [36]. The present knowledge of the structural and electronic properties of the molecular oxygen complexes has accrued as a result of the application of a wide range of measurements as outlined by Fig. 1.

Thermodynamic Measurements
of molecular oxygen adduct
formation

Infrared Spectroscopy
- measurement of vibrational
energy

ESR Spectroscopy
- detection of unpaired
electron, hyperfine effects

Photoelectron Spectroscopy
Mössbauer Spectroscopy
X-ray Absorption Edge
Spectroscopy from synchrotron
radiation
- measurement of electron
density at the metal.

X-ray Crystallography
- measurement of bond
distances, bond angles

Electrochemical Measurement
of ease of reduction of
metal centre.

Resonance Raman Spectroscopy
- measurement of cyclic structure
confirmation

UV-Visible Spectroscopy
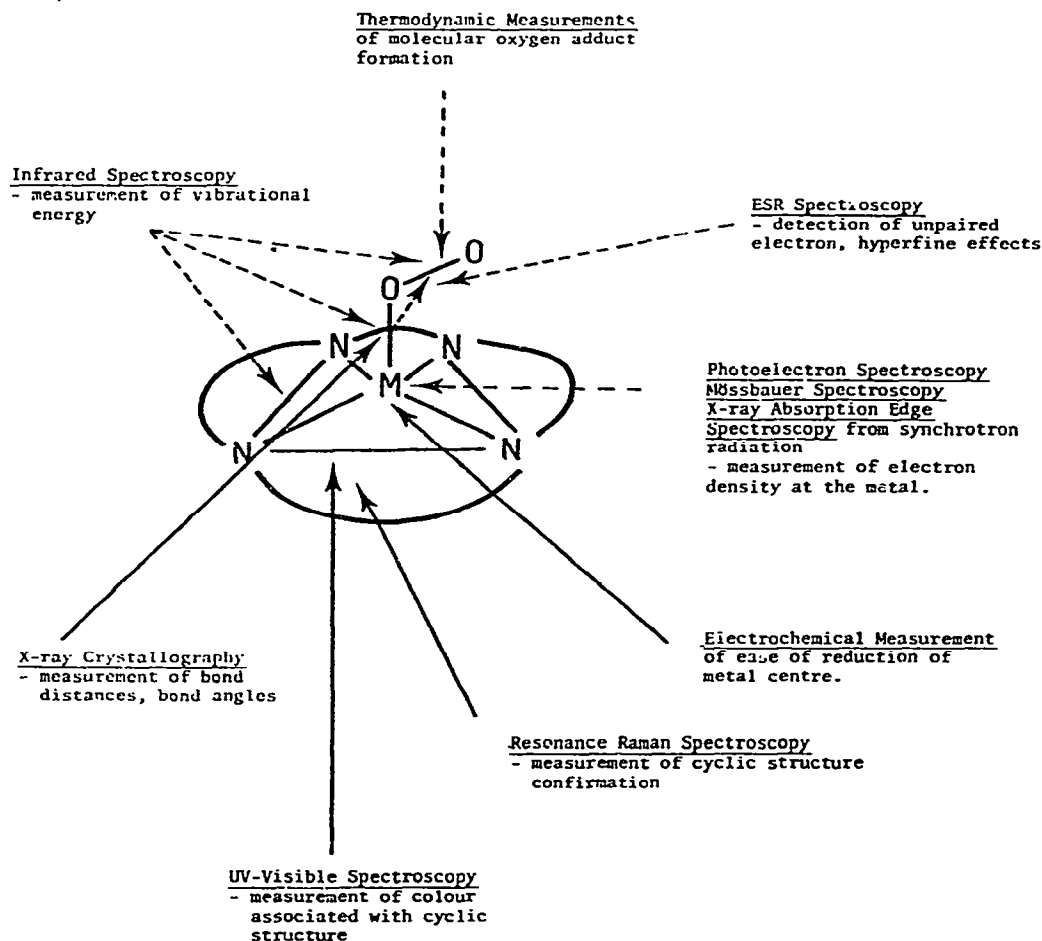- measurement of colour
associated with cyclic
structure

Fig. 1. Measurements used to determine the structural and electronic properties of molecular oxygen adducts.

## B. MEASUREMENT OF EQUILIBRIUM CONSTANTS OF OXYGEN UPTAKE

A large number of the early investigations [37–54], including the earliest report of the formation of a molecular oxygen adduct by N,N'-ethylene-bis(salicylideneiminato)cobalt(II) [55,56], were concerned with the reversible uptake of oxygen by cobalt(II) Schiff base chelates in the solid state, an aspect which has been the subject of recent work [57]. Whether the form of the cobalt(II) compound is a solid or in solution and possibly in the presence of base, equilibrium measurements have been used to quantify the influence of the ligand and its substituent groups and of the base with particular reference to finding correlations between base strength with the ability of the base to promote oxygenation. Equilibrium measurements on the iron protein and molecular oxygen have been reviewed [58].

The measurements are made possible by the fact that the colour of the cobalt chelate changes as a result of the formation of the adduct with molecular oxygen. Thus the oxygenation of the cobalt(II) Schiff base represented by Structure 1 causes the orange colour of the cobalt(II) chelate in
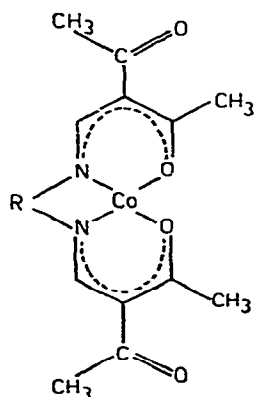
toluene containing a small amount of pyridine to turn purple when oxygen is passed through the solution at room temperature [59]. The orange colour is recovered when nitrogen is passed through the solution and warmed to about 60°C. The purple colour (525 nm) may be assigned to the charge-transfer transition from the π_ν^* orbital to the vacant $d_{x^2-y^2}$ orbital of the cobalt. The $\pi_\nu^*(O_2) \rightarrow d_{x^2-y^2}(Co)$ charge transfer bands are expected at wavelengths less than 400 nm [60] in most oxygen carriers and is thought to occur at higher wavelengths due to the electron withdrawing effect of the acetyl group which lowers the energy of the d orbital so that the charge-transfer band appears in the visible region.

The equilibrium constants for the system
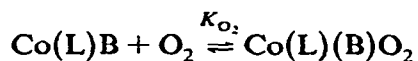
$$Co(L)B + O_2 \underset{}{\overset{K_{O_2}}{\rightleftharpoons}} Co(L)(B)O_2$$

measured at various partial pressures of oxygen have been computed using the Hill relation [62]:

$$Y/(1-Y) = \frac{[Co(L)(B) \cdot O_2]}{[Co(L)(B)]} = K_{O_2} P_{O_2}^{n} \text{ where } n = 1$$

The experimental data is plotted as log $Y(1-Y)$ versus log P_{O_2}, the concentrations of the cobalt species being determined spectrophotometrically. Thermodynamic data for the binding of molecular oxygen to cobalt chelates have been derived from measurements of the equilibrium constant at various temperatures using the following expression [62]:

$$K^{-1} = P_{O_2} \left[\frac{C_A b(E_c - E_A) - 1}{A - A^{\circ}} \right]$$

where K is the equilibrium constant for oxygenation, P_{O_2} is the partial pressure of oxygen above the solution, C_A is the initial concentration of cobalt chelate, b is the path length of the absorption cell, A is the total absorbance related to the concentration of oxygen adduct and to the cobalt chelate, A° is the absorbance of the solution before admission of oxygen and $(E_c - E_A)$ is the difference between the molar absorption coefficients of the oxygen adduct and cobalt chelate.

The large negative entropy change which is associated with the oxygenation process is consistent with the loss of translational degrees of freedom of the oxygen molecule upon coordination [63]. Amongst the various other conclusions reached are: (a) the oxygen carrying ability of the cobalt(II) chelates depends on the ease of oxidation [64]; (b) compared with species of similar redox potential but differing charge, neutral cobalt(II) chelates function as the best dioxygen carriers [64]; and (c) there is no simple relationship between ΔG, ΔH, and ΔS of oxygenation and the basicity of the ligand L, both σ and π donor effects need to be considered [65]. The ΔH and ΔS values found for the formation of the molecular oxygen carriers, as outlined by a selection of the data in Table 3, lie within a small range of values. The oxygenation process must offset an unfavourable ΔS term (~ 50 ea) by involving a sufficiently large enthalpy change with exothermic binding of the oxygen. From the thermodynamic point of view the compound will prove to be an effective oxygen carrier if there is a sufficiently large heat of formation of the metal–dioxygen bond.

C. STRUCTURES OF MOLECULAR OXYGEN COMPLEXES OF COBALT(II) COMPOUNDS

The geometric disposition of the dioxygen molecule in the molecular oxygen complexes of both iron and cobalt compounds has been of concern

TABLE 3

Thermodynamic parameters associated with the addition of molecular oxygen to cobalt(II) and iron(II) compounds

Compound	ΔG (kcal mol^{-1})	ΔH (kcal mol^{-1})	ΔS e.u.	Ref.
Fe(II)Mb	−0.4	−14.8	−49	a
Co(II)Mb	2.2	−12.7	−51	b
Co(II)(acacen)pyr	0.6	−15.1	−53	c
Co(II)(salen)pyr	1	−12.4	−47	c
Co(II)protoporphyrin IX dimethyl ester imidazole	+5.5	−11.5	−58	d
Co(II)protoporphyrin IX dimethyl ester pyridine		−7.80	−48.7	e
Co(II)protoporphyrin IX dimethyl ester; N methyl imidazole	5.7	−11.8	−59	f
Fe(II)TP·VPP·N−Me Im.	2.6	−13.3	−53	g
Fe(II)TP·VPP·N−Me Im.	~0	−15.6	−51	g
Co(II)Mb (Grey whale)	2.5	−9.4	−40	h
Co(II)Mb (sea lion)	2.4	−10.4	−43	h
Co(II)Mb (Sperm whale)	2.4	− 13.3	−53	h
Co(II)Mb (horse heart)	2.4	−11.3	−46	h
Fe(II)Mb (Grey whale)	~0	−15.3	−51	h
Fe(II)Mb (sea lion)	~0	−17.1	−57	h
Fe(II)Mb (Sperm whale)	~0	−19.1	−63	h
Fe(II)Mb (horse heart)	~0	−21.0	−70	h

[a] M.A. Keyes, M. Falley and R. Lumrey, J. Am. Chem. Soc., 93 (1971) 2035.

[b] C.A. Stillburg, B.M. Hoffman and D.H. Petering, J. Biol. Chem., 247 (1973) 4219.

[c] G.Tauzher, G. Amiconi, E. Antonini, M. Brunori and G. Costa, Nature: New Biology, 241 (1973) 222.

[d] H.C. Stynes and J.H. Ibers, J. Am. Chem. Soc., 94 (1972) 1559.

[e] T.J. Beugelsdijk and R.S. Drago, J. Am. Chem. Soc., 97 (1975) 6466.

[f] D.V. Stynes, H.C. Stynes, B.R. James and J.A. Ibers, J. Am. Chem. Soc., 95 (1973) 1796.

[g] J.P. Collman, J.I. Brauman, K.M. Doxsee, T.R. Halbert and K.S. Suslick, Proc. Natl. Acad. Sci., U.S.A., 75 (1978) 564.

[h] M.-Y.R. Wang, B.M. Hoffman, S.J. Shire and F.R.N. Gurd, J. Am. Chem. Soc., 101 (1979) 7394.

since the earliest investigations, with particular interest being shown in the bond angle made by the O−O molecule with the cobalt or iron atom and the O−O bond length which may be compared with the bond lengths in other chemical states of the oxygen molecule. The structural data drawn from X-ray crystallographic data of the 1:1 molecular oxygen complexes of a number of cobalt and iron compounds is summarized in Table 4. It shows that the molecular oxygen is tilted upwards from the plane containing the
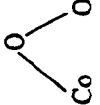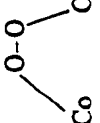
TABLE 4

X-ray crystallographic data for 1:1 molecular oxygen complexes of cobalt and iron compounds

Compound	M–O Å	O–O Å	M–O–O deg.	Ref.
Co(bzacen)(py)(O$_2$)	1.86	1.26	126	a
Co(acacen)(py)(O$_2$)	1.95		bent Co–O$_2$ group	b
[NEt$_4$]$_3$[Co(CN)$_5$(O$_2$)]·5H$_2$O	1.906	1.240	153	c
[Co(3-OMe-Saltmen)(H$_2$O)(O$_2$)]	1.88	1.25	117	d
[Co(t-Bsalten)(bzImid)(O$_2$)]	1.87	1.273	117.5	e
[Co(3-F-Saltmen)(1-Me-Imid)(O$_2$)·2(CH$_3$)$_2$CO]	1.881	1.302	117.4	f
[Co(saltmen)(BzImid)(O$_2$)]	1.889	1.277	120.0	g
[Co(salpeen)(O$_2$)]·MeCN(O$_2$)]	1.90	1.06	134	h
Co[3-tert-butyl salen]O$_2$·pyridine	1.870	1.35	116.4	i
[Fe($\alpha\alpha\alpha\alpha$TpVPP)](N-Me-imid)(O$_2$)]		1.26	137	j(1)j(2)
[Fe($\alpha\alpha\alpha\alpha$TplVPP)(1-Me-imid)(O$_2$)]	1.75	1.15	133	k
		1.17	129	
Oxymyoglobin	1.9	1.4	121	l

[a] G.A. Rodley and W.T. Robinson, Nature (London), 235 (1972) 438.

[b] M. Calligaris, Inorg. Nucl. Chem. Lett., 9 (1973) 419.

[c] L.D. Brown and K.H. Raymond, Inorg. Chem., 14 (1975) 2595.

[d] B.T. Huie, R.M. Leyden and W.P. Schaefer, Inorg. Chem., 18 (1979) 125.

[e] R.S. Gall, J.F. Rogers, W.P. Schaefer and G.G. Christoph, J. Am. Chem. Soc., 98 (1976) 5153.

[f] A. Avdelf and W.P. Schaefer, J. Am. Chem. Soc., 98 (1976) 5153.

[g] R.S. Gall and W.P. Schaefer, Inorg. Chem., 15 (1976) 2759.

[h] G.B. Jameson, W.T. Robinson and G.A. Rodley, J. Chem. Soc., Dalton Trans., (1978) 191.

[i] W.P. Schaefer, B.T. Huie, M.G. Kurilla and S.E. Ealick, Inorg. Chem., 19 (1980) 340.

[j](1) J.P. Collman, R.R. Gague, C.A. Reed, W.T. Robinson and G.A. Rodley, Proc. Natl. Acad. Sci., U.S.A., 71 (1974) 1326. (2) J.P. Collman, R.R. Gague, C.A. Reed, T.R. Halbert, G. Land and W.T. Robinson, J. Am. Chem. Soc., 97 (1975) 1427.

[k] G.B. Jameson, G.A. Rodley, W.T. Robinson, R.R. Gague, C.A. Reed and J.P. Collman, Inorg. Chem., 17 (1978) 850.

[l] S.E.V. Phillips, Nature (London), 273 (1978) 247; S.E.V. Phillips and B.P. Schoenborn, Nature (London), 292 (1981) 81.

TABLE 5

X-ray crystallographic data for the 2:1 molecular oxygen complexes of cobalt and iron compounds

Complex	Å O-O Bond length	degrees O⟨O,Co⟩ Bond angle	degrees O-O⟨Co⟩ Bond angle	Å Co-O Bond length	Å Co···Co Separation	Ref.
K_5[Co_2O_2(CN)_10]·H_2O	1.243	121.2	166	1.944	4.637	a
K_8[Co_2O_2(CN)_10](NO_3)_2·4H_2O	1.289	120.7	180	1.919	4.634	b
[Co_2O_2(NH_3)_12](NO_3)_5	1.447	118.8	180	1.985	4.899	c
[Co_2O_2(NH_3)_12](SO_4)(HSO_4)_3	1.317	117.3	180	1.895	4.545	d
[Co_2O_2(NH_3)_10(SO_4)_2·4H_2O	1.312	117.7	175.3	1.894	4.562	e
[Co_2O_2(NH_3)_10](SCN)_4	1.473	113	145.8	1.883	4.427	f
[Co_2O_2(en)_2(dien)_2](ClO_4)_4	1.469	110.8	180	1.879	4.495	g
[Co_2O_2(en)_2(NO_2)_2(NO_3)_2·4H_2O	1.488	110.8	180	1.896	4.523	h
(Co salen)_4(O_2)_2(H_2O)_2·pip·2CHCl_3	1.53	110	180	1.890	4.540	i
	1.308	118	122	1.930	—	
(Co salen)_2(O_2)(DMF)_2	1.339	120.3	110.1	1.910	—	j
(Co salen)_2(O_2)toluene	1.45	118.5	149.3	1.930	4.650	k
(Co salen)_2(O_2)·½acetone·½pip·	1.383	120	121.9	1.911	4.386	l

[a] F.R. Fronczek and W.P. Schaefer, Inorg. Chem., 14 (1975) 611.

[b] F.R. Fronczek and W.P. Schaefer, Inorg. Chim. Acta, 9 (1974) 143.

[c] R.E. Marsh and W.P. Schaefer, Acta Cryst., Sect. B, 24 (1968) 246.

[d] W.P. Schaefer and R.E. Marsh, J. Am. Chem. Soc., 88 (1966) 178.

[e] W.P. Schaefer, Inorg. Chem., 7 (1968) 725.

[f] F.R. Fronczek, W.P. Schaefer and R.E. Marsh, Acta Cryst., Sect. B, 30 (1974) 117.

[g] J.R. Fritch, G.G. Christoph and W.P. Schaefer, Inorg. Chem., 12 (1973) 2170.

[h] T. Shibahara, S. Koda and M. Mori, Bull. Chem. Soc. Jpn., 46 (1973) 2070.

[i] B.C. Wang and W.P. Schaefer, Science, 166 (1969) 1404.

[j] M. Calligaris, G. Nardin, L. Randaccio and A. Ripamonti, J. Chem. Soc. A, (1970) 1069.

[k] L.A. Lindblom, W.P. Schaefer and R.E. Marsh, Acta Cryst., Sect. B, 27 (1971) 1461.

[l] A. Ardeef and W.P. Schaefer, Inorg. Chem., 15 (1976) 1432.

ligand atoms surrounding the cobalt or iron atom with a lengthening of the O–O distance compared with that in molecular oxygen though shorter than the O–O distances encountered in the 2:1 compounds, the structural data for which are summarized in Table 5. An interesting structural comparison may be made with the molecular chlorine complex with cobalt(II) in cobalt(II) exchanged sodium Zeolite A $(Co_4Na_4–A \cdot 4Cl_2)$ [66]. The Co–Cl(1)–Cl(2) angle is 114° with a Co–Cl distance of 2.24 Å which is comparable with that found in chloride complexes of cobalt(II). The Cl–Cl bond is 2.52 Å which is 0.53 Å longer than free dichlorine. A surprising observation is that the colour of the cobalt(II) exchange zeolite does not change on absorption of dichlorine. An interpretation of the infra-red spectral data for matrix isolated Fe · O_2 suggests that the complex possesses a triangular structure analogous to that formed by similar complexes of Ni^0, Pd^0 and Pt^0 [67].

D. ELECTRONIC STRUCTURES OF MOLECULAR OXYGEN COMPLEXES

The nature of the chemical bond between the metal ion and molecular oxygen, particularly in those compounds containing iron or cobalt has been of paramount interest. A number of formulations have been put forward to account for some measurable property as outlined in Table 6. While it may be semantic to describe in simplistic terms the electron distribution in the molecular oxygen complexes of iron compounds in terms such as $Fe(II)–O_2$ or $Fe(III)–O_2^-$, such representations assist in delineating the various formulations which seek to describe the extent of charge transfer between the metal ion and the dioxygen ligand [68].

Heitler–London calculations with configuration interaction among the various basic configurations belonging to the structures $Fe(II)–O_2$, $Fe(III)–O_2^-$ and $Fe(I)–O_2^+$ have been carried out, while calculations relating to the $Fe–O_2$ group with the oxygen in the inclined position show that the electronic state is complicated involving a mixture of the following wave functions: $\psi(^3E; \ Fe^{2+})\phi(^3\Sigma^-; \ O_2); \ \psi(^1A_1; \ Fe^{2+})\phi(^3\Sigma_g; \ O_2)$ and $\psi(^2E; \ Fe^{3+})\phi(^2\Pi_{,g}; \ O_2^-)$ [69]. More recently the FeO_2 unit has been shown to be represented as an equal mixture of Fe^{2+} $(S = 0),O_2$ $(S = 0)$ and Fe^{2+} $(S = 1)$, O_2 $(S = 1)$ valence state pairs [70]. In the Fe^{2+} $(S = 0)$, O_2 $(S = 0)$ model, the iron is ferrous low spin (t_{2g}^6) while the oxygen molecule resides in a spin paired singlet configuration analogous to that in the $^1\Delta_g$ molecular state; the spin pairing in molecular oxygen occurs because the Π_g orbital in the FeO_2 plane has a lower energy than its out-of-plane partner. The other configuration has both iron and oxygen in the $S = 1$ state. The iron is in an excited ferrous state in which one electron has been moved from the d_{xz} orbital, which is antisymmetric with respect to the FeO_2 plane, and placed into the d_{z^2} orbital which points along the Fe–O bond; the oxygen remains a

TABLE 6

Electronic configurations of the iron–dioxygen bond

Iron–dioxygen bond	Description	Ref.
Formal $Fe(II) - O_2$ configuration	Semi-empirical calculations on a totally spin paired iron(II)–dioxygen configuration. Larger degree of backbonding from iron to the dioxygen than forward donation into the d_{xz} and d_{yz} orbitals results in net negative charge on dioxygen	a
Formal $Fe(II) - O_2$ configuration	Theoretical analysis of ground and excited states. An equal mixture of Fe^{2+} ($S=0$), O_2 ($S=0$) and Fe^{2+} ($S=1$),O_2 ($S=1$) valence state pairs. The bonding of oxygen is mainly covalent with little charge transfer	b(1),b(2)
$Fe(II)$–O_2 "ozone model"	Valence bond considerations (GVB – CI calculation). Iron is essentially of intermediate spin ($S=1$), oxygen retains its triplet ground state character	c(1),c(2) ·
$Fe(II) - O_2$ intermediate spin valence formula	Valence bond considerations. High-spin iron(II) promoted to an intermediate spin state $S=1$ with two unpaired electrons of the latter spin pairing with a triplet ground state O_2. Explains infra-red data on O–O stretching frequency which is reduced from 1556 to 1107 cm^{-1}	d(1),d(2)
$Fe(III)$–O_2^-	Mössbauer spectroscopy on oxymyoglobin. Temperature dependence of the electric field gradient tensor can be calculated from an Fe^{2+} term. Ground state is a diamagnetic singlet $|J| \gg 300$ cm^{-1}	e
$Fe(IV)$–O_2^{2-}	Valence bond explanation of infra-red spectroscopic data	

[a] R.F. Kirchner and G.H. Loew, J. Am. Chem. Soc., 99 (1977) 4639.
[b](1) B.H. Huynh, D.A. Case and M. Karplus, J. Am. Chem. Soc., 99 (1977) 6103. (2) D.A. Case, B.H. Huynh and M. Karplus, J. Am. Chem. Soc., 101 (1979) 4433.
[c](1) B.D. Olafson and W.A. Goddard, Proc. Natl. Acad. Sci., U.S.A., 74 (1977) 1315. (2) W.A. Goddard and B.D. Olafson, Proc. Natl. Acad. Sci., U.S.A., 72 (1975) 2335.
[d](1) R.D. Harcourt, J. Inorg. Nucl. Chem., 39 (1977) 243. (2) R.D. Harcourt, International J. Quant. Chem., 4 (1977) 143.
[e] D. Bade and F. Parak, Z. Naturforsch. C, Bio. Sci., 33c (1978) 488.
[f] H.B. Gray in Adv. Chem. Series, 100 (1971) 365.

$^3\Sigma_g$ configuration. The resulting complex is diamagnetic due to spin pairing of the $S = 1$ states. Since the charge on the ferrous ion is nearly neutralized by the five nitrogen atoms of the ligands, the bonding of oxygen is mainly covalent with little charge transfer. The σ donation to the iron, primarily from the $2s$ orbital of the oxygen atom linked to the iron is almost exactly balanced by the π back donation into the 2_{p_x} orbitals of both oxygen atoms.

The back donation is into an antibonding orbital and it appears to be mainly responsible for the lengthening of the O–O bond. A study of the optical spectra of oxy- and deoxyhemoglobin provides some useful experimental data to compare with these theoretical considerations [71]. In addition, it is .worth bearing in mind the results of a study of the magnetic properties of oxyhemoglobin which allow the conclusion that, contrary to widely accepted opinion, oxyhemoglobin is not diamagnetic above 50 K. Spin pairing occurs with $J = -73$ cm^{-1} [72]. The results of the configuration interaction calculations on model oxy–heme compounds definitely establish a diamagnetic ground state with a very lowlying triplet state (129 cm^{-1}) and an antiferromagnetic singlet state at a much higher energy (13500 cm^{-1}) above it [73]. This provides a simple rationale for the temperature dependent magnetic susceptibility observed for oxyhemoglobin, namely a thermal equilibrium between a diamagnetic ground state and a paramagnetic excited triplet state lying very close in energy to the ground state. The efficacy of the empirical parametization in INDO for giving a good description of the ground state of model oxyheme is demonstrated by the agreement between the calculated and experimental electric field gradient. The aspherical charge distribution on the iron atom corresponding to a $Fe(III)-O_2^-$ complex is consistent with the anomalously large electric field gradient.

The identification of an Fe–O bond at 567 cm^{-1} [74], and the observation of an $^{16}O-^{16}O$ stretch frequency at 1107 cm^{-1} [75], as well as measurements of polarized optical spectra [76], lend support to the concept of multiple bonding between the iron dioxygen along with lengthening of the O–O bond distance as emphasized by the "ozone" and intermediate spin valence formula. Despite the fact that these explanations include anisotropic covalent bonding interactions which account for the Mössbauer spectra of the iron–dioxygen complexes, the interpretation of the Mössbauer spectra, sometimes in uncompromising terms, is still expressed in the $Fe(III)-O_2^-$ form. Some of the data are shown in Table 7 which shows that the deoxygenated materials show large isomer shifts and large temperature-dependent quadrupole splittings characteristic of high spin ferrous compounds [77]. The quadrupole splittings in the dioxygen compounds are fairly large and strongly temperature dependent whereas those in the carbonyl compounds are very small. While earlier interpretations of the data have either been non-committed or tending to support the $Fe^{2+}-O_2$ form [78] the more recent data referred to in Table 6 support an $Fe^{3+}-O_2^-$ unit. The use of X-ray absorption spectroscopy using synchroton radiation for the structural investigation of certain molecules of biological interest has been described [79]. These techniques applied to deoxy and oxy forms of hemoglobin in aqueous solution at pH 7.4, the essential results being illustrated in Fig. 2 show that there is a shift in the K edge absorption as a result of

TABLE 7

Mössbauer measurements on compounds of myoglobin (Mb) and hemoglobin (Hb) [a]

Compound	Temperature (K)	Isomer shift relative to iron at room temperature (mm sec^{-1})	Quadrupole splitting (mm sec^{-1})
Deoxy Mb	4.2		2.28
	77	0.90	2.21
	195		1.85
Mb–O$_2$	4.2	0.27	2.31
	77	0.22	2.27
	195		1.96
Mb CO	4.2	0.27	0.36
	77		
	195		
Deoxy Hb	4.2	0.92	2.43
	77		2.37
	195		2.05
Hb–O$_2$	4.2	0.28	2.25
	77	0.26	2.19
	195	0.20	1.89
Hb CO	4.2	0.26	0.36
	77		0.36
	195	0.18	0.36

[a] Y. Maeda, Adv. Biophys., 11 (1978) 199.

molecular oxygen complex formation [80]. The results compared with other forms of hemoglobin, namely, hemin chloride and the carbonyl complex of hemoglobin are shown in Fig. 3. These preliminary results tend to favour an electronic formulation of $Fe^{3+}-O_2^-$ for the oxygen bonding unit of hemoglobin.

In the case of the molecular oxygen complexes formed by cobalt(II) compounds the greater weight of discussion is used to support a $Co(III)-O_2^-$ configuration where the π orbitals of dioxygen are relatively destabilized by the formal negative charge whereas the $3d$ orbitals of cobalt are relatively stabilized by the increased formal positive charge [81]. These considerations are supported by X-ray photoelectron spectroscopic studies of cobalt(II) Schiff base complexes and their adducts with dioxygen [82,83], and point to an 86 ± 17% extent of electron transfer between cobalt and oxygen, a result in broad agreement with similar determinations of charge transfer from ESR spectral data [84], and the O–O stretching frequency determined by infra-red and resonance Raman spectroscopy [85,86]. Indeed the $Co(III)-O_2^-$ formu-
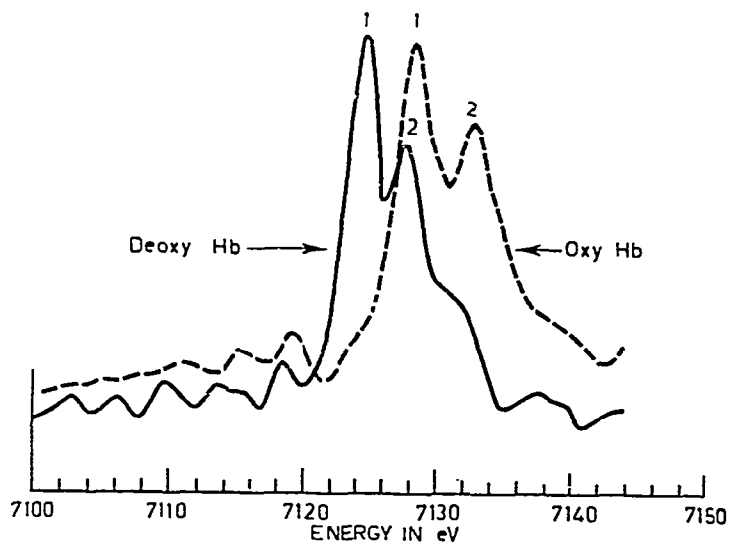
Fig. 2. First derivatives of the iron K-edge spectra of oxy- and deoxyhemoglobin solutions at pH 7.4 obtained by fluorescence measurements. 1 and 2 indicate the first and second inflection points along the rising position of the K-edge.
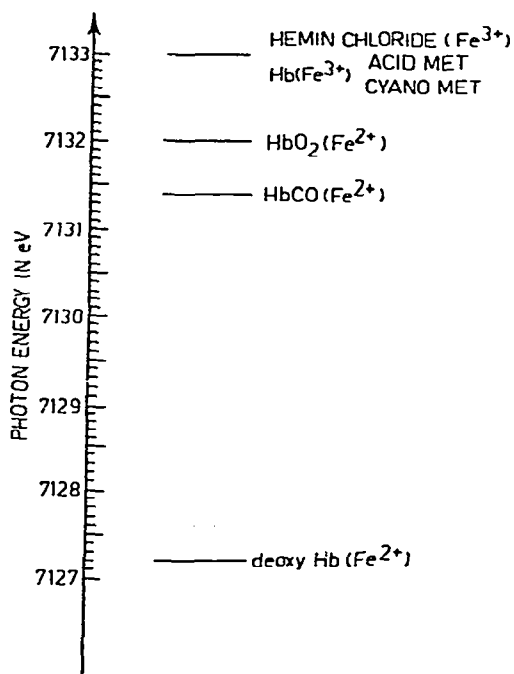

Fig. 3. Iron K-edge positions described by the second inflection points for various heme compounds.

lation of the molecular oxygen adducts prompted the experiment to show that the molecular oxygen adducts can be formed by addition of superoxo ligand to a cobalt(III) chelate [87], while a somewhat similar result was noted for the reaction of superoxoide ion with iron(III) protoporphyrin IX dimethylester perchlorate [88]. On the other hand a molecular orbital study of the molecular oxygen adducts of cobalt(II) chelates indicates that the coordinated dioxygen resembles the oxygen molecule more than the superoxo species [89]. The calculations point out that the function of the axial base invariably present to promote molecular oxygen adduct formation, localizes the spin density, into the d_{z^2} cobalt atom orbital, and increases the nucleophilicity of the cobalt atom. The interaction of penta-coordinated cobalt(II) chelates with dioxygen is thought not to involve a large transfer from cobalt to dioxygen, but only a spin polarization process which produces a negative spin density on the oxygen moiety.

Fantucci and Valenti's [89] calculations were based on Co(acacen)O$_2$ using an INDO–UHF method and Co(acacen)NH$_3$O$_2$ using a semi-empirical method. They assumed the C$_s$ symmetry reported by Rodley and Robinson [90] from an X-ray study of Co(bzacacen)pyO$_2$ where the Co–O–O angle was taken to be 126° and the Co–O bond length 1.26 Å. In their model, one of the oxygen π^* orbitals interacts with d_{z^2} (Co) to give a negative spin density of -0.0816 for Co(acacen)O$_2$ and -0.3971 for Co(acacen)NH$_3$O$_2$. Spin densities on other d-orbitals are very much smaller, sometimes negative and sometimes positive. For Co(acacen)O$_2$ it was found that 0.3 electron transfer had occurred into the bonding region. Oxygen spin densities are 0.4 and 0.6, respectively, for the middle and terminal oxygens of both systems. The general conclusions of this work lend support to the ideas put forward independently by Tovrog et al. [60] based on an earlier model due to Wayland et al. [91]. The idea of spin pairing may also be found in work reported by Harcourt [92].

Dedieu et al. [93] considered Co(acacen)O$_2$ within a fixed molecular framework by means of an ab initio LCAO–MO–SCF calculation with a minimal basis set. They found that a bent model with a Co–O–O angle of 126° has lower energy than either a linear model or one where the angle was 153°. From a population analysis (their Table X), the electron transfer to oxygen is calculated to be ~ 0.5, though it does include ligand effects. Spin densities on the oxygens are reversed compared with Fantucci and Valenti's calculation [89].

Similar general conclusions regarding particularly the bond angle have been reached for peroxy radicals using semi-empirical SCF–INDO calculations where energy was minimized by varying the O–O bond length and the X–O–O angle [94].

The O–O distance of 1.26 Å [90], normally thought of as being close to

the value of 1.28 Å observed in KO_2 [95] is decidedly smaller than the more recently determined value of 1.34 Å for the O_2^- species in the gaseous phase [96,97]. It is suggested that the value of 1.28 Å observed in the ionic structure of KO_2 is related to electrostatic polarization in the lattice structure. It is concluded that the 1.26 Å observed for the O–O distance in the cobalt complexes is in keeping with a charge transfer of about 0.3 electron thus preserving a certain character of the initial dioxygen molecule.

E. ESR STUDIES OF MOLECULAR OXYGEN COMPLEXES OF COBALT(II) COMPOUNDS AND RELATED SYSTEMS

A great many cobalt(II) complexes reversibly bind molecular oxygen and the resulting adducts have an ESR spectrum attributable to *one* unpaired electron. Typically, the g-values are 2.0, 2.0 and 2.08, while the corresponding hyperfine constants are ~ 0.001, 0.001 and 0.002 cm^{-1} [60,98–107].

The first problem to be overcome in the interpretation of ESR signals due to dioxygen adducts of cobalt(II) complexes concerns the molecular geometry. From X-ray structural data such as those summarized in Table 4, it has been long known that the Co–O–O angle was $\sim 120°$ in many cases. Preliminary single crystal ESR data for oxy cobalt myoglobin ($CoMbO_2$) indicated a low symmetry configuration for at least one of the two centres; aspects of that earlier study have been refined recently. When the authors and their colleagues first considered the interpretation of oxygen binding in frozen solutions of CoTPPS [104], they considered the possibility that principal g- and hyperfine axes might not necessarily coincide. Consideration of the g-values obtained for O_2^- trapped in KCl crystals [108] suggested that the largest g-value (~ 2.08) for Co–O_2 adducts would probably lie along the O–O direction. Principal cobalt hyperfine axes were expected to lie within the ligand plane and normal to it. Even since that time only a handful of papers have reported non-coincident g- and hyperfine axes [101,104–107,109]. A general discussion of low symmetry effects in ESR has been given elsewhere [110].

The second issue to consider is the description of the electronic structure of Co–O_2 adducts as a necessary step to interpreting both g-values and hyperfine structure. While there is some hope that the hyperfine structure can be understood in relatively simple terms, the g-values are a different matter with maximum values ranging from 2.44 (KCl:O_2^-) [108] through ~ 2.08 (Co–O_2) to 2.02 for peroxy radicals [94]. The g-value calculation reported by Kanzig and Cohen [108] for KCl:O_2^- is probably not quite appropriate, as it stands, for Co–O_2 and peroxy radicals where the two oxygens are inequivalent. In any event, g-values are very susceptible to excited state energies and these are not well known.

(i) ESR theory for molecular oxygen adducts of cobalt(II) compounds and related systems

ESR (electron spin resonance) or EPR (electron paramagnetic resonance) is the resonant absorption of energy by a spin system in an applied magnetic field. For a spin 1/2 system, which has two energy levels in a magnetic field, resonance is observed at a *fixed* microwave frequency, v, according to the relation

$$hv = g\beta B_0 \tag{1}$$

where h is Planck's constant and β the Bohr magneton. B_0 is the resonance magnetic field. Figure 4 illustrates resonance in a two level system, which is usually nowadays recorded as the first derivative of absorption with respect to magnetic field $(d\chi''/dB)$. When $g \sim 2$ and the measurement is recorded at X-Band (9–10 GHz), $B_0 \sim 300$ mT or 3000 G.

The presence of nuclear hyperfine coupling due to a nucleus with nuclear spin I leads to the occurrence of a set of $2I + 1$ equally spaced hyperfine lines in place of the single transition depicted in Fig. 4, e.g. for cobalt (II) where $I = 7/2$, each electron level becomes eight closely spaced nuclear sublevels (Fig. 5). Normally allowed magnetic dipole transitions where $\Delta M_s = \pm 1$ occur between pairs of levels which have the same values of M_I (Fig. 5). For interaction with a single Al nucleus as observed by Miller and Haneman [111] $I = 5/2$ and there are six hyperfine lines observed for some orientations within the system.

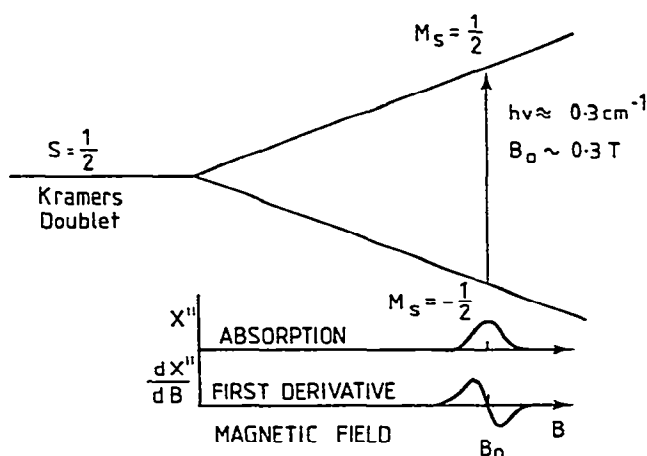In ESR the properties of the energy levels which give rise to the observed

Fig. 4. EPR in an $S = \frac{1}{2}$ doublet. Resonance absorption of energy occurs when the microwave energy (hv) exactly equals the energy difference between the levels.

spectrum, as depicted in Fig. 5, are summarized by a spin Hamiltonian which is limited to the set of lowest energy levels responsible for the resonance. Anisotropic effects due to the immediate environment of the paramagnetic centre are incorporated in anisotropic g- and A-values. The spin Hamiltonian for this case is as follows:

$$\mathcal{H} = \beta \sum_{i=x_g, y_g, z_g} g_i B_i S_i + \sum_{I=X,Y,Z} A_I S_I I_I \tag{2}$$

Here S is the effective electron spin which has the value $1/2$ and $I = 7/2$ for cobalt(II). x_g, y_g, z_g replace x, y, z in earlier papers of the authors. In this review we wish to choose x, y, z to be standard coordinates centred on cobalt(II) for discussion of the models of the centre. In the most general case, x_g, etc. will not coincide in orientation with X, etc. In order to keep the analysis and necessary computer simulations manageable, the lowest symmetry for Co–O$_2$ complexes will be considered C_s. This requires coordinates whose directions are summarized in Fig. 6 [112] and which are related to the likely molecular geometry in Fig. 7(a) [104]. When $\alpha = 0$ the model reduces to one with orthorhombic symmetry.

There are some very useful relationships which hold when the Zeeman interaction is much larger than the hyperfine terms in eqn. (2), a condition
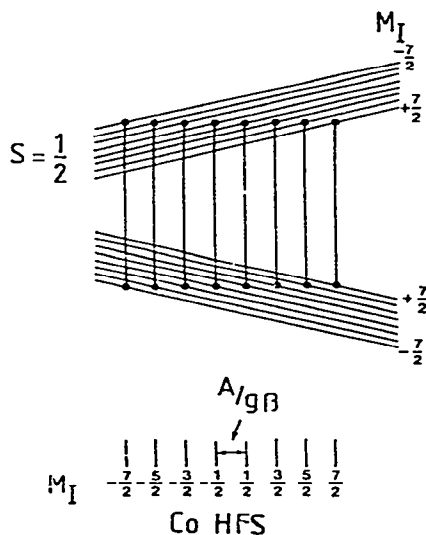

Fig. 5. Schematic representation of energy levels for cobalt where $S=\frac{1}{2}$ and $I=7/2$. Each level of Fig. 4 now consists of eight nuclear sublevels. ESR magnetic dipole transitions occur when $\Delta M_I = 0$.

well satisfied for Co–O_2 adducts. For the g-value angular variation

$$g^2 = g_x^2 l_x^2 + g_y^2 l_y^2 + g_z^2 l_z^2 \qquad (x = x_g, \text{etc.})$$ (3)

and, within the monoclinic symmetry limit [112],

$$g^2 A^2 = A_X^2 \left[g_x l_x \cos\alpha + g_y l_y \sin\alpha \right]^2 + A_Y^2 \left[-g_x l_x \sin\alpha + g_y l_y \cos\alpha \right]^2$$

$$+ A_Z^2 g_z^2 l_z^2 \qquad (x = x_g, \text{etc.})$$ (4)

At a particular orientation of B, then the resonance fields are given by

$$B = B_0 - \frac{A}{g\beta} M_I - a\left[I(I+1) - M_I^2 \right] - b M_I^2$$ (5)

where a and b, which are second-order corrections due to hyperfine interactions, are both dependent upon θ and ϕ. These are minor considerations for O_2 adducts of cobalt (II).

Because of anisotropy in g, the intensity of the lines also varies with orientation. In a powder this is complicated by the fact that although the resonance field depends only on θ and ϕ values, the intensities due to given molecules with the same values of θ and ϕ differ because they do not all have the same orientation relative to the microwave magnetic field in the cavity. The correct average value when $B \perp B_{rf}$ is [112(a),(b)]

$$\bar{g}_I^2 = \left[g_x^2 g_y^2 \sin^2\theta + g_y^2 g_z^2 (\sin^2\phi + \cos^2\theta \cos^2\phi) \right.$$

$$\left. + g_x^2 g_z^2 (\cos^2\phi + \cos^2\theta \sin^2\phi) \right] / (2g^2) \qquad (x = x_g, \text{etc.})$$ (6)

An additional factor $1/g$ is required in field swept ESR experiments for accurate comparisons of intensities as a function of orientation. This is particularly important for computer simulations [113].

Linewidths may also be anisotropic and for simulation purposes can be treated according to relationships such as

$$\sigma^2 = \sigma_{x^2} l_{x^2} + \sigma_{y^2} l_{y^2} + \sigma_{z^2} l_{z^2} \qquad (x = x_g, \text{etc.})$$ (7)

Single crystal studies of oxygenated CoMb [101,107] and B_{12r} [109] have used the spin Hamiltonian (2) and methods of collection and analysis of angular dependent ESR spectra which are nowadays quite commonplace [114,115].

By far the majority of the studies of Co–O_2 adducts have been done with powders or frozen solutions. Anisotropy information can then only be deduced from comparisons between experimental and computer simulated spectra. Computer simulation programs must sum spectra due to all possible orientations of the molecules with intensities weighted by the solid angle element $-1/2\Delta\cos\theta\Delta\phi$ for the range $[\theta, \theta + \Delta\theta; \phi, \phi + \Delta\phi]$. Programs used

by the authors sum the contributions from each particular transition as it is calculated.

Since a good many of the ESR results for Co–O_2 adducts have not been analysed on the basis of models such as implied by Fig. 7(a), where allowance must be made for non-coincident g and A axes ($\alpha \neq 0$), we must digress to consider some of the specific implications of the low symmetry. When the Zeeman interaction is much larger than hyperfine constants, turning directions in a crystal correspond to principal g-directions (x_g, y_g, z_g). When translated into powder ESR, it is the turning directions, where $\partial B/\partial \theta = 0$ and or $\partial B/\partial \phi = 0$ which produce the sharp features observed. Only when the symmetry is at least as high as orthorhombic ($\alpha = 0$ in figs. 5, 6 and 7) do the observed hyperfine splittings correspond to principal
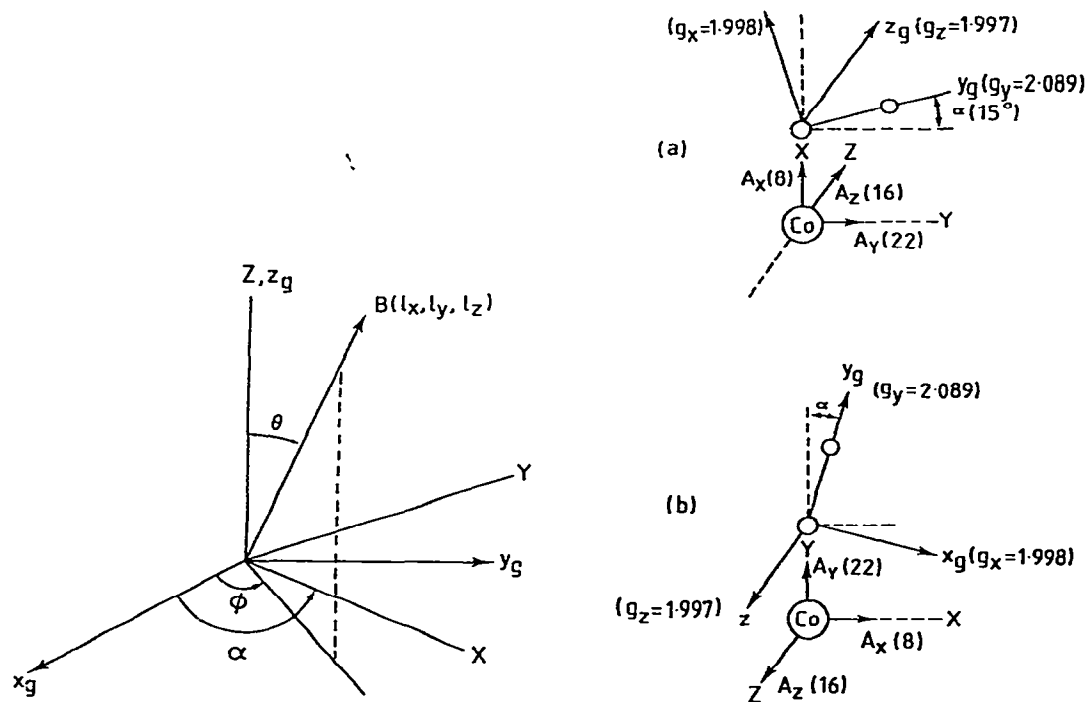
Fig. 6. Coordinate system for paramagnetic centre with monoclinic point symmetry ($\alpha \neq 0$), orthorhombic symmetry ($\alpha = 0$) and axial symmetry ($g_x = g_y$, $A_x = A_y$).

Fig. 7. Arrangement of principal axes for two possible models of the Co(II)TPPS·O_2 complex (a) Co–O–O angle 105°, YZ plane is the porphyrin plane; (b) Co–O–O angle 165°, XZ plane is the porphyrin plane. A values in 10^{-4} cm^{-1}. The orientation of the in-plane axes in relation to the four atoms is not known. (Reproduced with permission from de Bolfo et al. [104].)

hyperfine components. When $\alpha \neq 0$, and the complex has C_s symmetry, only A_z could, in principle, be read off directly from a powder spectrum. It may, nevertheless, be masked by other contributions. In single crystals where the symmetry is low, hyperfine splittings maximize or minimize at directions different from the g-axes. Therefore, if the symmetry of a paramagnetic complex is low, one *cannot, in general,* read the values of hyperfine constants directly from the spectral charts. This is an important point and must be borne in mind in connection with the later discussion of the electronic structure and its relationship to ESR parameters.

As a corollary to this, it is sometimes possible to obtain computer simulations of true low symmetry systems by means of an orthorhombic approximation and to obtain correct peak positions. It is not possible, at the same time, to match intensities satisfactorily. Furthermore, the hyperfine constants so obtained will not be the correct ones; at least one of them will be too high, another too low. The point is that monoclinic symmetry spectra have a different spatial distribution of spectral density compared with

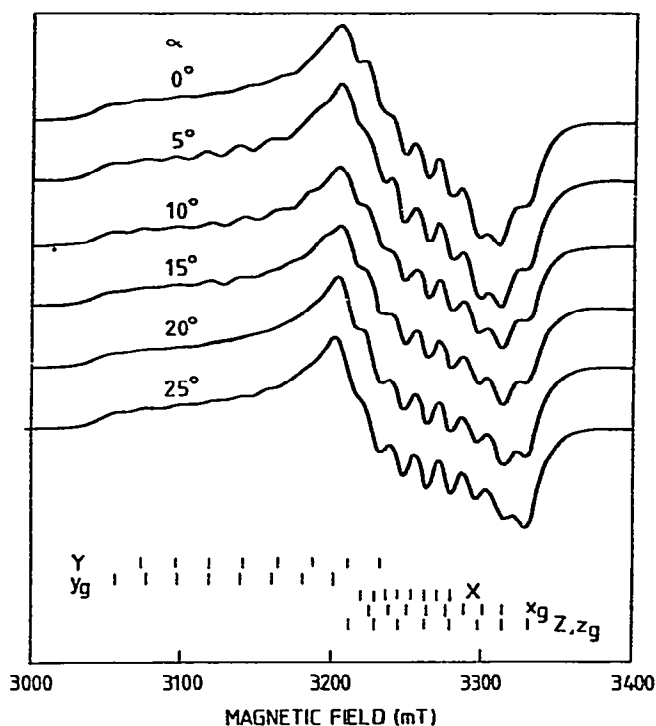Fig. 8. Simulated ESR spectra for Co(II)·O_2 adduct illustrating the effect of changing the angle α. g- and A-values as for CoTPPS·O_2 in Table 8. Linewidths used are $\sigma_x = \sigma_y = 1.2$ mT, $\sigma_z = 1.0$ mT. Microwave frequency 9.143 GHz.

orthorhombic spectra arising from identical g- and A-values. In the former.
case where $\alpha \neq 0$ one must integrate over ϕ from 0–180° whereas, when
$\alpha = 0$, ϕ ranges only from 0 to 90°. Figure 8 illustrates the effect of changing
α while keeping everything else constant. Figure 9 makes a different point in
·showing changes to one part of the spectrum caused by modest changes in
g_y. In Figs. 10 and 11 are shown two of the many examples which the
authors and their colleagues have studied. Errors in g-, A-values and α are
based upon the possible range of good fits judged by eye as automatic
least-squares fitting methods have been potentially too time consuming.

Analysis of powder or frozen solution spectra permit as one alternative to
Fig. 7(a), the situation depicted in Fig. 7(b) [104]. This would lead to a
Co–O–O angle of 180° $- \alpha$ rather than the 90° $+ \alpha$ for Fig. 7(a) but it is
rejected on the basis of the structural data such as given in Table 4.

Finally we consider the effect of the neglect of $g - A$ non-coincidence for
some Co–O$_2$ adducts. In the XY (zy) plane (Fig. 12) eqn. (4) reduces to

$$g^2 A^2 = A_X^2 \left(g_x l_x \cos\alpha + g_y l_y \sin\alpha \right)^2 + A_Y^2 \left(g_x l_x \sin\alpha + g_y l_y \cos\alpha \right)^2 \tag{8}$$

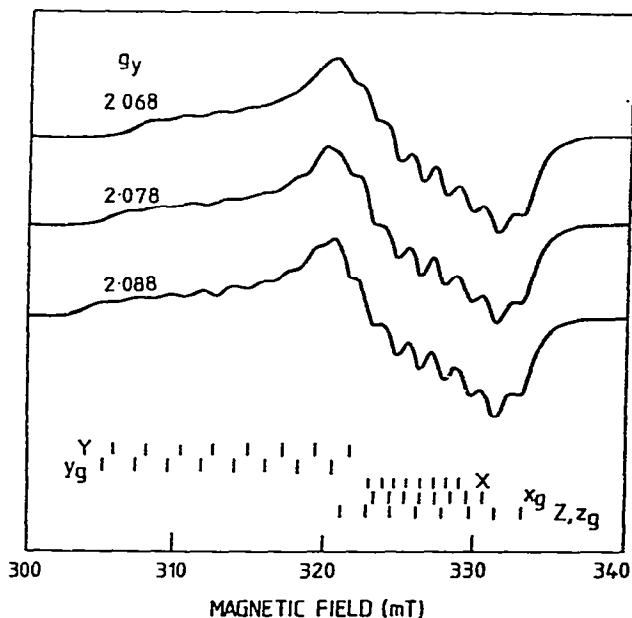and we use this equation to calculate the A values along principal x_g and

Fig. 9. Simulated ESR spectra for Co(II)–O$_2$ adduct illustrating the effect of changing g_y, the
maximum g-value. $\alpha = 15°$. All other parameters as in Fig. 8.

y_g-directions $A(x_g)$ and $A(y_g)$, respectively. When $l_x = 1$ and $l_y = 0$,

$$A(x_g)^2 = A_X^2 \cos^2 \alpha + A_Y^2 \sin^2 \alpha \tag{9a}$$

and for $l_y = 1$, $l_x = 0$

$$A(y_g)^2 = A_X^2 \sin^2 \alpha + A_Y^2 \cos^2 \alpha \tag{9b}$$

In Table 8 we list values of A_X, A_Y and α obtained from a number of computer simulation analyses of Co–O$_2$ spectra and, in one case, single crystal data. Included are six examples originally reported by Niswander and Taylor [116] for a series of Schiff's base complexes but initially interpreted using an orthorhombic symmetry model. The spectra from their paper have been digitized and the resulting spectra simulated using the model described in Fig. 12. (It was necessary to relabel the axes to conform to our simulation
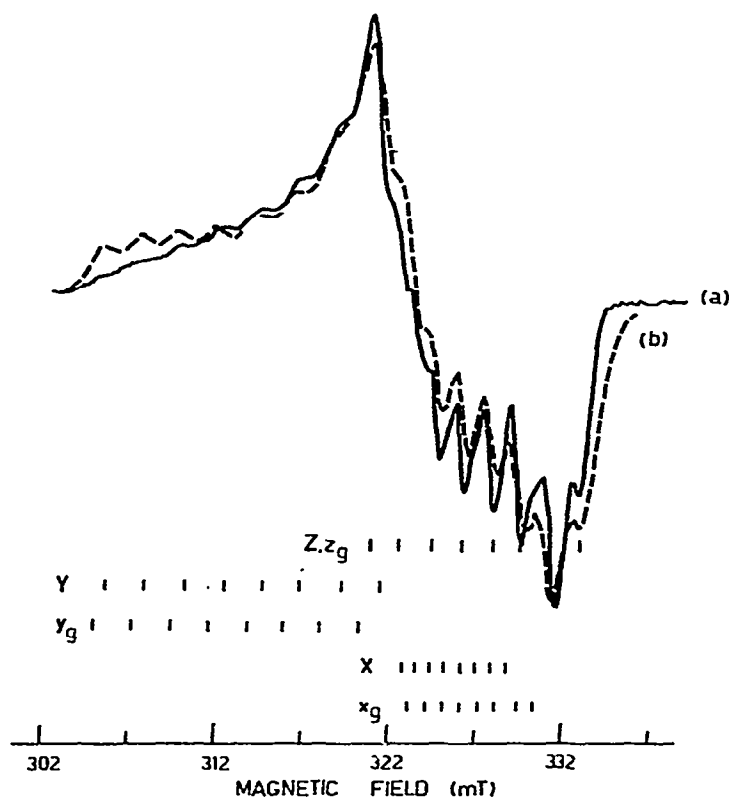

Fig. 10. ESR spectrum at 77 K of oxygenated form of Co(II)TPPS: (————) in aqueous solution containing 75% v/v DMF at 77 K; (- - - - -) computer simulated spectrum using parameters given in Table 8. Stick spectra labelled according to Fig. 12. Microwave frequency 9.143 GHz.
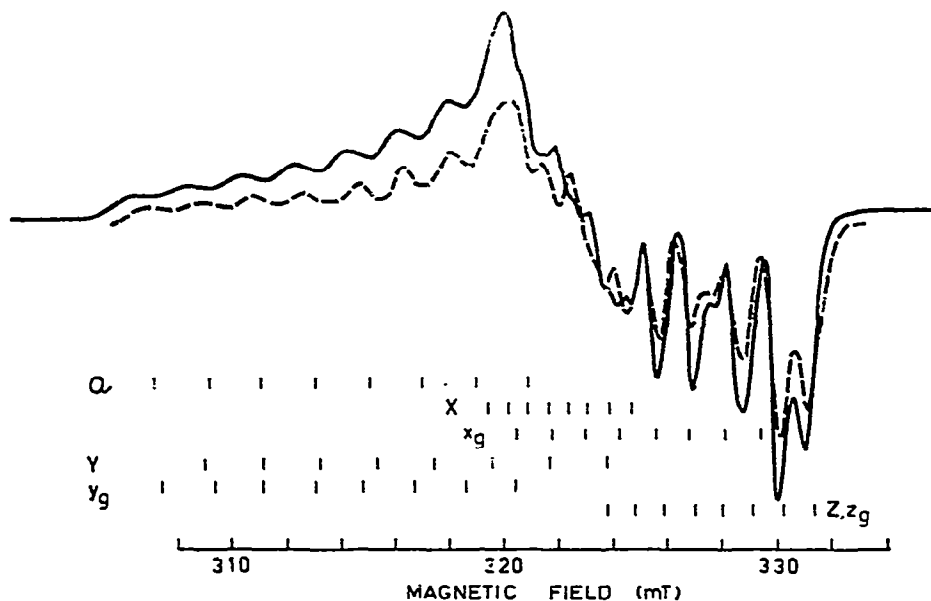
Fig. 11. ESR spectrum at 77 K due to oxygenated Co(II) (77' Diethylsalen) pyridine at 9.143 GHz. g-values, A-values and α as in Table 15 for α methyl salen. Linewidths 0.5, 0.5 and 0.85 mT.

program.) Comparison of the calculated values of $A(x_g)$ and $A(y_g)$ with those obtained from their interpretation (in parentheses) show that misleading A-values can be obtained. Table 8 also lists g-values including those reported by Niswander and Taylor [116] for the Schiff's bases given in parentheses, differences being most marked for g_x, the intermediate value.

Caution should be exercised in using the results of Table 8 to try to work backwards from reported A-values in the literature to the true values of A_x

Fig. 12. Coordinates based on Fig. 7(a) with addition of x, y and z to describe cobalt site for later discussion of hyperfine structure.

TABLE 8

ESR Parameters [1] for some Co-O₂ adducts

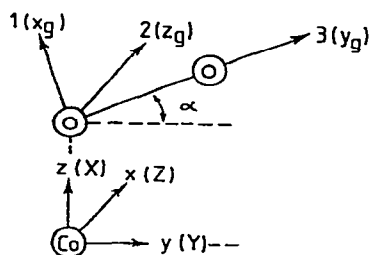| Compound	α^o	$A_X(z)^2$	$A_Y(y)^2$	$A_Z(x)^2$	$\langle A \rangle$	$A(x_g)$	$A(y_g)$	$g_x{}^3$	$g_y{}^3$	$g_z{}^3$	Ref.
		(×10⁻⁴ cm⁻¹)									
B₁₂·O₂(crystal)	21	9	21	7	12.3	11.2	20.3	1.994	2.079	2.012	a
CoTPPS·O₂	15	8	22	16	15.3	9.5	21.4	1.998	2.088	1.997	b
Co(saldpt)O₂	26 (0)	5.7	24	9.9 (13.5)	13.2	11.7 (13.3)	21.7 (22.7)	2.016 (2.007)	2.084 (2.0850)	1.996 (2.000)	c, Fig. 4(a)
Co(3-CH₃OsalMedpt)O₂	28 (0)	6.5	20.0	10.0 (14.5)	12.2	11.0 (12.1)	17.9 (18.6)	2.014 (2.009)	2.090 (2.090)	1.995 (1.988)	c, Fig. 4(b)
Co(α-CH₃salMedpt)O₂	28 (0)	6.3	22.4	11.0 (14.9)	13.2	11.8 (13.0)	21.2 (19.7)	2.009 (2.004)	2.088 (2.089)	1.993 (1.998)	c, Fig. 5(a)
Co(salphdpt)O₂	27 (0)	8.2	24.8	12.2 (17.0)	15.1	13.4 (16.0)	22.4 (22.6)	2.012 (2.004)	2.088 (2.083)	1.990 (1.997)	c, Fig. 5(b)
Co(5-Cl saldape)O₂	27–28 (0)	7.5	31.3	15.0 (19.1)	17.9	15.7 (16.4)	28.1 (27.6)	2.013 (2.003)	2.089 (2.090)	1.988 (1.995)	c, Fig. 6(a)
Co(3-CH₃OsalMcdapp)O₂	29 (0)	6.4	27.0	12.3 (19.1)	15.2	14.2 (14.3)	23.8 (23.6)	2.014 (2.009)	2.086 (2.097)	1.987 (2.000)	c, Fig.6(b)

[1] For definitions of axes see Fig. 12.
[2] Errors in A-values ±0.5×10⁻⁴ cm⁻¹; assumed negative for hyperfine analysis.
[3] Errors in g-values <±0.001.

[a] E. Jörin, A. Schweiger and Hs. H. Günthard, Chem. Phys. Lett., 61 (1979) 228.
[b] J.A. de Bolfo, T.D. Smith, J.F. Boas and J.R. Pilbrow, J. Chem. Soc., Dalton Trans., (1976) 1495.
[c] R.F. Niswander and L.T. Taylor, J. Mag. Res., 26 (1977) 491. (Published spectra were digitized and simulated at Monash University by I. Ruzic. Axes relabelled to conform to monoclinic simulation program. g- and A-values in parentheses are those reported by Niswander and Taylor.)

and A_γ. More information is needed than is contained, as has frequently been the case, in two reported values, viz. $A_\parallel$ and $A_\perp$.

There is another note of caution. In general, as exemplified by the single crystal study of Jörin et al. [109] on $B_{12r}\cdot O_2$, none of the g- and A-axes coincide, and the symmetry is very low indeed but it nevertheless approximates well to the model assumed in Fig. 12.

F. ESR STUDIES OF SUPEROXIDE AND OTHER OXYGEN RADICAL SPECIES

The exposure of activated, coloured, magnesium oxide to nitrous oxide, carbon dioxide, sulphur dioxide, hydrogen sulphide, and oxygen leads to the formation of stabilized paramagnetic radical anions which may be detected by e.s.r. spectroscopy [117,118].

The characterization of oxygen radical species formed on oxide surfaces or zeolites is of long-standing interest due to the role of these species in heterogenous catalytic oxidation [119–122]. For example, the species O^-, formed on the surface of magnesium oxide by the treatment of a sample of magnesium oxide, with about 0.5% of electrons trapped at discrete surface anion vacancies, with nitrous oxide, gives the g tensor values summarized in Table 9. The treatment of oxide surfaces or zeolite material with UV or γ radiation may lead to the formation of O_2^+ and O_2^- species at surface sites. The former species has g tensor values less than 2.00 [123]. The existence of O_3^- on oxide surfaces and zeolite material has been shown by ESR and chemical evidence [123–134] and assigned the g values shown in Table 9. The criteria for the choice of which of these radical species formed is based on their chemical reactivity toward some gases (e.g. SO_2, N_2O) and on their temperature of formation or decay [135]. As outlined in Table 9 the superoxide radical can be trapped and stabilized by an assembly of molecular dipoles as well as by discrete charged ions in ionic lattices. The formation of the O_2^- radical on the surface of silver has been confirmed by means of ESR measurements, which assist in elucidating the mechanism of the vapour phase oxidation of certain organic substrates catalyzed by silver [136–140]. Potassium superoxide, solubilized in dimethyl-sulphoxide by cyclohexyl-18-crown 6 [141], gives the characteristic ESR spectrum of the superoxide radical with $g_\parallel = 2.11$; $g_\perp = 2.00$. Addition of tetraphenylporphyrinato zinc(II) to the dimethylsulphoxide solution of superoxide results in a shift of $g_\parallel$ to 2.07 [142]. Further addition of pyridine to the solution effects the disappearance of the resonance $g = 2.07$, a result consistent with the replacement of O_2^- by pyridine. The ESR spectrum due to the complex $^{67}Zn(TPP) \cdot O_2^-$ (^{67}Zn, $I = 5/2$) show a shift by 2–3 G of the $g_\parallel$ resonance. A similar experiment involving the reaction of superoxide ion with iron(III) porphyrins in aprotic solvents has been shown to lead to the formation of a high-spin ferric porphyrin peroxo complex [143].

TABLE 9

ESR parameters of oxygen radicals

	g_x or $g_\perp$	g_y	g_z or $g_\parallel$	Ref.
O^- on oxides				
MgO	2.0016	2.0297	2.0505	a
	2.0016	2.0193	2.0472	
MgO	2.0016	2.041	2.041	b(1),b(2)
U_2O_5/SiO_2	2.003	2.023	2.023	c(1)
O^- in ice	2.07		2.002	c(2)
O_2^+ on rutile	2.024	2.002	1.980	d(1)
ESR data reinterpreted to be due to a species containing nitrogen	1.977	1.999	2.072	d(2)
O_2^- on oxides				
MgO	2.001	2.0073	2.077	e
ZnO	2.002	2.0082	2.051	e
TiO	2.003	2.0090	2.024	f(1),f(2),f(3)
SnO_2	2.002	2.0090	2.028	g
V_2O_5/SiO_2	2.005	2.0010	2.025	h
ZrO_2	2.002	2.0100	2.032	i
$CdO-Al_2O_3$	2.002	2.0090	2.039	j
MoO_3-TiO_2	2.003	2.009	2.019	k
O_2^- on zeolites				
Sodium Y zeolite	2.009	2.0046	2.057	l
Barium Y zeolite	2.0087	2.0047	2.058	m
Na X zeolite	2.001	2.008	2.027	n
O_3^- on oxides				
MgO	2.0014	2.010	2.0172	o
O_3^- in different matrices				
a. Ionic matrices				
Na_2O_2	2.002		2.175	p,q
	1.991		2.188	r
KCl	1.9512	1.9551	2.4359	s
b. Molecular matrices				
H_2O_2 + urea	2.009	2.0084	2.0886	t
c. Solvent matrices				
water, 0.2 M formate pH 11.7	2.006		2.11	u
water	2.001		2.101	r
methanol	2.0031		2.077	r
ethanol	2.0025		2.079	r
isopropanol	2.0022		2.084	r
pentan-3-ol	2.0018		2.092	r
benzene	2.0008		2.123	r
			2.180	

324

TABLE 9 (continued)

[a] A.J. Tench, T. Lawson and J.F.G. Kibblewhite, J. Chem. Soc., Faraday I, 68 (1972) 1169.

[b] (1) W.B. Williamson, J.H. Lunsford and C. Naccache, Chem. Phys. Lett., 9 (1971) 33. (2) W.B. Wong and J.H. Lunsford, J. Chem. Phys., 55 (1971) 3007.

[c] (1) V.A. Shvets, V.M. Vorotyntser and V.B. Kazanskii, Kin. Kat., 10 (1969) 356. (2) M.C.R. Symons, J. Chem. Soc., Chem. Commun., (1980) 675.

[d] (1) R.D. Iyengar, M. Codell, J.S. Karra and J. Turkevich, J. Am. Chem. Soc., 88 (1966) 5055. (2) R.D. Iyengar and R. Kellerman, J. Colloid Interfac. Sci., 35 (1971) 424.

[e] J.H. Lunsford and J.P. Jayne, J. Chem. Phys., 44 (1966) 1487.

[f] (1) I.D. Mikheikim, A.I. Maschenko and V.B. Kazanskii, Kin. Kat., 8 (1967) 1363. (2) C. Naccache, P. Meriaudeau, M. Che and A.J. Tench, Trans. Faraday Soc., 67 (1971) 506. (3) P.C. Gravelle, F. Juillet, P. Meriaudeau and S.J. Teichner, Discuss. Faraday Soc., 52 (1971) 40.

[g] J.H.C. Van Hoof and J.F. Van Helden, J. Catal., 8 (1967) 199; 11 (1968) 277.

[h] V.A. Shvets, M.E. Saricher and V.B. Kazanskii, J. Catal., 11 (1968) 378.

[i] M. Setaka and T. Kwan, Bull. Chem. Soc. Jpn., 38 (1965) 1414.

[j] M. Setaka and T. Kwan, Bull. Chem. Soc. Jpn., 43 (1970) 2727.

[k] M. Akimoto and E. Echigoya, J. Catal., 29 (1973) 191.

[l] P.H. Kasai, J. Chem. Phys., 43 (1965) 3322.

[m] K.M. Wang and J.H. Lunsford, J. Phys. Chem., 74 (1970) 1512; 73 (1969) 2069; 75 (1971) 1165.

[n] N. Kanzaki and I. Yasumori, Bull. Chem. Soc. Jpn., 51 (1978) 991.

[o] N.-B. Wong and J.H. Lunsford, J. Chem. Phys., 56 (1972) 2664.

[p] J.E. Bennett, D.J.E. Ingram, M.C.R. Symons, P. George and J.S. Griffith, Phil. Mag., 46 (1955) 443.

[q] J.E. Bennett, D.J.E. Ingram and D. Schonland, Proc. Phys. Soc. A, 69 (1956) 556.

[r] J.E. Bennett, B. Mile and A. Thomas, Trans. Faraday Soc., 64 (1968) 3200.

[s] W. Kanzig and M.H. Cohen, Phys. Rev. Lett., 3 (1959) 509; W. Kanzig, J. Phys. Chem. Solids, 23 (1962) 479.

[t] T. Ichikawa, M. Iwasaki and K. Kuwata, J. Chem. Phys., 44 (1966) 2979.

[u] R.A. Holroyd and B.H.J. Bielski, J. Am. Chem. Soc., 100 (1978) 5796.

Miller and Haneman [111] investigated the ESR spectra due to oxygen adsorbed onto the surfaces of a number of III–V semiconductors, viz. p-type GaP, GaAs, GaSb and InAs as well as n-type GaAs, AlSb and GaSb. For AlSb, where the g-values were 2.041 and 2.005, respectively, partially resolved Al hyperfine structute was observed. They concluded that the unpaired electron had 5% Al character in an orbital with 90% p-character. From computer simulations of the ESR, they concluded that g- and A-axes were not necessarily coincident. Their results were not inconsistent with an Al–O–O angle of between 120° and 130°. The g-values were interpreted using the equations derived for O_2^- in KCl by Känzig and Cohen [108].

In a molecular orbital calculation using an SCF–INDO method, Biskupič and Valko [94] calculated g-values for the HO_2^- radical. They found the

maximum g-value to be along the O–O direction but to have its least value when the H–O–O angle was 111°, corresponding to the configuration where the energy was a minimum.

To explain the results for O_2 trapped by surfaces, formation of O_2^- has often been assumed (see Table 9). Exceptions appear to be peroxy radicals where the view is much more that of the formation of a σ-bond involving one of the oxygen π^* orbitals spin paired with a p-orbital on the substrate while the ESR is due to the other π^* orbital already present on the oxygen molecule.

G. OXYGENATION OF IRON(II) AND COBALT(II) PROTEIN COMPOUNDS

(i) Hemoglobin

Since a number of studies of the oxygenation of cobalt(II) chelates are thought to serve as model systems for hemoglobin it is as well to consider some aspects of the properties of this important compound. The globular protein has four protein subunits each of which has an iron protoheme group. Two of the four units have the same amino acid sequence and are designated as α chains, the other two are termed the β chains. The α chain possesses 141 amino residues while the β chain has 146. Each heme group is embedded in a crevice in the globin such that the two propionic acid groups emerge from the surface of the protein which is packed tightly with side chains of the amino acids forming dispersion forces bonding with each other and the heme group. The multiple contacts with the heme form a hydrophobic environment and control the orientation of the heme plane while guarding access to the oxygen binding site such that even oxygen is admitted with some difficulty. The multiple heme-globin contacts include the proximal (F8) and distal(E7) histidines and the invariant residues phenylalanine (CD1) and leucine (F4). Position (E11) is always occupied by valine or the structurally similar isoleucine. In general terms the heme group can be regarded as being suspended between the F and E helices with bonding of the proximal (F8) histidine to the iron of the heme group and the leucine (F4) forming a hydrophobic bond with the heme. Distally, the heme is maintained in its plane by phenylalanine (CD1) which also guards the ligand site along with histidine (E7) and valine (E11). The replacement of any of these amino acids has a profound effect on the whole molecule. The γ_2 methyl of valine (E11) is in van der Waals contact with the porphyrin only in the β subunit of deoxyhemoglobin, where it overlaps the van der Waals radii of heme ligands, so that the heme pocket must widen before ligands can bind. Thus a marked widening of the heme pocket occurs on combination of oxygen with the β subunits but little change occurs in the α subunits.

The assembly of the α and β chains of hemoglobin into the $\alpha_2\beta_2$ tetramer results in the quaternary structure with a markedly lower affinity for oxygen compared with the isolated chains. Interactions between the assembled subunits are propagated to the heme sites in a manner which reduces the oxygen affinity by a factor of about 1/250 for the first oxygen bound [144]. This reduction in affinity is generally believed to be the result of constraints imposed at the heme sites as a result of subunit interaction. As additional oxygen molecules are bound these constraints are altered in such a way that affinities are increased, until at the last step the affinity more nearly approximates that of the isolated chains. An effect of the opposite kind has been observed in chains of β hemoglobin such that interactions between the assembled subunits are propagated to the heme sites such that there is an enhancement of affinity for oxygen [145]. The cooperative mechanisms arise from the small difference between larger energetic quantities, and it is possible that the enhancement effects may be critical in the final stages of oxygen binding by the hemoglobin tetramer [146].

A possible explanation of the trigger mechanism which sets off the conformational changes with the protein suggests that spatial changes occur within the heme group such that combination of the iron with molecular oxygen results in a movement of the iron atom and of the heme linked histidine (F8) relative to the plane of the porphyrin, caused by the electronic transition in the iron on going from the five coordinated high-spin deoxyhemoglobin to the six coordinated low-spin oxyhemoglobin, which will involve some electronic redistribution between the iron and oxygen molecule. The acquisition of molecular oxygen by hemoglobin, which does not appear to involve a large difference in the bonding affinity between the α and β subunits, has been explained in terms of the existence of two conformational states of the hemoglobin tetramer. There is a tense (T) state in which the heme groups have a low affinity for ligand and a relaxed (R) state in which the heme groups have a high affinity for ligand. It is the concerted structural transition from the low affinity state to the high affinity state that is responsible for the observed sigmoidal rather than hyperbolic ligand saturation curve. Reaction with ligand alters the allosteric equilibrium between the two alternative stable quaternary structures of mammalian hemoglobin which is thought to involve two distinct subunit interaction processes by changing the distance of the proximal histidine from the plane of the porphyrin ring and by the direct steric effect of the ligand on the β subunits.

The molecular changes which occur on deoxygenation involve structural changes at the $\alpha_1\beta_1$ contact face due to a sliding rotation of the $\alpha_1\beta_1$ dimer with respect to the $\alpha_2\beta_2$ dimer which causes a structural change at the $\alpha_1\beta_2$ contact. The rotation occurring at the $\alpha_1\beta_2$ junction on deoxygenation

produces a widening of the gap between the two β chains in the central axis of the molecule. The opening of this gap allows the entry of a molecule of 2,3-diphosphoglycerate (2,3-DPG), which results in a strengthening of the deoxy configuration. With the loss of the first oxygen molecule, possible from α chain, the iron changes from low to high spin and moves out of the plane of the heme. In doing so it presses on the F helix, opening a gap between the F and H helices. In deoxyhemoglobin this gap is of the appropriate dimensions to accept the aromatic side chain of tyrosine HC2, the second to last amino acid of both the α and β chains. The nc̃ -helical terminal portion of the globin which has been free to take up random positions in oxyhemoglobin is fixed in the deoxygenated subunit by the bonding of the penultimate tyrosine. This also fixes the terminal arginine of the α-subunit, a change resulting in the formation of salt bridges. Therefore from the time of loss of the first oxygen, changes occur which favour the switching of the molecule to the T conformation. Deoxygenation of the next subunit will similarly result in fixation of its penultimate tyrosine with the potential formation of salt bridges. At a critical stage, which may vary from molecule to molecule, a conversion to the T conformation will occur which involves the sliding rotation about the $\alpha_1\beta_2$ interface with a widening of the space between the β chain. 2,3-DPG enters this space, its phosphate groups forming three ionic bonds with the positively charged side chains on each of the two β chains. The most critical adjustments to the oxygen supply accrue from changes in the 2,3-DPG concentration which provide a subtle and long-term means of controlling the efficiency of oxygen transport. Inositol pentaphosphate plays a similar role in avian red cells. Other organic anions have been shown to interact with deoxyhemoglobin through electrostatic interactions which lower its oxygen affinity. The isolated dimers bind oxygen non-cooperatively and with the same affinity as the isolated α and β chains. The effects of organic phosphates on the functions of hemoglobin oxygenation have been reviewed [147]. Using pulse radiolysis techniques on phosphate stripped methemoglobin, it has been shown that the heme-iron in a single subunit within the tetramer is reduced to iron(II). The valence hybrid thus formed reacts with oxygen. The results support the description of stripped methemoglobin as residing in an R state. In the presence of inositol hexaphosphate the methemoglobin is stabilized in a T state but it switches to a high affinity state when the pH is raised above pH 8.0. This structural transition was not found to coincide with the switch of spin state of the heme iron that accompanies the ionization of water in aquomethemoglobin [148].

Detailed accounts of the structure and function relationships in oxy and deoxy hemoglobin have been given [149–152] while the mode of action of the allosteric effecting protons, chloride, carbon dioxide and 2,3-DPG has been outlined [153]. This description of the oxygenation process which stems

from X-ray crystallographic studies projects the view of a protein structure able to undergo few structural changes. However, in the solution environment it has been pointed out that in general proteins experience structural fluctuations on the nanosecond time scale which permit the diffusion into their structures of small molecules such as dioxygen and carbon monoxide [154,155]. Measurements of the transient optical anisotropic decay and triplet lifetime quenching of the protoporphyrin IX in myoglobin by dioxygen and carbon monoxide support the model of a protein in solution as one with fluctuating conformations, and show the small gas molecule is able to enter a region near the binding site at a solvent diffusion-limited rate [156,157]. Myoglobin which may be non-spherical in solution is thought to possess intermediate reaction path wells which do not seem to be directly sensitive to heme modifications but instead are related to other parts of the protein [156]. Within the protein, dioxygen experiences barriers of about equal height and moves smoothly toward the binding site. An important barrier is the narrow entrance to the pocket. Having finally reached the heme, binding by the iron and possibly the distal histidine occurs [158].

Measurements of the heme structure of photo-deligated hemoglobin by picosecond time-resolved Raman resonance spectroscopy, shows that the oxygen affinity of hemoglobin depends on the integrity of the protein structure such that the protein plays its part by acting directly on the charge of the iron atom and does not affect the geometric state of the heme and in turn the protein relaxation process should be influenced by the structural and electronic state of the heme [159]. Recent findings based on the extended X-ray absorption fine structure (EXAFS) spectra show that the distortions of structure associated with the oxygenation of the heme in deoxyhemoglobin are transmitted through general changes of the heme rather than being localized to a simple driven motion of the iron atom [160]. This is in keeping with an earlier description of the heme–heme interactions in hemoglobin as distributed among many degrees of freedom of the protein and not in the relatively rigid heme such that the strain energy due to oxygenation tends to be stored primarily in the weaker binding region of the hemoglobin assembly [161,162]. Chemical modifications of the side chains of the prosthetic group cause significant changes in the oxygen binding properties of hemoglobin and myoglobin. A study of the effect of chemical modification, particularly of the vinyl groups, on oxygen and carbon monoxide bonding to myoglobin has been made by comparison with oxygen-binding by apo-myoglobins reconstituted with different hemes with various side chains [163].

The laser flash-photolysis experiments on these reconstituted myoglobins show that the combination rate constants for oxygen and carbon monoxide are closely related to the electron attractive properties of the side chains

[164]. The rate constants tend to increase as the electron-withdrawing power of the side chains increases indicating that reduced electron density of the iron atom of the heme favours the combination reaction for both oxygen and carbon monoxide. In general terms the ligand binding for the "on" reaction depends largely on σ bonding while in the "off" reaction disruption of π bonding is more important.

Proton nuclear magnetic resonance studies of hemoglobin M. Milwaukee, a naturally occurring valence hybrid containing two permanently oxidized hemes on the β chains are consistent with a sequential model for the oxygenation of this mutant hemoglobin. In view of the similarities between normal adult hemoglobin and HbM Milwaukee it has been suggested that a two-state concerted allosteric model does not provide an adequate description of the structure function relationships in normal hemoglobin [165]. Raman difference spectroscopy measurements on native and chemically modified human deoxyhemoglobins indicate that the free energy of cooperativity for a variety of ligated proteins follows the same order as that of the degree of charge depletion of the π^{*} orbitals upon ligation as determined from the frequency of a Raman mode. The electronic interaction between the protein and the heme could result in energies large enough to provide a significant contribution to the energetics of hemoglobin cooperativity. The electronic interaction arises from heme–aromatic residue interactions which affect the charge density of the antibonding orbitals.

An interesting aspect of the dimeric myoglobin isolated from the radular muscle of the gastropod, Nassa mutabilis, is that oxygen equilibrium curves show that the myoglobin (M.W. 28000 $\pm$ 1000 daltons) binds oxygen cooperatively with an interaction coefficient 1.5, without any Bohr effect [166]. The values of the oxygen affinity constants are $K_1 = 0.142$ and $K_2 = 0.317 p_{O_2}^{-1}$. Oxygen partial pressure at half saturation is 4.7 mm Hg. More detailed structural studies of the cooperative effects in this oxygen binding protein might well help to unravel the more complicated sequence of events which occur in hemoglobin.

(ii) Coboglobin

In order to shed light on the nature of the hydrophobic pocket of the protein as well as on other aspects of the oxygenation process the expedient of substituting the iron atom of the prosthetic group by cobalt(II) to form coboglobins has made possible a number of measurements, particularly those involving ESR spectroscopy on the deoxy and oxy forms. The introduction of cobalt instead of iron into the heme decreases the stability of the T structure relative to that of FeHb [167]. This partially destabilized T structure allows the R/T transition to occur between the second and third

ligation steps [168]. It is interesting to note that cobalt is not incorporated into protoporphyrin formed in hepatocytes incubated in the presence of the metal [169]. The major conclusions of other studies are summarized in Table 10. The opportunity to confirm the influence of the distal histidine group on the binding of molecular oxygen is presented by those proteins where either the distal histidine group is replaced by some other amino acid residue or where the distal group is absent. The former possibility is realized by monomeric hemoglobin Glycera where the distal group is replaced by a leucyl residue while the latter circumstance is presented by myoglobin Aplysia which possesses only one histidine group. Turning to the results of substitution of the iron in hemoglobin by cobalt(II) some prospects of unravelling the complicated effects due to interactions between the subunits arise from a study of cobalt(II) substitution into the individual α and β chains. The opportunity to measure the effect of the distal histidine on oxygen binding by the cobalt derivative of hemoglobin is made possible by a study of the molecular oxygen complex of cobalt(II) substituted hemoglobin Zürich where the distal histidine in the β subunits is replaced by arginine which is thought to have an effect on the entrance of ligands into the heme pocket. The parameters associated with the ESR spectra due to a range of coboglobins derived largely by recalculations from published spectra are summarized in Table 11.

Chien and Dickinson [101,107] have reported the results of two studies of the ESR of oxygenated cobalt substituted myoglobin ($CoMbO_2$). The first of their papers focused on the g- and A-values at $-195°C$ for two different sites. Their recent study was particularly concerned with use of O^{17} enriched oxygen and this has aided the elucidation of likely structural models for the two centres. The more abundant centre (I, 60%) has equivalent oxygen atoms where the O^{17} hyperfine constants are 12, -72.5 and 60 G, along, ζ, ξ and η, respectively. Spin densities on cobalt d-orbitals are calculated by them to be -0.02 (d_{yz}) and 0.09 (d_{yz}). (Figure 13 compared with Fig. 12 shows that x and y must be interchanged.) The orientation of the various tensors is not precisely determined but the O–O projection bisects N_2–Fe–N_3 and is parallel to the imidazole group of histidine F8. The oxygen hyperfine constants were temperature dependent. Figure 13, adapted from Figs. 5(a) and 5(c), and Table 2, of the paper by Dickinson and Chien, summarizes their proposed model for centre II. The oxygens are not equivalent for centre II and the oxygen hyperfine constants are 5, -67.5 and 22.4 G and 5.4, -83.3 and 30.3 G respectively. Orbital spin densities, based on both O^{17} and cobalt h.f.s. are $O_\alpha(p_\eta) = 0.48$, $O_\alpha(p_\zeta) = -0.11$, $O_\beta(p_\eta) = 0.74$, $O_\beta(p_\zeta) = -0.16$, $Co(d_{xz}) = -0.01$ and $Co(d_{yz}) = 0.06$. These results lead to a total spin density of 1.01. It is concluded that the O–O axis points towards histidine E7, suggesting possible hydrogen bonding interactions, and that the

TABLE 10

Studies of the oxygenation of coboglobins

Compound and type of experiment	Conclusions of the investigations	Ref.
1. Measurement. Oxygenation of artificial myoglobins and hemoglobins containing cobalt(II) proto- meso- and deutero porphyrins. Equilibrium measurements and thermochemical parameters.	1. Partial pressure of oxygen at half-saturation ($p_{0.5}$) value of CoMb 50–100 times greater than corresponding Fe compounds 2. Variation of $p_{0.5}$ with temperature is stereochemical rather than electronic 3. Protoporphyrin is required for a minimal oxygen affinity but maximal coperativity in CoHb 4. Metal substitution is primarily enthalpic whereas the effect of the apoprotein binding on oxygen affinity of cobalt(II) porphyrins is essentially entropic 5. The substitution of cobalt(II) for iron(II) results in decreased O_2 affinity related mainly to a decrease in heat of reaction	a
2. Temperature jump relaxation measurements on oxygenation of Co(II)-Mb and Co(II)Hb.	1. Association rate constant, k_{on} for Co(II)Mbs in the same order of magnitude as those for Fe(II)Mbs whereas k_{off} values about 10^2 times greater than those for the corresponding Fe(II)Mbs 2. Kinetics of oxygenation reactions of Co(II)Mbs in the same range as typical enzyme-substrate association-dissociation reactions	b
3 Oxygen equilibrium measurements on α and β subunits each containing cobalt(II). ESR characteristics of the subunits in deoxy and oxy states.	1. Oxygen affinity of the individual chains higher than tetrameric CoHb and independent of pH 2. Rates of oxygenation similar to those reported for iron(II) α and β chains whereas deoxygenation 10^2 times larger 3. ESR of oxy α chain shows distinctly narrowed hyperfine structure in comparison with oxy β chain indicating different environments around the paramagnetic centre 4. Inequivalences between α and β chains might exist near the distal histidine group	c
4. ESR of oxy CoHb.	Formation of a hydrogen bond between the bound oxygen and the distal histidine group	d
5. X-ray structural analysis of deoxy Co(II)Mb.	Cobalt(II) mesoporphyrin lies in a hydrophobic crevice of the apoprotein similar to iron porphyrin	e

TABLE 10 (continued)

Compound and type of experiment	Conclusions of the investigations	Ref.
6. Raman resonance spectra of oxy and deoxy.	Tension imposed on the cobalt porphyrin by the globin results in little distortion of the metal-porphyrin moiety from its unconstrained geometry	f
7. ESR measurements on oxy CoMb and cobalt form of monomeric Glycera hemoglobin. Oxygen equilibrium studies.	1. Confirmation that the hydrogen bond is formed between the bound oxygen and the distal histidyl group in CoMb 2. The orientation of the bound oxygen in CoHb(Glycera) is different from that in CoMb 3. The oxygen affinity, the light absorption and ESR spectrum of CoMb affected by pH changes 4. Oxygen affinity of CoHb(Glycera) is about 50 times lower than CoMb attributed to large k_{off} value for CoHb(Glycera)	g
8.(a) Oxygen affinity of CoHb Zürich. ESR measurements of oxy and deoxy forms. 8.(b) Similar study on CoHb(Rainer).	1. Oxygen affinity of CoHb(Zürich) higher, cooperativity smaller than that of CoHb·A. 2. Hydrogen bond between the distal amino acid residue and bound oxygen is not formed in the abnormal β subunits 3. ESR of Co(II)Hb(Zürich) similar to that of Co(II)Hb·A 4. Electronic structure of the normal α subunits in CoHb(Rainer) is different from that of CoHb·A	h(1), h(2)
9. ESR measurements on oxy cobalt Mbs(Aplysia) Photodissociation measurements. Equilibrium and kinetic measurements.	1. In oxy CoMbs(Aplysia) the bound oxygen interacts with amino acid adjacent to it, the interaction is weaker than in oxy CoMb (Sperm whale) 2. k_{on} for oxygenation of proto-CoMb (Aplysia) order as proto-FeMb(Aplysia), k_{off}CoMb(Aplysia)>k_{off}FeMb(Aplysia) by three orders of magnitude	
10. ESR measurements on hybrid hemoglobins $\alpha(Co)_2\beta(Fe)_2\alpha(Fe)_2$ $\beta(Co)_2$ protoporphyrin IX.	1. Different ESR spectra for $\alpha(Co)_2\beta(Fe)_2$ and $\alpha(Fe)_2\beta(Co)_2$ showing different environment of oxygen bound to cobalt. 2. Comparison of ESR spectra with that of deoxy CoHb suggests that the electronic state of cobalt(II) in deoxy $\alpha(Co)_2\beta(Fe)_2$ exists in the α subunits of deoxy Hb 3. Ligation in the β subunits changes greatly the electronic state of metal in the α subunit which in turn contributes to the alkaline Bohr effect	

TABLE 10 (continued)

Compound and type of experiment	Conclusions of the investigations	Ref.
11. PMR measurements on the subunit interaction in iron–cobalt hybrid hemoglobins in deoxy and oxy form.	1. PMR spectral data of the α subunits in deoxy CoHb as well as deoxy $\alpha(Co)_2\beta(Fe)_2$ are different from those of $\beta(Co)_2$ subunits 2. Substantial electron spin delocalization from the cobalt(II) ion to bound oxygen 3. State of the prosthetic groups in the isolated chains differs from those in tetrameric Hb 4. The electronic structure of the prosthetic groups in deoxy-α subunits is more closely related to the state of the quaternary structure of the Hb molecule than in the deoxy β subunits	k
12. ESR measurements of single crystal oxy Co(Mb). and deoxy Co(Mb).	1. About 1/2 to 2/3 of unpaired electron density is transferred to oxygen when protein is oxygenated 2. There are two paramagnetic species in oxy CoMb having identical g tensors but different A^{Co} tensors 3. Results consistent with the model for oxy-hemoglobin proposed by Griffith (J.S. Griffith, Proc. Roy. Soc. Ser. A, 235 (1956) 23), i.e. a parallel π-bonded structure	l(1), l(2)
13. ESR and Raman circular dichroism resonance measurements on copper(II) protoporphyrin IX as reporter group for heme environment in myoglobin.	1. Packing of the amino acid side chains around the porphyrin is different than on metamyoglobin 2. Copper(II) is five coordinate, probably through coordination to the F-8 proximal histidine with no appreciable distortion from square-planar solution conformation	m

[a] T. Yonetani, H. Yamamoto and G.V. Woodrow, J. Biol. Chem., 249 (1974) 682.

[b] H. Yamamoto, F.J. Kayne and T. Yonetani, J. Biol. Chem., 249 (1974) 691.

[c] M. Ikeda-Saito, H. Yamamoto, K. Imai, F.J. Kayne and T. Yonetani, J. Biol. Chem., 252 (1977) 620.

[d] T. Yonetani, H. Yamamoto and T. Iizuka, J. Biol. Chem., 249 (1974) 2168.

[e] E.A. Padlan, W.A. Eaton and T. Yonetani, J. Biol. Chem., 250 (1975) 7069.

[f] W.H. Woodruff, D.H. Adams, T.G. Spiro and T. Yonetani, J. Am. Chem. Soc., 97 (1975) 1695.

[g] M. Ikeda-Saito, T. Iizuka, H. Yamamoto, F.J. Kayne and T. Yonetani, J. Biol. Chem., 252 (1977) 4882.

[h] (1) M. Ikeda-Saito, M. Brunori, K.H. Winterhalter and T. Yonetani, Biochim. Biophys. Acta, 580 (1979) 91. (2) T. Yonetani, H. Yamamoto, G.V. Woodrow, J. Biol. Chem., 249 (1974) 682.

334

TABLE 10 (continued)

[i] M. Ikeda-Saito, M. Brunori and T. Yonetani, Biochim. Biophys. Acta, 533 (1978) 173.
[j] M. Ikeda-Saito, H. Yamamoto and T. Yonetani, J. Biol. Chem., 252 (1977) 8639.
[k] M. Ikeda-Saito, T. Inubushi, G.G. McDonald and T. Yonetani, J. Biol. Chem., 253 (1978) 7134.
[l] (1) J.C.W. Chien and L.C. Dickinson, Proc. Natl. Acad. Sci. U.S.A., 69 (1972) 2783. (2) L.C. Dickinson and J.C.W. Chien, Proc. Natl. Acad. Sci. U.S.A., 77 (1980) 1235.
[m] K. Alston and C.B. Storm, Biochemistry., 18 (1979) 4292.

O–O projection approximately bisects N_1–Fe–N_3. There is a surprise, however, in that the x axis for cobalt h.f.s. due to $CoMbO_2$ is tilted away from the heme normal by $28°$ in contrast to CoMb where the same angle is $1-2°$. The resulting Co–O–O bond angle is found to be $120°$.

In comparing the results for sites I and II, Dickinson and Chien conclude that the O–O directions are at right angles to one another. A significant puzzle remains. Preliminary X-ray results indicate only *one* type of centre at $-16°C$ [170].

The signs of cobalt h.f. constants are all assumed to be negative and the analysis of the h.f.s. makes it clear that $Co(d_{z^2})$ orbitals are not significantly involved.

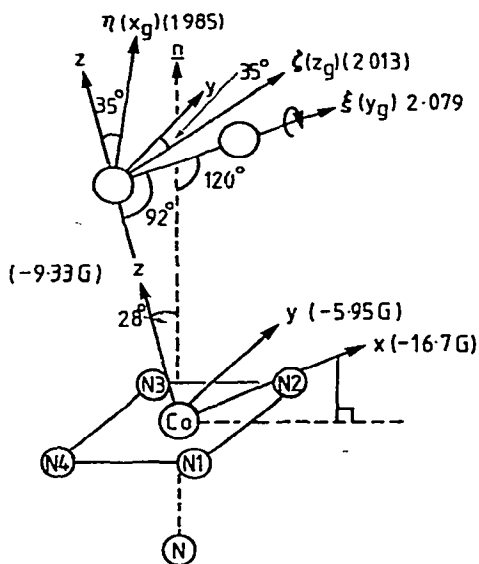Fig. 13. Molecular arrangement of Co–MbO_2 complex, site II adapted from Fig. 5(a) and 5(c) and information in the text of paper by Dickinson and Chien [107]. Comparison with Fig. 12 shows that x and y axes need to be interchanged.

TABLE 11

ESR parameters associated with molecular oxygen adducts of cobalt(II) porphyrins in protein pockets

Apo-protein	cobalt(II) porphyrin	Solvent conditions	g_x	g_y	g_z	$A_x(z)$ [1]	$A_y(y)$ [1]	$A_x(x)$ [1]	$\alpha°$	Ref.
						($\times 10^{-4}$ cm^{-1})				
Sperm whale Mb	MeP	H_2O	2.0123	2.0782	1.9850	5.5	21.3	8.5	18	a, Fig. 4(a)
	MeP	D_2O	2.0136	2.0790	1.9850	5.0	22.0	8.5	22	a, Fig. 4(a)
	PPIX	Phosphate buffer pH 7.0	2.0130	2.0748	1.9878	4.0	20.0	8.0	23	a, Fig. 2(a)
	PPIX	Phosphate pH 7.0	2.0127	2.0760	1.9905	5.5	19.0	7.7	23	e
	PPIX	H_2O pH 7.0	2.0027	2.0627	1.9870	5.0	20.5	8.0	23	a, Fig. 2(a)
Hb Glycera	MeP	H_2O	2.0008	2.0680	1.9778	4.0	16.5	6.8	23	a, Fig. 4(b)
Aplysia Mb	MeP	H_2O pH 7.0	2.0068	2.0885	1.9836	5.8	21.5	9.6	22	b, Fig. 2
α chain Hb	PPIX	H_2O	2.0077	2.0760	1.9870	5.0	17.8	7.9	25	c, Fig. 4
β chain Hb	PPIX	H_2O	2.0095	2.0680	1.9912	4.0	20.5	7.9	26	c, Fig. 4
Hb Zürich	PPIX	H_2O	2.0093	2.0680	1.9850	4.0	19.8	7.9	26	d, Fig. 5

[1] A-values assumed negative for hyperfine analysis.
a F.J. Kayne and T. Yonetani, J. Biol. Chem., 252 (1977) 4882.
b M. Ikeda-Saito, M. Brunori and T. Yonetani, Biochim. Biophys. Acta, 553 (1978) 173.
c F.J. Kayne and T. Yonetani, J. Biol. Chem., 252 (1977) 620.
d M. Ikeda-Saito, M. Brunori, K.M. Winterhalter and T. Yonetani, Biochim. Biophys. Acta, 580 (1979) 91.
e I.M. Ruzic, Ph.D. Thesis, Monash University, 1981.

An inspection of the results obtained from the ESR spectra due to Sperm whale apo-myoglobin containing cobalt(II) mesoporphyrin where the value of α increases from 18° to 22° as a result of replacement of the solvent, water, by deuterium oxide, could be considered support for the concept of a structural change brought about by the release of hydrogen bonding from the distal histidine group in deuterium oxide, with little change in the electronic structure of the dioxygen moiety since there is little attraction in g or A tensors. This view is strengthened by the results from Co(II)Mb(Aplysia) where the value of α is 22° and again in Co(II)Hb(Glycera) where α is 23°. However, there are important changes to the value of g_y such that it increases to 2.0885 in the molecular oxygen complex of Co(II)Mb(Aplysia) and falls to 2.068 in the molecular oxygen complex of Co(II)Hb(Glycera). This indicates that the molecular oxygen, which is sensitive to its surroundings, experiences environmental changes within these proteins.

A comparison of the results obtained from the apo-myoglobin containing cobalt(II) protoporphyrin IX with those of the protein containing cobalt(II) mesoporphyrin show that the substituent effects arising from certain regions of the periphery of the porphyrin are transmitted to the molecular oxygen moiety so as to increase the value of α and enable a discernable change in the value of g_y with little effect on the hyperfine tensors.

Turning to the results associated with the substituted hemoglobins the expected differences in the environments of the superoxo group in the α and β subunits are borne out by the significant difference in the value of g_y for the α and β subunits and though the value of α is not very different for the α and β subunits both values are higher than those found in the myoglobins. Here for the first time the values of the hyperfine tensor A_y are different. The results of the cobalt substituted hemoglobin Zürich suggest that the environment of the molecular oxygen within this protein is closely similar to one which could be experienced within the β chain of a normal hemoglobin.

In an analysis of the acid base properties of peroxidase and myoglobin it has been concluded in myoglobin ionization of the distal histidine does not influence its reactivity. The interaction of the distal base with a sixth ligand is weak in myoglobin but is strong in peroxidases [171,22]. It has been reported that horseradish peroxidase can be reconstituted with cobalt porphyrin to give a cobalt(III) haloenzyme with physico-chemical properties quite similar to those of the native iron(III) protein [172]. The cobalt(III) horseradish peroxidase can be reduced to Co(II)HRP, an analogue of iron(II) peroxidase and the reduced cobalt protein can bind dioxygen to form an analogue of oxy-iron(II) peroxidase. At pH 8.2 and room temperature the oxy-cobalt peroxidase undergoes decay to form cobalt(III) peroxidase rather more slowly than the oxyferroperoxidase ($T_{1/2}^{Co}$ 10 min, $T_{1/2}^{Fe}$ 4 min).

It has been shown recently that ruthenium(II) mesoporphyrin(IX) undergoes reversible oxygenation in dimethylformamide; the apo-myoglobin complex of the ruthenium porphyrin is oxidized reversibly by dioxygen to give $RuMb^+$ by an outer sphere electron transfer mechanism [173].

In related studies of isoelectronic species, Symons and Peterson [174,175] have investigated the ESR spectra of γ-irradiated HbO_2 and MbO_2 in frozen solutions at 77 K and MbO_2 crystals. For HbO_2 the ESR resembled that due to low spin Fe^{3+} but O^{17} hyperfine structure suggested that the two oxygens are inequivalent with considerable electron density on oxygen (0.7) and also on iron (0.3). In the single crystal study on irradiated MbO_2 it was found that the maximum g-value axis was tilted 15° away from the heme normal, well away from the O–O direction. In that case the measured g-values were 2.205, 2.114 and 1.96 respectively.

(iii) Vitamin $B_{12r}(Cbl^{II})$

That oxygen binds to Cbl^{II} and cobinamides (Cba) has long been known [176–178]. Figure 14 shows one of the early results for oxygenated Cbl^{II} in methanol at 218 K (A) and 77 K (B) while (C) is the spectrum for DMB Cba at 77 K. Curves (B) and (C) are reminiscent of oxygenated cobalt porphyrins [176] which were interpreted, by means of simulated spectra, as having a Co–O–O angle of 105° [104].

The early studies due to Bayston et al. [176] were concerned with oxygenation of Cbl^{II} in solution at low temperature. The ease with which oxygen combines with Cbl^{II} at low temperatures and in solution suggested direct addition to the cobalt atom, rather than substitution for a coordinated solvent molecule. There is no evidence to suggest that oxygen ever displaces the nucleotide. For cobinamides, with various ligands bound to the fifth position, oxygen binds with increasing difficulty for the following sequence of fifth position ligands: methanol, adenine, DMB and CN^-. In other words, the stronger the binding of the ligand at the fifth position, the weaker the oxygen binding. EPR spectra due to oxygen bound to the cobinamides [177] show two kinds of sites with obviously different coupling constants and g-values.

Recently Jörin et al. [109] have reported EPR spectra due to oxygenated Cbl^{II} in crystals of OH–Cbl (B_{12r}) and conclude from their study that the Co–O–O angle is 111° and that the Co–O–O plane is nearly at right angles to DMB. Their experiments were carried out on both OH–$Cbl^{II}(B_{12b})$ crystals doped with both B_{12r} and $B_{12r}O_2$. The spectrum due to each of the four magnetically equivalent sites consists of eight lines due, of course, to hyperfine interaction with the cobalt nucleus. At −190°C, only a single eight line spectrum is observed when the magnetic field is along either of the
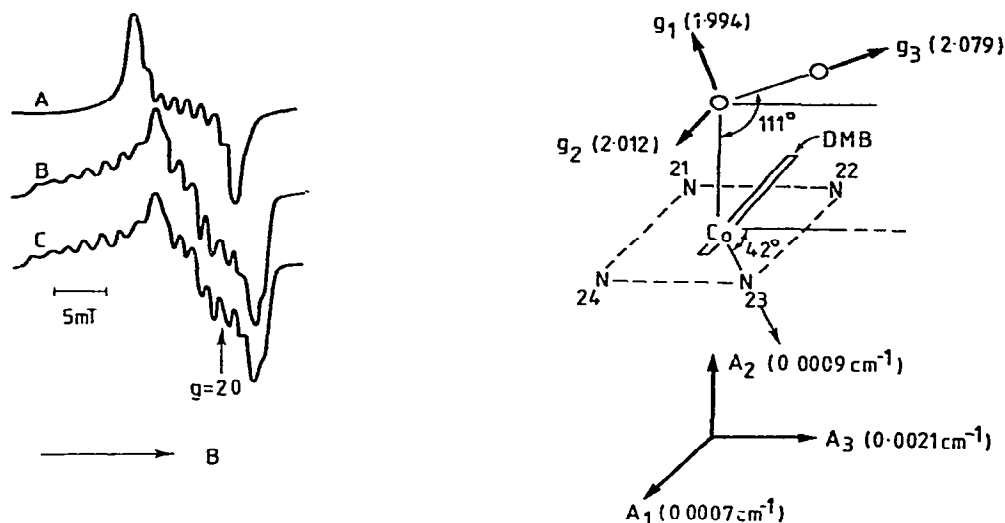
Fig. 14. (a) ESR spectrum of oxygenated B_{12r} in methanol at 218 K. (b) ESR spectrum of oxygenated B_{12r} in methanol at 77 K. (c) ESR spectrum due to oxygenated dimethyl benzimidazole cob(II)inamide in methanol at 77 K. (Reproduced from Bayston et al. [176].)

Fig. 15. Schematic representation of $B_{12r} \cdot O_2$ complex in B_{12b} crystals based on data found in article by Jorin et al. [109]. Angle between projection of g_3 and A_3 in corrin plane $= 7°$; angle between A_3 and $g_3 = 26°$; angle between g_1 and $A_2 = 15°$. Numbering of corrin nitrogens differs from that used by Jörin et al. but agrees with standard nomenclature.

crystal b or c axes, indicating that the oxygen radical is located in a single minimum potential. Figure 15 summarizes the results due to Jörin et al. [109] where the largest g-value is believed to be along the O–O direction. The symmetry of the O_2 centre is triclinic, none of the g and A axes coinciding. This is more general than the monoclinic symmetry indicated by Fig. 12 for a single angle, α, is insufficient to describe the $B_{12r}O_2$ spectra. Preliminary ^{17}O data obtained with powder samples at an oxygen pressure of 20 atm were used to argue for a $Co(III)O_2^-$ model for the $B_{12r}O_2$ centre. As the temperature is raised, the g anisotropy is reduced but the orientation of the principal axes remains unchanged.

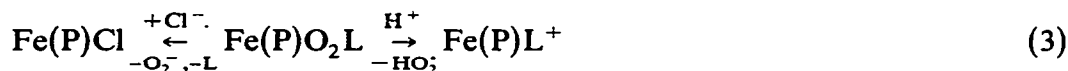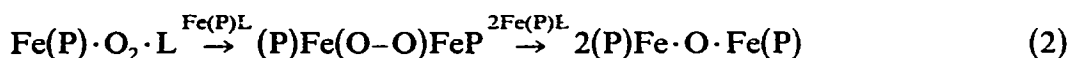## H. OXYGENATION OF METALLO-PORPHYRINS WITH SOME CONTROL OF FACIAL REGIONS

The ability of hemoglobin or myoglobin to bind oxygen reversibly may be considered to be anomalous when compared with the oxidative instability of simple iron(II) compounds in the presence of oxygen and water [179]. The advantages possessed by the protein include the following:

(a) The existence of a hydrophobic pocket around the iron porphyrin site which retards oxidative electron transfer from iron to oxygen in the non-polar environment. About 3% of the circulating hemoglobin of an adult person is oxidized each day to methemoglobin. A methemoglobin reduction system, one of the few oxidation–reduction reactions known to occur in the mature red blood cell, keeps this level of methemoglobin at less than 1% of the total hemoglobin. The reduction of methemoglobin by NADH in the red blood cell is accomplished by the following sequence:

NADH → cytochrome b_5 reduction → cytochrome b_5 → methemoglobin [180,181]
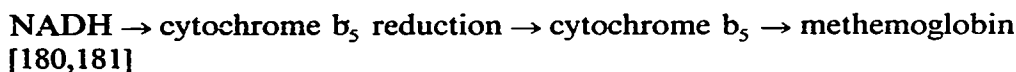
(b) The inability of the iron–porphyrin units to approach closely enough in the metalloprotein system to permit μ-oxo-dimer formation as a consequence of oxidation to the iron(III) species.

(c) The existence of an environment of low acidity, since acidic media assists in the oxidation of the iron proteins.

The oxidation of hemes to hemins in solution occurs more rapidly than the oxidation of iron in heme proteins. The iron(II) porphyrins are generally thought to be oxidized by an inner sphere mechanism the first step being coordination of the dioxygen molecule to heme iron. The second stage is the attachment of a second heme to the dioxygen ligand while the third step is the nucleophilic substitution of the superoxide ion by, for example, a chloride or proton assisted dissociation in suitable solvent conditions as follows [182,183]:
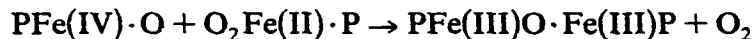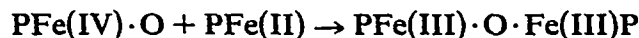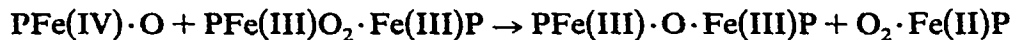
$$Fe(P)L_2 \underset{-L}{\rightleftharpoons} Fe(P)L \rightleftharpoons Fe(P)\cdot O_2\cdot(L) \tag{1}$$

$$Fe(P)\cdot O_2\cdot L \xrightarrow{Fe(P)L} (P)Fe(O-O)FeP \xrightarrow{2Fe(P)L} 2(P)Fe\cdot O\cdot Fe(P) \tag{2}$$

$$Fe(P)Cl \underset{-O_2^-,-L}{\xleftarrow{+Cl^-}} Fe(P)O_2L \xrightarrow[-HO_2^-]{H^+} Fe(P)L^+ \tag{3}$$

The steps in (3) are followed by the superoxide disproportionation reactions in protic media.

$$O_2^- + H^+ \rightarrow HO_2^- \rightarrow H_2O_2 + O_2$$

Evidence for the existence of an Fe–O–O–Fe structure at low temperatures has been presented [184]. More recently it has been shown that the reaction of a Por·Fe·O$_2$·Fe·Por compound with nitrogenous bases, yields new complexes described best as ferryl species [185]. An outer sphere oxidation process [186] can occur in the presence of a suitable proton source [187], while reaction of molecular oxygen with pyridine hemochromes is thought to

proceed by an outer sphere mechanism [188]. The participation of a ferryl species in the oxidation process has been put forward to occur as follows in non-coordinating solvents [189]:

$$PFe(III)O_2Fe(III)P \rightarrow 2PFe(IV) \cdot O$$

$$PFe(IV) \cdot O + PFe(III)O_2 \cdot Fe(III)P \rightarrow PFe(III) \cdot O \cdot Fe(III)P + O_2 \cdot Fe(II)P$$

$$O_2Fe(II)P \rightleftharpoons O_2 + PFe(II)$$

$$PFe(IV) \cdot O + PFe(II) \rightarrow PFe(III) \cdot O \cdot Fe(III)P$$

$$PFe(IV) \cdot O + O_2Fe(II) \cdot P \rightarrow PFe(III)O \cdot Fe(III)P + O_2$$

It has also been suggested that cytochrome autoxidation may proceed by an outer-sphere mechanism in water to produce a solvated superoxide ion [190]. In addition the reduction of molecular oxygen ruthenium(II) amines proceeds by a one-electron outer-sphere electron transfer process [191].

Attempts to provide a facial control of the iron porphyrin environment, which in some way offers a control of irreversible oxidation and encourages molecular oxygen adduct formation has given rise to the synthesis of a number of iron(II) or cobalt(II) porphyrins whose structures are outlined in Table 12. In the more recent studies, the synthesis of a doubly bridged oxygen carrier has been described [192]. The iron(II) porphyrin is equipped with an anthracene bridge across one face and a pyridino bridge across the other, so as to mimic the structural features of natural oxygen carrying systems. The iron(II) porphyrin in this compound forms reversibly a molecular oxygen complex at 20°C of decomposition to oxidation product with $T_{1/2}$ of 15 min in chloroform and $T_{1/2}$ of $2\frac{1}{2}$ hours in dimethylformamide.
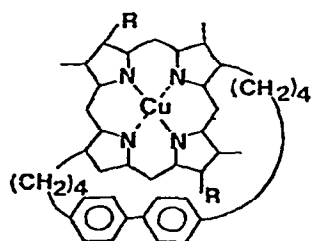
The synthesis of two forms of iron(II) "basket-handle" porphyrins having double face protection or double face protection and covalently attached imidazole has been described [193]. The iron(II) porphyrin binds reversibly nitrogenous bases and carbon monoxide [194]. The protecting chains enable molecular oxygen complexes to form and inhibit μ-oxo dimer formation as in systems described earlier [195,196]. When a dilute (5×10^{-5} M) benzene solution of the iron(II) "basket porphyrin" with covalently attached base is exposed to molecular oxygen the adduct is formed immediately and its existence has a $T_{1/2}$ of 30 min at 1 atm of oxygen.

A Raman resonance study [197] of the structure sensitive bands of the oxygenated iron "picket-fence" porphyrins has identified the iron–oxygen stretching mode at 568 cm^{-1} which is close to that obtained in oxyhemoglobin [198], thus helping to establish the similarity of the iron–oxygen bond in the protein and model compound. The relatively high frequency is consistent with a multiple bond character of the iron–dioxygen linking involving substantial π back-donation from iron(II) to O_2 with concomitant reduction in the O–O bond order to that of a superoxide. From a study of the oxygen

TABLE 12

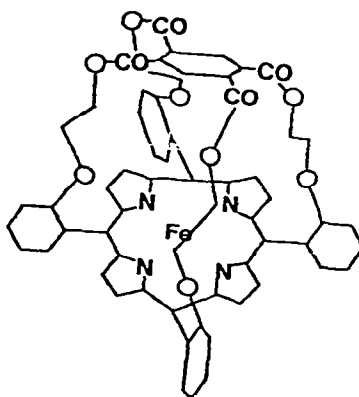Metallo porphyrin structures with some control of facial regions

1. Cyclophone porphyrin		Ref.
		a

| 2. "Capped" porphyrin "cap" and "homologous cap" porphyrin | | b(1), b(2), b(3) |

| 3. Porphyrin with covalently limited axial base | | c |
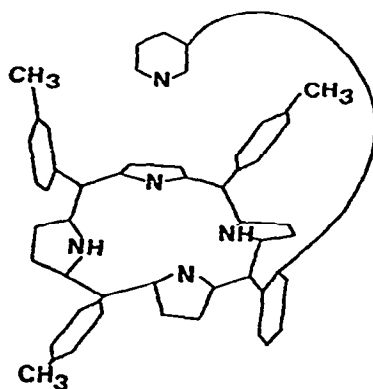
TABLE 12 (continued)

4. Double "capped" porphyrin   d
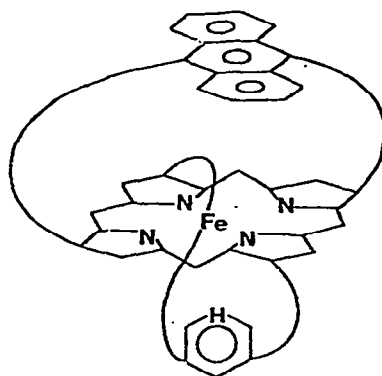
5. Strati-bisporphyrin   e
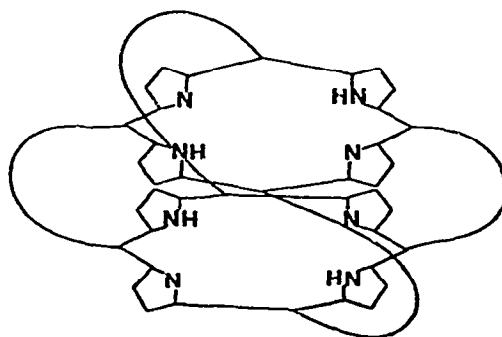
6. "Face to face" diporphyrin   f(1), f(2)
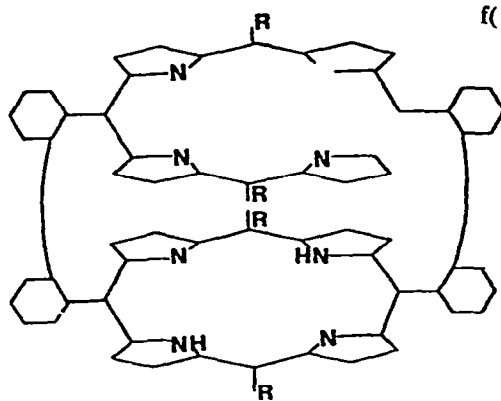
7. "Bridged" or "strapped"   g
   porphyrin

343

TABLE 12 (continued)

8. "Crowned" porphyrin

9. "Picket fence" porphyrin
   αααα, H₂TpIVPP

10. Bismetallo tetrabispyridine
    "capped" porphyrin

11. "Double" porphyrin

h

i

j

k(1), k(2), k(3)

TABLE 12 (continued)

12. Basket handle porphyrin

[a] H. Dickmann, C.K. Chang and T.G. Traylor, J. Am. Chem. Soc., 93 (1971) 4068.

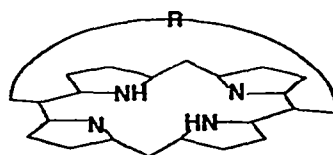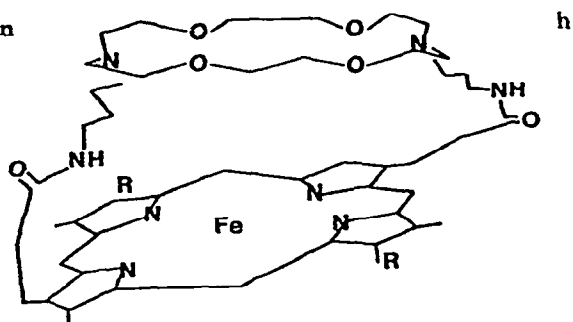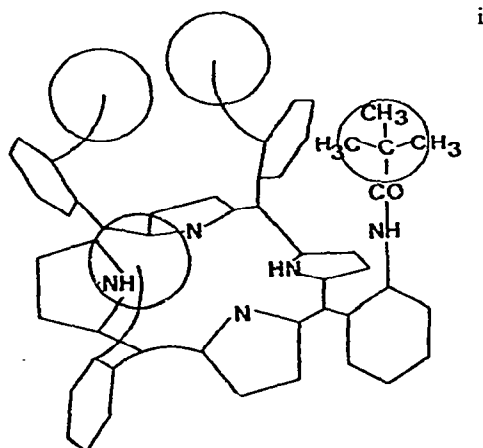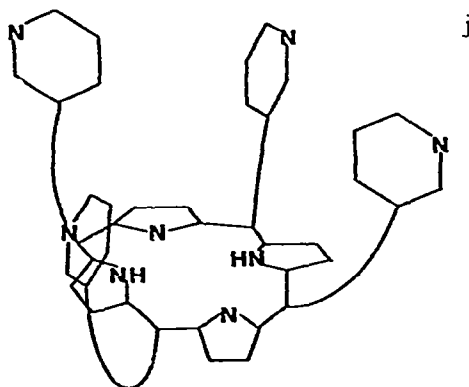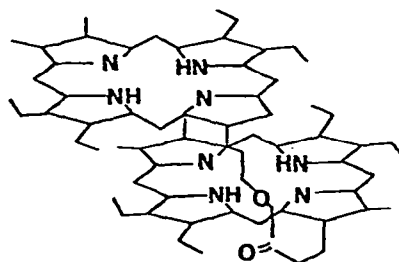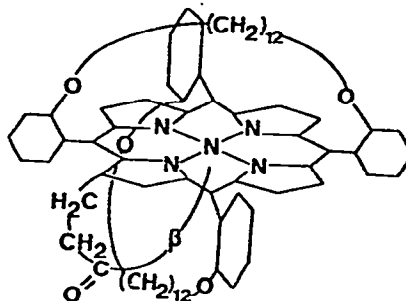[b] (1) J. Almog, J.E. Baldwin, R.L. Dyer and M. Peters, J. Am. Chem. Soc., 97 (1975) 226. (2) J. Almog, J.E. Baldwin and J. Huff, J. Am. Chem. Soc., 97 (1975) 228. (3) J.R. Budge, P.E. Ellis, R.D. Jones, J.E. Linard, T. Szymanski, F. Basolo, J.E. Baldwin and R.L. Dyer, J. Am. Chem. Soc., 101 (1979) 4762. (4) P.E. Ellis, J.E. Linard, T. Szymanski, R.D. Jones, J.R. Budge and F. Basolo, J. Am. Chem. Soc., 102 (1980) 1889. (5) J.E. Linard, P.E. Ellis, J.R. Budge, R.D. Jones and F. Basolo, J. Am. Chem. Soc., 102 (1980) 1896.

[c] F.S. Molinaro, R.G. Little and J.A. Hep, J. Am. Chem. Soc., 99 (1977) 5628.

[d] A.R. Battersby and A.D. Hamilton, J. Chem. Soc., Chem. Commun., (1980) 117.

[e] N.E. Kagan, D. Mauzerall and R.B.M. Merrifield, J. Am. Chem. Soc., 99 (1977) 5484.

[f] (1) J.P. Collman, C.M. Elliot, T.R. Halbert and B.S. Tovrog, Proc. Natl. Acad. Sci., U.S.A., 74 (1977) 18. (2) C.K. Chang in R.B. King (Ed.), Inorganic Compounds with Unusual Properties, Advances in Chemistry Series, 173 (1979) 162.

[g] (1) A.R. Battersby, D.G. Buckley, S.G. Hartley and M.D. Turnbull, J.Chem. Soc., Chem. Commun., (1976) 879. (2) J.E. Baldwin, T. Klose and M. Peters, J. Chem. Soc., Chem. Commun., (1976) 881.

[h] C.K. Chang, J. Am. Chem. Soc., 99 (1977) 2819.

[i] J.P. Collman, R.R. Cagne, T.R. Halbert, J.-C. Marchon and C.A. Reed, J. Am. Chem. Soc., 95 (1973) 7868.

[j] D.A. Buckingham, M.J. Gunter and L.M. Mander, J. Am. Chem. Soc., 100 (1978) 2898.

[k] (1) H. Ogoshi, H. Sugimoto and Z. Yoshida, Tetrahedron Lett., (1977) 169, 1515. (2) F.P. Schwarz, M. Gruterman, Z. Muljiani and D. Dolphin, Bioinorg. Chem., 2 (1972) 1. (3) D. Arnold, A.W. Johnson and M. Winter, J. Chem. Soc., Perkin I, (1977) 1643.

[l] M. Momenteau and B. Loock, J. Mol. Catal., 7 (1980) 315.

affinities for the iron"picket-fence" porphyrins and the available data on the iron proteins it has been concluded that a special interaction between the protein and bond oxygen is not needed to explain the oxygen affinities of the hemoproteins [199] and that the system provides a model for the T state of hemoglobin. Other compounds have been proposed as models for the R and T state of hemoglobin. In studies of imidazole-appended iron porphyrins, it has been concluded that the axial imidazole "tension" is of general impor-

tance in dictating electronic spectroscopic and chemical properties of heme proteins [200–203].

A comparison has been made of the thermodynamic parameters of dioxygen binding to native myoglobins and their cobalt analogues with those of iron(II) and cobalt(II) "picket-fence" porphyrins [204]. The results show constant free energies of binding, ΔG^{Fe} (25°C) for the native iron proteins and ΔG^{Co} (25°C) for the cobalt substituted analogues, an expected result for a homeostatic process where the oxygen affinity is of primary importance at the constant temperatures of the organism. Taking the data for the corresponding iron and cobalt compounds, all three of the thermodynamic quantities $\delta(\Delta G)$, $\delta(\Delta H)$ and $\delta(\Delta S)$ are quite similar for each protein, such that differences in the prosthetic group environments are equally experienced whether the metal is iron or cobalt. There appears to be an intrinsic difference between the thermodynamics of dioxygen binding by the cobalt and iron porphyrins embedded in the various apo-myoglobins such that: $\delta(\Delta H) \sim 6\,\text{kcal mol}^{-1}$, $\delta(\Delta S) \sim 12$ eu, and $\delta(\Delta G)$ 298° $\sim 2.5\,\text{kcal mol}^{-1}$. Comparisons of the values of $\delta(\Delta S)$ and $\delta(\Delta H)$ drawn from the data concerned with the oxygenation of the "picket-fence" porphyrins reveal a substantial difference in the oxygen binding environments of proteins and the model compound. The essential point is that while the values of ΔH° and ΔS° for the iron "picket fence" porphyrin are similar to those of iron proteins, the exchange makes a bigger difference in the values of $\delta(\Delta H)$ and $\delta(\Delta S)$ in the proteins than in the model compound, thus assisting in establishing a role played by the protein which does not appear in the model compound.

(i) Role of iron(II) porphyrinic materials in artificial blood

The view is sometimes expressed that the iron porphyrin compounds which have been synthesized to provide some information about important features of the binding of oxygen to the oxygen transport protein may, in addition, offer the long range biomedical prospect as substitutes for hemoglobin. Bearing in mind the wholly unpleasant effects of human congenital erythroprietic porphyria [205], and the inherent toxicities of the hemoglobin model compounds, one would have to be at death's door to allow their transfusion into the bloodstream. On the other hand considerable progress has been made in the use of stroma free modified hemoglobin and perfluorohydrocarbons as blood substitutes. A study of the intravascular persistence and oxygen delivery of pyridoxylated stroma free hemoglobin and related observations clearly indicate that this material is a leading candidate as an oxygen carrying blood substitute [206–208].

The physiological and toxicological aspects of perfluoro compounds as

TABLE 13

Polymer bound compounds capable of binding dioxygen

Metal compound bound to the polymer	Polymer matrix or polymer solution	Ref.
1. Imidazolyl-heme analogue	1. Covalent binding to poly(ethylene oxide) 2. Covalent binding to poly(ethylene oxide)—urethane copolymer	a
2.(a) Iron(II) porphyrins and Iron(III) porphyrins	Copolymers prepared from styrene and vinylimidazole or 2-phenyl-1-vinyl-imidazole—low spin adducts with iron(II) porphyrins and iron(II) porphyrins when imidazolyl groups in polymer>10 mol%. High spin when imidazolyl content <1 mol%. Oxygenation of high spin forms of iron(II) and cobalt(II) occur for coordination and covalent binding to polymer	b
3.(a) Iron(II) hematoporphyrin	Covalent binding to a peptidyl polyethylene glycol	c(1)
3.(b) Cobalt(II) hematoporphyrin	Water soluble functionalized polymers	c(2)
4. Iron(II) porphyrins	Surface particles of silica gel	d
5. Iron(II) porphyrins	Bilayer of phospholipid membrane	e
6. Iron(II) protoporphyrin(IX)	Aqueous solution of poly(vinyl-pyridine) or poly(N-vinyl-2-methylimidazole)	f–i
7. Iron(II) porphyrin	Water soluble polyphosphazenes	j
8. Cobalt(II) protoporphyrin IX dimethyl ester	1. Coordination binding to copoly-(styrene-N-vinyl-imidazole) in toluene solution	k

2.		Covalent binding to copoly-(styrenestyrylamide) in toluene solution containing *N*-ethylimidazole	
9.	Cobalt(II) protoporphyrin IX dimethyl ester	Copolymer of 4-vinylpyridine and styrene	l
10.	Cobalt(II) protoporphyrin IX styrylamide	Radical copolymerization of protoporphyrin IX styrylamide with styrene in toluene solution	m
11.	Cobalt(II) etioporphyrin	Poly(4-vinylpyridine) with pyridine base	n
12.(a)	Cobalt(II) Schiff base	Metal Schiff base formation by a polydentate amine base attached to poly(methylstyrene)	o
12.(b)	Iron(II) Schiff base		
13.	Cobalt(II) Schiff base	Poly(vinylpyridine)	p
14.	Cobalt(II) complexes with ammonia, methylamine or ethylenediamine	Cobalt(II) complex formed on Amberlyst cation exchange resin	q
15.	Trout heme	Covalently bound to sepharose or Sephadex	r
16.	Titanium(III) chloride complexes	Coordination by copolymers of 4-vinylpyridine, dioxinyl benzene and styrene	s
17.	Cobalt(II) functionalized tetraphenylporphyrin	Porous polystyrene	t
18.	Cobalt(II) compound polymerized	Polymer prepared from tetracyano ethylene and cobalt(II) acetylacetonate	u

TABLE 13 (continued)

[a] E. Bayer and G. Holzbach, Angew. Chem. Int. Ed. Engl., 16 (1977) 117.

[b] J.H. Fuhrhop, S. Beserke, W. Vogt, J. Ernst and J. Subramanian, Makromol. Chem., 178 (1977) 1621.

[c] (1) E. Bayer and G. Holzbach, Ger. Offen. 2, 645,079, Chem. Abstr., 89 48878g. (2) E. Bayer and G. Holzbach, Angew. Chem., 89 (1977) 120.

[d] O.Leal, D.A. Anderson, R.G. Bowman, F. Basolo and R.L. Burwell, J. Am. Chem. Soc., 97 (1975) 5125.

[e] I.A. Vasilenko, I.P. Radyukhin, E.I. Filippovich, G. Serebrennikova and R.P. Evstigneeva, Dokl. Akad. Nauk SSR, 241 (1978) 963.

[f] E. Tsuchida, K. Honda and H. Sata, Biopolymers, 13 (1974) 2147.

[g] E. Tsuchida, K. Honda and E. Hasegawa, Biochim. Biophys. Acta, 393 (1975) 483.

[h] E. Tsuchida, E. Hasegawa and K. Honda, Biochem. Biophys. Res. Commun, 67 (1975) 846.

[i] E. Tsuchida, K. Honda and H. Sata, Inorg. Chem., 15 (1976) 352.

[j] H.R. Allcock, P.P. Greigger, J.E. Gardner and J.L. Schmutz, J. Am. Chem. Soc., 101 (1979) 606.

[k] E. Hasegawa, T. Kanayama and E. Tsuchida, Biopolymers, 17 (1978) 651.

[l] A. Nishide, S. Hata, K. Mihayashi and E. Tsuchida, Biopolymers, 17 (1978) 191.

[m] E. Hasegawa, T. Kanayama and E. Tsuchida, J. Polymer. Sci., Polymer Chem. Ed., 15 (1977) 3039.

[n] A.V. Saritskii and N.K. Zheltukhin, Koord. Chem., 4 (1978) 591.

[o] R.S. Drago, J. Gaul, A. Zombeck and O.K. Strant, J. Am. Chem. Soc., 102 (1980) 1033.

[p] A. Misono, S. Koda and Y. Uchida, Bull. Chem. Soc. Jpn., 42 (1969) 3470.

[q] S.M. Davis, R.F. Howe and J.H. Lunsford, J. Inorg. Nucl. Chem., 39 (1977) 1069.

[r] M. Brunori, B. Giadina, S.G. Condo, G. Falcioni and E. Antonini, Biochim. Biophys. Acta, 494 (1977) 426.

[s] Y. Chimura, M. Beppa, S. Yoshida and K. Tarama, Bull. Chem. Soc. Jpn., 50 (1977) 691.

[t] L.D. Rollmann, J. Am. Chem. Soc., 97 (1975) 2132.

[u] A. Andreev, L. Prakhov, D. Shopov, N. Neshev and D. Zidarov, React. Kinet., Catal. Lett., 7 (1977) 175.

blood substitutes has been outlined [206–211]. Other studies have shown that fluorocarbon emulsions cause arteriolar constriction, vessel wall damage and blood cell aggregation in rabbits. Thus emulsions with comparatively high concentrations of fluorocarbons could be used as blood substitutes if their pharmacological effect on microcirculation can be controlled [212]. Methods of evaluating vapour pressures and the solubility of oxygen in fluorocarbons that may be used in artificial blood formulations have been outlined [213].

(ii) Polymer bound compounds capable of binding oxygen

The concept of combining prosthetic groups with polymer materials was explored by the attachment of hemin and chlorophyll structures to prepared polymers [214]. Since the early description of the reversible formation of a molecular oxygen adduct of the diethyl ester of heme embedded in a matrix of polystyrene and organic base [215,216] a number of studies have described the uptake of molecular oxygen by metal ion complexes in polymer matrices [217] as outlined in Table 13. The metal chelate group is either covalently attached to the polymer structure or as illustrated by the binding of cobaloxime, a vitamin B_{12} model, coordinatively bound by the nitrogeneous base of the polymer structure [218].

I. OXYGENATION OF COBALT(II) PORPHYRINS

Since the iron(II) protoporphyrin (IX) plays a fundamental role in oxygen binding by the oxygen transport and storage proteins in mammalian physiology studies of the oxygenation of iron(II) and cobalt(II) porphyrins acquire a particular importance. It has been shown that the natural heme prosthetic group is able to bind molecular oxygen reversibly in solution in the absence of the apoprotein or covalent linkage of any grouping provided suitable chemical and physical conditions prevail [219]. A number of aspects which concern the oxygenation process of cobalt porphyrins such as axial ligand interactions [220], stereochemistry of low-spin porphyrins [221–223], ESR and spectroscopic properties of the oxygen adducts [224–226], thermodynamics [227,228] and kinetics [229] of oxygen binding to cobalt(II) porphyrins, have been reviewed recently [230]. Generally, the 1:1 complexes of the form $B \cdot Co \cdot P \cdot O_2$ are stable at low temperatures and are formed rapidly. The formation constants of the adducts in polar aprotic solvents are much higher than in toluene solution. The instability of the 1:1 complex at room temperatures is due to the influence of an unfavourable entropy contribution to the free energy of formation. Molecular oxygen complex formation by the cobalt(II) chelate of protoporphyrin IX dimethylester in

TABLE 14

ESR Parameters for some cobalt porphyrin O_2 adducts [1]

	g_x	g_y	g_z	$A_x(z)^2$ $(10^{-4} cm^{-1})$	$A_y(y)^2$	$A_z(x)^2$	α^o	$A(x_g)$	$A(y_g)$	Ref.
$\alpha\beta\gamma\delta$-Co·TCPP·O_2 in CHCl₃/MeOH	2.005	2.086	1.987	12	22	12	27	14.6	20.3	a
$\alpha\beta\gamma\delta$-Co·TCPP·O_2 in pyridine	2.007	2.080	1.991	7.8	16.5	6.5	26	10.1	15.2	a
$\alpha\beta\gamma\delta$-Co·pMeO·PP·O_2 pyridine	2.004	2.079	1.987	6.0	19.0	7.0	25	9.7	17.4	a
	$g_\perp 2.002$	$g_{\parallel} 2.079$		$A_{\parallel} 16.6$	$A_\perp 10.7$		0			b
CoPPIXDiMe·ester·O_2 pyridine	2.004	2.079	1.987	5.0	16.7	7.5	35	10.4	15.4	a
	$g_\perp 1.99$	$g_{\parallel} 2.08$		$A_{\parallel} 17.5$	$A_\perp 9.0$		0			c
CoTPP·O_2	1.993	2.09	1.959	28	9	14	25	26.9	20.0	a
	1.998	2.05	1.993	27	12	28	0			d
CoTPPS·O_2	1.998	2.088	1.997	8	22	16	15	9.5	21.4	e

[1] Re fitting errors–see Table 8.

[2] A-values assumed negative for hyperfine analysis.

[a] R.L. Lancashire, Ph.D. Thesis, Monash University, 1976.

[b] F.A. Walker, J. Am. Chem. Soc., 92 (1970) 4235.

[c] B.M. Hoffman and D.H. Petering, Proc. Natl. Acad. Sci., U.S.A., 67 (1970) 637.

[d] B.B. Wayland, M.E. Abd-Elmageed and L.F. Meline, Inorg. Chem., 14 (1975) 1456.

[e] J.A. de Bolfo, T.D. Smith, J.F. Boas and J.R. Pilbrow, J. Chem. Soc., Dalton Trans., (1976) 1495.

the presence of 2-(methylthio)ethanol or mercaptoethanol in toluene solution has been described [231], while more recently the ESR spectra due to the molecular oxygen complex of tetraphenylporphyrinato (Co II) in the presence of thiophene has been reported [232]. The oxygenation of the more rarely encountered cobalt(II) carboranyl porphyrinates in the solid state, non-aqueous and aqueous solution has been outlined [233].

A study of the oxygenation of the cobalt(II) chelate of tetraphenylporphyrin tetrasulphonate (Co(II)TPPS) shows that the addition of N,N-dimethylformamide or dimethyl sulphoxide to aqueous solutions of Co(II)TPPS results in a disaggregation of the metalloporphyrin and provides conditions for its oxygenation [234]. Additions of ethanol lead to formation of a monomeric six coordinate cobalt(II) porphyrin which does not undergo a reaction with molecular oxygen to any great extent. On long storage in air, Co(II)TPPS in the solid state forms a complex with molecular oxygen. The magnetic parameters associated with the ESR spectrum due to the molecular oxygen adduct are given in Table 14. The ESR spectrum of the molecular oxygen adduct of $\alpha,\beta,\gamma,\delta$-tetra($p$-carboxyphenyl)porphyrinato cobalt(II) (Co(II)TCPP) formed in chloroform/methanol and pyridine solutions as outlined previously [235], gives the magnetic parameters outlined in Table 14 which contains similar information for the oxygen adducts of $\alpha,\beta,\gamma,\delta$-tetra($p$-methoxyphenyl)porphyrinato cobalt(II) (Co(II)MeO · PP), the cobalt(II) chelates of porphyrin IX dimethyl ester (Co(II)PPIXDiMeester) and $\alpha,\beta,\gamma,\delta$-tetraphenylporphyrin (Co(II)TPP). Marked changes in the ESR spectra due to the molecular oxygen adduct of Co(II) · MeOPP in the presence of various heterogenous bases have been reported to take place [234]. (A cursory examination of the ESR spectra reported as Figs. 4 and 5 of [224] indicate that for the A values quoted to be of the correct order of magnitude the field scales are apparently out by a factor of two in both cases, one by ca. 1/2, the other by ca. 2.)

J. OXYGENATION OF COBALT(II) SCHIFF-BASE CHELATES

The molecular oxygen complexes of cobalt(II) Schiff base chelates assume an historical importance in the development of understanding of the formation of such complexes. The electronic structures of cobalt(II) Schiff base chelates, which are of interest in the oxygenation process have been described [236]. Recently it has been shown that substituent groups on the Schiff base ligand as well as the base present in solution of the cobalt(II) Schiff base chelate have some influence on the magnetic parameters associated with the ESR spectra due to the molecular oxygen complexes [237]. The structural variations used in this investigation are shown by Structure 2. A further structural variation is possible by the use of different bases added to

TABLE 15

ESR parameters for some cobalt Schiff's base O_2 adducts[1]

Ligand	g_x	g_y	g_z	$A_x(y)$[3]	$A_y(Z)$[3]	$A_z(x)$[3]	$\alpha°$	$A(x_g)$	$A(y_g)$	Ref.
salen	2.081±0.002	2.010±0.005	1.990±0.002	19±1	7.3±0.5	7.5±0.5	28±1	11.0	17.0	a
salpd	2.081	2.010	1.990	18	7.3	7.5	28			a
salpn	2.081	2.010	1.990	19	7.3	7.5	28			a
αMe-salen	2.081	2.010	1.994	20.5	7.0	10.0	30	12.0	18.0	a
αEt-salen	2.081	2.010	1.994	20.5	7.0	10.0	30			a
3OMe-salen	2.083	2.008	1.996	20.0	11.4	8.0	25	13.4	18.7	a
salen[2]	2.083	2.008	1.996	20.0	11.4	8.0	25			a
t-salen in DMF	2.077	2.014	2.002	21	12	11	0±10			b
t-salen in pyridine	2.086	2.001	2.003	20	7	14	15±5			b

[1] Hyperfine constants are in units of 10^{-4} cm^{-1}. Fitting errors are constant in each column. The magnetic diluant was 50% v/v py–CHCl$_3$ except where stated otherwise

[2] Diluant was 2,6-Me$_2$-py–CHCl$_3$.

[3] A-values assumed negative for hyperfine analysis.

[a] R.L. Lancashire, T.D. Smith and J.R. Pilbrow, J. Chem. Soc., Dalton Trans., (1979) 66.

[b] M.F. Corrigan, K.S. Murray, B.O. West, P.R. Hicks and J.R. Pilbrow, J. Chem. Soc., Dalton Trans., (1977) 1478.

$[Co^{II}L]$ (1)
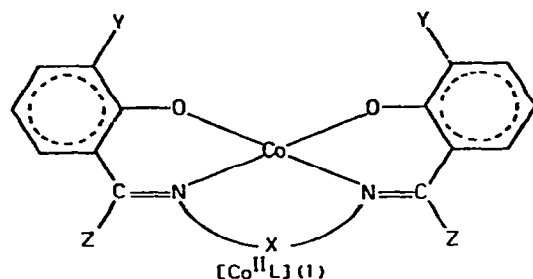
X	Y	Z	L
[CH$_2$]$_2$	H	H	salen
[CH$_2$]$_3$	H	H	salpd
CH(Me)CH$_2$	H	H	salpn
[CH$_2$]$_2$	H	Me	αMe-salen
[CH$_2$]$_2$	H	Et	αEt-salen
[CH$_2$]$_2$	OMe	H	30Me-salen

the cobalt(II) chelates to assist the dioxygen addition. The bases used were pyridine and 2,6-dimethylpyridine. Table 15 summarizes the magnetic parameters for the molecular oxygen adducts of the various cobalt(II) Schiff base chelates studied. Taking as a point of comparison the structural and magnetic parameters associated with the dioxygen complex of Co(II)salen, increasing the length of the bridging group in Co(II)salpd and Co(II)salpn has little or no effect on the g, A or α values. The result of substitution of H by methyl or ethyl as in Co(II)αMe-salen or Co(II)αEt-salen is to increase the values of A_z and α while A_x and A_y remain close to the values observed for Co(II)salen. On the other hand, substitution in the phenyl groups as in Co(H)30Me-salen results in a decrease in the value of α and a clearly discerned increase in A_x while A_y and A_z remain largely unaltered. These effects on α and A_x also occur as a result of substitution of the base pyridine by the stronger base 2,6-dimethyl pyridine.

A further structural variation of the cobalt(II)salen is the omission of the $-CH_2-CH_2-$ bridging unit as in the cobalt(II)salicylaldinate chelates, which are high spin but form molecular oxygen adducts at room temperature in chloroform solution containing various nitrogenous bases [238]. Again, as shown by Table 16, substitution of the methoxy group into the phenyl ring of salicylaldazine leads to a diminution in the size of α and an increase in the value of A_x as observed previously for the Co(II)salen chelates. A similar effect is also observed in the dioxygen adducts of cobalt(II) chelates of salicylaldehyde hydrazones, the parent chelates of which are high spin and again form molecular oxygen complexes at room temperature in the presence of various nitrogenous bases [238]. The magnetic parameters drawn from the ESR spectra due to molecular oxygen complexes of the cobalt(II)salicylaldehyde hydrazones are summarized in Table 17. Table 18 shows that

TABLE 16 [1]

Magnetic parameters[2] associated with the molecular oxygen adducts of the cobalt(II) chelates of salicylaldazine, 3,3'-dimethoxysalicylaldazine and 5,5'-dichlorosalicylaldazine in chloroform containing 20% v/v of pyridine at 77 K. (Salicylaldazine=S.)

Ligand	g_x	g_y	g_z	$A_X(x)$	$A_Y(y)$	$A_Z(z)$	α°
3,3'-dimethoxy S	2.010	2.081	1.994	10.3	20.2	7.6	27
	±0.0005	±0.0002	±0.0002	±0.5	±1.0	±0.5	±1
S	2.016	2.082	1.991	7.2	20.3	11.6	29
5,5'-dichloro S	2.010	2.081	1.994	7.3	19.0	7.0	30

[1] S. Tirant, M.Sc. Thesis, Monash University, 1979. [2] Hyperfine constants are in units of 10^{-4} cm^{-1}.

marked effects on the magnetic parameters occur as a result of changes of the base associated with the cobalt(II)salicylaldazinate-molecular oxygen adduct. For the purposes of comparisons taking pyridine as the starting point, the presence of 2,4,6-collidine causes a marked drop in the value of α and an increase in the value of A_x, whereas the presence of 2,6-lutidine favours an increase in the value of α and a decrease in the value of A_x. Again comparing the structural and hyperfine effects which accrue from taking the bases 2,4-lutidine and 2-picoline both of which have similar steric requirements at the nitrogen but differ in the substituent in the 4-position, the 2,4-lutidine favours a low value of α while 2-picoline lends its influence to a higher value of α. A reasonable conclusion from these limited comparisons of the nitrogen bases is that a controlling influence is provided by the methyl group in the 4-position of the nitrogenous base in determining the value of α. Presumably electron density push from the methyl group to the nitrogen is able to offset the effect of steric hindrance caused by the methyl groups in

TABLE 17 [1]

Magnetic parameters[2] associated with the molecular oxygen adducts of the cobalt(II) chelates of salicylaldehyde hydrazone, 3-methoxysalicylaldehyde hydrazone and 5-chlorosalicylaldehydehydrazone in chloroform containing 20% v/v of pyridine at 77 K. (SH=salicylaldehyde hydrazone.)

Ligand	g_x	g_y	g_z	$A_X(x)$	$A_Y(y)$	$A_Z(z)$	α°
3-methoxy SH	2.0170	2.0810	1.9950	8.3	18.5	10.0	18
	±0.005	±0.002	±0.002	±0.5	±1.0	±0.5	±1
SH	2.0190	2.0910	1.9977	6.2	18.5	9.6	21
5-chloro SH	2.0190	2.0830	1.9990	10.3	17.4	10.5	25

[1] S. Tirant, M.Sc. Thesis, Monash University, 1979. [2] Hyperfine constants are in units of 10^{-4} cm^{-1}.

TABLE 18 [1]

Magnetic parameters[2] associated with the molecular oxygen adducts of the cobalt(II) salicylaldazinate chelate in chloroform containing 20% v/v of various bases and in DMF solution at 77 K ($\nu = 9.149$ GHz)

Base	g_x	g_y	g_z	$A_x(x)$	$A_y(y)$	$A_z(z)$	α
2,4,6-collidine	2.0170±0.005	2.0810±0.002	1.9950±0.002	10.5±0.5	17.5±1.0	11.6±0.5	22±1
2,4-lutidine	2.0176	2.0816	1.9930	5.0	20.5	8.8	27
Acridine	2.0120	2.0827	1.9946	5.8	20.2	10.5	27
Pyridine	2.0161	2.0820	1.9910	7.2	20.3	11.6	29
2-picoline	2.0154	2.0810	1.9940	5.8	20.5	10.6	30
2,6-lutidine	2.0170	2.0810	1.9930	5.0	20.5	8.8	32
DMF	2.0106	2.0810	1.9940	7.0	20.5	10.0	28

[1] S. Tirant, M.Sc. Thesis, Monash University, 1979. [2] Hyperfine constants are in units of 10^{-4} cm^{-1}.

the 2 or 2,6 positions. That steric factors are involved is supported by comparisons of the value of α which occur when 2-picoline or 2,6-lutidine is present and compared with the influence of the presence of pyridine. The simplistic argument is that electron density made available at the nitrogen from the 4-methyl group makes it relatively easier to transfer electron density from the cobalt(II) to the dioxygen molecule reducing back bonding and increasing the bending of the $Co–O_2$ unit in keeping with the argument put forward by Wayland et al. [239]. The preparation of a number of high spin cobalt(II) chelates of linear pentadentate Schiff base ligands has been described along with their combination with molecular oxygen in solution at room temperature and frozen solution [116,240,241]. The ESR spectra of the molecular oxygen adducts were considered in the light of spin polarization and electronic delocalization effects. ESR measurements have shown the thioiminato Schiff base chelate, N, N'-ethylenebismonothioacetylace-toneiminato cobalt(II) forms reversibly a monomeric 1:1 complex with molecular oxygen in the presence of nitrogenous bases [242].

K. OXYGENATION OF M/,CROCYCLIC COBALT(II) CHELATES

Low pH equilibrium and kinetic studies on cobalt(II) complexes of the form $[CoL]^{2+}$ where L is a 12, 13 or 14 membered fully saturated macro-cyclic amine have been described. The ring size influences the stability of the oxygenated products formed by these chelates [243]. The stoichiometry of oxygenated products, established by potentiometric titration and polaro-graphic measurements, takes the form $[(CoL)_2 \cdot O_2 \cdot (OH)]^{3+}$ and $[(CoL)_2 \cdot O_2]^{4+}$. When the data are compared with similar information derived from measurements on a linear tetra-amine chelate system it is apparent that while the macrocycle serves to raise the $[CoL]^{2+}$ stability there is a marked decrease in the molecular oxygen affinity of these chelates. Kinetics measurements show that the formation of the complex CoL^{2+} is the slowest step in oxygen uptake. The presence of the macrocyclic ligand slows down considerably the overall rate of molecular oxygen uptake compared with the linear tetra-amine systems. Studies on the stabilities of monobridged binuclear cobalt dioxygen complexes have shown that the primary factors governing the stability of the cobalt–dioxygen bond in complexes of the type $(CoL)_2 \cdot O_2$ is the increase of σ-donation by the ligands to cobalt with π-bonding effects having little influence [244]. The structural and electronic factors involved in the formation of μ-peroxo cobalt(III) species have been described [245], while electrochemical studies of peroxo-bridged [246] and μ-superoxo compounds [247] have been reported. The formation of a number of μ-peroxo and μ-superoxo cobalt complexes containing cyclic amine ligands has been described [248]. The cobalt(II) chelate of deprotonated 1,4,8,11-

tetraazacyclotetradecane-5,7-dione forms a 1:1 complex with oxygen at low temperatures when imidazole is present and a μ-superoxo complex when pyridine is added to an ethanol solution of the chelate [249]. The cobalt(II) complexes of macrocyclic Schiff base ligands function as a reversible oxygen carrier in several solvents and in the presence of several Lewis bases [250]. The oxygenation of the iron(II) chelate of 5,14-dihydrodibenzo [b,i][5,9,14,18]tetraaza[14]annulene incorporated into apomyoglobin has been described [251]. It has been pointed out that macrocyclic cobalt chelates comprise a useful series of compounds for investigation of molecular oxygen reactivity since their redox activities as well as spin states involved in the reaction pathway may be altered systematically by structural changes in the equatorial ligand [252]. It has been shown that out-of-plane structural modifications of cobalt(II) macrocyclic chelates, which involve different hydrocarbon linkings across the facial regions results in wide variation of the ability of the cobalt(II) to bind molecular oxygen [253,254].

L. FORMATION OF MOLECULAR OXYGEN COMPLEXES ON ZEOLITES AND CATION EXCHANGERS

Transition metal complexes may be formed in zeolites by a variety of techniques which include: (a) exchange of the hydrated ion followed by dehydration and addition of the ligand from the gas phase; (b) direct exchange of the complex ion; and (c) the exchange of the ligand followed by the addition of metal ion. ESR spectroscopy has been used to study the reactions of bis(acetylacetonato)copper(II) adsorbed on an X-type zeolite with various bases [255,256]. The formation, characterization and catalytic activity of transition metal complexes in zeolites, including molecular oxygen complexes of cobalt(II) compounds adsorbed on to zeolites has been described [257–259]. An ESR study of some cobalt amine oxygen adducts in faujasite-type zeolite Y showed the reversible formation of low spin $[Co(III)L_XO_2^-]^{2+}$ adducts within the large cavities of a Co(II)–Y zeolite, where $L = NH_3$, CH_3NH_2 or $n\text{-}CH_3CH_2CH_2NH_2$ and X is probably equal to 5. Dimeric μ-superoxo $[L_XCo(III)O_2^- Co(III)L_X]^{3+}$ adducts can also be formed with $L = NH_3$ or CH_3NH_2 [260]. It has been shown that nitrosyl complexes are formed by reaction of nitric oxide with cobalt(II) ions or cobalt(II) amine complexes in cobalt-exchanged zeolites [261]. The reversible oxygen binding by a divalent chromium(II) ion exchanged zeolite A has been reported [262]. One of the simplest of all systems to be described is the formation of monomeric dioxygen adduct of cobalt(II) complexes with ammonia, methylamine or ethylenediamine formed in an Amberlyst A15 cation exchange resin [263].

M. ACTIVATION OF MOLECULAR OXYGEN

(i) Role of cobalt(II) compounds in catalytic oxidation processes

The roles of transition metal chelates as catalysts for the addition of molecular oxygen to reactive organic substrates have been described [264–268] while similar processes occurring on the surfaces of metal oxides have been outlined [269]. The ability of a number of cobalt(II) compounds to act as carriers of molecular oxygen, which achieves a degree of reduction as a result of combination with the cobalt(II), ensures that cobalt(II) chelates occupy a prominent position in these reactions. Some general reaction mechanisms which emerge are: (1) Ternary complex formation by the cobalt chelate, the substrate and molecular oxygen as a reactive intermediate in the overall process. (2) Redox changes whereby the cobalt(II) chelate is reduced by the substrate and subsequently oxidized by molecular oxygen. (3) Radical abstraction whereby coordinated oxygen abstracts a hydrogen atom from the substrate with formation of radicals. (4) Atom transfer processes where the two oxygen atoms of molecular oxygen are distributed among substrate molecules.

The reaction of coordinated oxygen with an uncoordinated organic substrate has been postulated for a number of metal catalyzed autoxidations [270]. The liquid phase oxidation of acetaldehyde by molecular oxygen to give peracetic acid catalyzed by tetraphenylporphyrinato cobalt(II) and cobalt(II)polyphthalocyanines has been reported [271–274]. In a study of the autoxidation reactions of hydrocarbons catalyzed by cobalt(II)tetra(p-tolyl)porphyrin the reactivity of the molecular oxygen adduct of the cobalt(II) chelate was compared with that of the superoxide ion resulting from other sources [275]. The quite valuable point is made in this study that cobalt(II)tetra(p-tolyl)-porphyrin and π-allyl Fe(CO)$_3$Br form less reactive molecular oxygen than electrogenerated superoxide which can catalyze autoxidation reactions of 9,10-dihydroanthracene (71 kcal mol^{-1}), cumene (79 kcal mol^{-1}), tetralin (82 kcal mol^{-1}) and cyclohexene (95 kcal mol^{-1}) where the quantities in parentheses are the C–H bond dissociation energies. The former two metal complexes failed to catalyze the autoxidation reaction of cumene and tetralin which possess C–H bond dissociation energies above 79 kcal mol^{-1}.

The oxidation of molecular oxygen of 3,5-di-t-butyl catechol in the presence of metal acetylacetonates has been studied [276]. The catalytic activity of the chelates decreases in the order Mn(II) > Co(II) > Ni $\gg$ Fe(II) and the product is 3,5-di-t-butyl-o-benzoquinone. The kinetics of the reaction suggests a mechanism in which the radical chain reactions involving 3,5-di-t-butyl-o-benzosemiquinone and hydroperoxyl radical are initiated by

the reaction of the catechol with molecular oxygen bound to the chelate. The results of this study may be usefully compared with the base catalyzed regiospecific oxygenations of t-butylated phenols. Catalysis by some manganese(II) or cobalt(II) Schiff base chelates of the oxidation by molecular oxygen of β-isophorone to the corresponding 3,5,5-trimethylcyclohexene-1,4-dione has been studied [277].
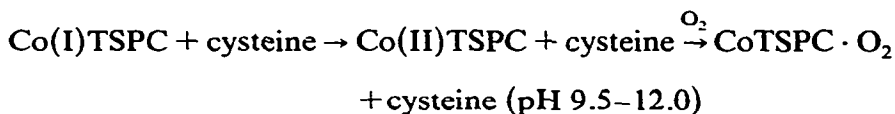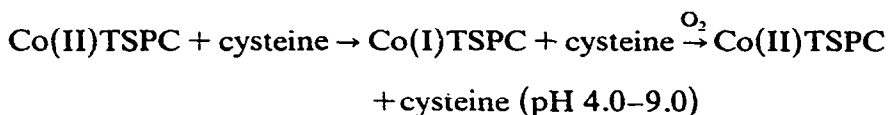
Cobalt(III) and iron(III) porphyrins have been found to catalyze the autoxidation of cyclohexene to allylic hydroperoxides which then decompose to give 2-cyclohexenone as the main product [278]. The initial step is the reduction of cobalt(III) or iron(III) porphyrin to cobalt(II) or iron(II) porphyrin by cyclohexene. In a similar manner hemin dimethyl-ester and cobalt(II)/(III) octaethylporphyrins have been found to catalyze the autoxidation of squalene [279]. Cobalt(II), cobalt(III) and manganese(III) mesotetraphenylporphyrins catalyze the oxygenation of simple alkyl-substituted indoles [280]. In the reaction catalyzed by cobalt(II)tetraphenyl-porphyrin (Co(II)TPP) a Co TPP $\cdot$ O$_2$ indole ternary complex is formed initially. This complex gives rise to the formation of indolenyl hydroperoxide which decomposes to the final product under the influence of the cobalt porphyrin. The preparation of surfactant solutions containing cobalt(II) complexes which activate molecular oxygen has been described [281].

The autoxidation of hydrazine catalyzed by transition metal ion tetra-sulphophthalocyanines has been described [282]. A study of the kinetics of the reaction concludes that a ternary complex [N$_2$H$_4$ $\cdot$ Co tetra-sulphophthalocyanine $\cdot$ O$_2$] is an active intermediate in the reaction. A similar conclusion was reached in a study of the autoxidation of ascorbic acid catalyzed by cobalt(II)tetrasulphophthalocyanine [283]. In the oxidation of hydroxylamine by molecular oxygen, catalyzed by cobalt(II)tetra-sulphophthalocyanine the products are nitrogen, dinitrogen oxide and nitrite. Oxygen is reduced to water and hydrogen peroxide whose reaction with hydroxylamine is also catalyzed by the cobalt(II) chelate [284].

In an ESR study of the autoxidation of hydrazine, hydroxylamine and cysteine catalyzed by cobalt(II)tetrasulphophthalocyanine (Co(II)TSPC) the catalytic reactions were unravelled first by the observation of an ESR spectrum due to the molecular oxygen complex of Co(II)TSPC formed substantially in aqueous solution over the pH range 10–13 containing 10% v/v of dimethylformamide [285]. The spin-Hamiltonian parameters for the complex were found to be as follows: $g_x = 2.005$; $g_y = 2.084$; $g_z = 2.001$; $A_x = 8.0 \times 10^{-4}$ cm^{-1}; $A_y = 18.0 \times 10^{-4}$ cm^{-1}; $A_z = 9.0 \times 10^{-4}$ cm^{-1}; $\alpha = 10 \pm 5°$. The ESR spectrum due to molecular oxygen adducts of cobalt(II)tetrasulphophthalocyanine formed in methanol containing a trace of ammonia has been recorded [286], whilst the 1:1 adduct of molecular oxygen with cobalt(II)phthalocyanine in the presence of nitrogenous base has been

characterized [287]. The formation of the hydrazine adduct of Co(II)TSPC, as monitored by the intensity of the ESR signal, can be controlled reversibly by adjusting the pH provided the pH is kept below 11.5. Above this pH reduction to Co(I)TSPC occurs. Thus the autoxidation of hydrazine involves the initial formation of a binary adduct with Co(II)TSPC the catalytic process being most effective at pH 11.5 where the concentration of the binary adduct reaches a maximum. However, no evidence for the formation of a ternary adduct involving Co(II)TSPC, hydrazine and oxygen was found. At high pH reduction to a cobalt(I) species indicates that hydrazine is oxidized by a simple electron transfer reaction. In a similar series of experiments involving the autoxidation of hydroxylamine a surprising aspect is the observation of an ESR signal due to an oxygen adduct of cobalt(II)TSPC in the pH range 3.5–4.5, which requires the presence of hydroxylamine for its appearance.

The ESR studies indicate that the catalytic autoxidation of cysteine may be summarized by the equations [285]:

$$Co(II)TSPC + cysteine \rightarrow Co(I)TSPC + cysteine \xrightarrow{O_2} Co(II)TSPC$$

$$+ cysteine \ (pH \ 4.0–9.0)$$

$$Co(I)TSPC + cysteine \rightarrow Co(II)TSPC + cysteine \xrightarrow{O_2} CoTSPC \cdot O_2$$

$$+ cysteine \ (pH \ 9.5–12.0)$$

These equations represent the fact that the effective catalytic autoxidation of cysteine proceeds in the range pH 4.0–9.0.

The autoxidation of thiols which occur in certain petroleum distillates has been of interest for a number of years. Cobalt(II) phthalocyanines play a prominent role in these processes and in more recent years have been used in conjunction with solid supports in basic media [288–292]. The gas phase autoxidation of 2-propane thiol catalyzed by crystalline phthalocyanines of the first transition group has been described [293]. The characterization by ESR of a polymer attached cobalt(II)phthalocyanine has been outlined [294]. The autoxidation of mercaptans catalyzed by bifunctional catalysts prepared by polymer attachment of cobalt(II)phthalocyanine has been carried out [295]. Polymer attachment of the cobalt(II)phthalocyanine was achieved by complexation through polymeric amine groups, as well as by formation of a peptide linkage between the phthalocyanine ring system and the polymeric carrier. The means by which polymer–metal complexes may be formed and aspects of their catalytic activity have been reviewed [296,297], while some aspects of the catalytic behaviour of polymeric azaporphyrin compounds have been outlined [298]. An interesting aspect of the catalytic oxygenation

reaction is the possibility of oxygen atom transfer reactions. An example of this type of reaction is the reaction of Co(saloph)py · NO$_2$ (saloph = N, N'-bisalicylidene-o-phenylene diamino) with triphenyl phosphine to form triphenyl phosphine oxide by an oxygen transfer mechanism where the resulting reduced ligand is reoxidized by molecular oxygen completing the catalytic cycle [299]. An atom transfer process is thought to be involved in formation of an acetonyl adduct of N, N'-ethylene-bis(3-fluor-salicylideneiminato)cobalt(II) which is thought to be formed as a result of transfer of hydrogen from acetone to a coordinated dioxygen intermediate [300].
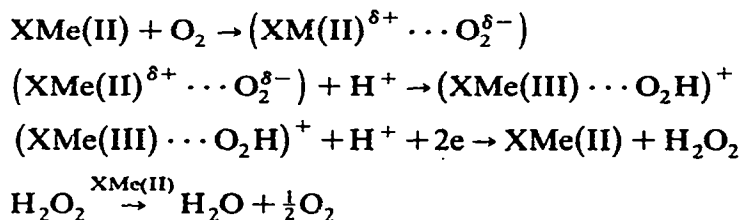
The reaction of the molecular oxygen complex of N, N'-ethylene-bis(acetyl-acetoniminato)cobalt(II) with general acids (HX) in pyridine and other organic solvents has been observed to produce oxygen and hydrogen peroxide, which is relatively stable in the reaction conditions used, as follows [301]:

$$Co(II)(acacen) \cdot O_2 + HX \xrightarrow{py} [Co(acacen)py_2] X + \tfrac{1}{2} O_2 + \tfrac{1}{2} H_2O_2$$

Hydrogen peroxide is also generated in the reaction of alcohol bound to a ruthenium complex with molecular oxygen. In this reaction the alcohol is converted to a ketone [302]. The preparation and catalytic oxidizing potential of polymer supported chelating amine and Schiff's base complexes have been described [303]. In an atmosphere of air or oxygen and under mild conditions the pyridine complex of bis(dimethylglyoximato)cobalt(II) catalyzes the oxidation of hydroquinone, triphenyl phosphine or hydrazobenzene added in five to fifty fold excess over the catalyst [304]. The cobalt(II) chelate of the Schiff base formed in condensation of o-aminobenzaldehyde and ethylenediamine (Co(II)amben) assists in electron transfer from N, N, N', N'-tetramethyl-p-phenylenediamine to molecular oxygen [305].

(ii) Catalysis of electrochemical reduction of molecular oxygen

The catalytic electrochemical reduction of molecular oxygen is of interest in the design and composition of electrodes used in fuel cells, batteries and electrochemical solar energy conversion devices. Effective electrocatalysis at the oxygen cathode has been shown to occur with metal chelates of porphyrins, dibenzotetraazaannulenes and tetraphenylporphyrins [306,307]. In the relatively few cases where comparisons under uniform conditions can be made the order of decreasing activity for different central metal ions is as follows: Mn $\approx$ Pd $\geqslant$ Fe $\geqslant$ Pt > Co > Cu $\geqslant$ Mo > Ni [308,309]. The catalyzed pathway for electrochemical reduction of molecular oxygen may comprise the following steps [310]:

$$XMe(II) + O_2 \rightarrow \left(XM(II)^{\delta+} \cdots O_2^{\delta-}\right)$$

$$\left(XMe(II)^{\delta+} \cdots O_2^{\delta-}\right) + H^+ \rightarrow \left(XMe(III) \cdots O_2H\right)^+$$

$$\left(XMe(III) \cdots O_2H\right)^+ + H^+ + 2e \rightarrow XMe(II) + H_2O_2$$

$$H_2O_2 \xrightarrow{XMe(II)} H_2O + \tfrac{1}{2}O_2$$

The incorporation of the metal chelates into the cathode has been achieved by vacuum sublimations of the metal macrocyclic chelate onto inert electrodes, by precipitation from a solution, by painting the electrode with a suspension of the catalyst, or by mixing the catalyst with suitable material to fabricate the electrode. It has been argued that the one-electron transfer process in the oxidation of oxygen is reversible and independent of electrode materials and solution conditions [310], such that the belief that the electrode surface is catalytic for the electron transfer process is unjustified [311,312]. However the more conventional view has been put forward that there is ample evidence that the process, $O_2 + e^- \rightarrow O_2^-$ is catalyzed by some electrode surfaces [313–328] but that a rewarding goal would be a catalyst that promotes the direct dissociation of molecular oxygen [329].

N. INTERPRETATION OF ESR PARAMETERS FOR Co–O₂ ADDUCTS

Two different kinds of models have been invoked to account for the electronic properties of Co–O₂ adducts and their ESR parameters. The most often discussed picture is of the proposed formation of an O_2^- radical resulting from more or less complete electron transfer from cobalt(II) to O_2. Both the work of Drago et al. [60,330–333] and recent work on CoMbO₂ by Dickinson and Chien [107], suggests the importance of indirect spin polarization contributions to hyperfine structure and the formation of a σ-bond. Electron transfer occurs in the bonding region. Nevertheless, it is the view of the authors that both direct and indirect mechanisms must operate if a consistent view of anisotropic h.f.s. is to be achieved. We begin with a brief summary of the O_2^- picture and then later discuss spin pairing models.

(i) Superoxide formulation

Within the superoxide, O_2^-, formulation, cobalt hyperfine structure is understood on the basis of partial occupation of cobalt d-orbitals by the unpaired electron on the oxygen. If the hyperfine structure were due solely to d_{z^2} admixture [98] where the mixing was governed by the coefficient, τ,

$$A_{max} = A_z \simeq P\left[-K + \tfrac{4}{7}\tau^2\right] \tag{10a}$$

and

$$A_{min} = A_x = A_y \simeq P[-K - \tfrac{2}{7}\tau^2] \tag{10b}$$

where

$$P = 2\beta g_n \beta_n <r^{-3}>_{3d} \tag{11}$$

Here τ is used instead of α so as to avoid confusion with the non-coincidence angle α. Parameters not previously defined are g_n and β_n which are the cobalt nuclear g-factor and the nuclear magneton, respectively, while $<r^{-3}>_{3d}$ is the mean inverse cubed radius of $3d_{z^2}$ electrons. K is the Fermi-contact parameter which will include direct admixture of cobalt $4s$ density and indirect core polarization. For parent cobalt(II) compounds typically $P \simeq 0.02$ cm^{-1} whereas, as mentioned in Section E, Co-O_2 adducts have $(A_{max}) \simeq 0.002$ cm^{-1}. The eqns. (10a) and (10b) are sometimes combined to yield

$$A_{max} \simeq \langle A \rangle + \tfrac{4}{7}P\tau^2 \tag{12}$$

where

$$\langle A \rangle = \tfrac{1}{3}(A_x + A_y + A_z) \tag{13}$$

Hoffman et al. [98] pointed o. that on the basis of likely crystal geometries of Co-O_2 adducts, A_{max} which has often been called $A_{\parallel}$ or A_z, probably lies along y (Fig. 14) and *not* along z. Therefore, the major contribution to cobalt h.f.s. would come from d_{xz} and *not* d_{z^2}. Then

$$A_{max} = A_y \simeq P[-K - \tfrac{4}{7}\tau^2] \tag{14b}$$

In place of eqn. (12) one may write

$$|A_{max}| \simeq |\langle A \rangle| + \tfrac{4}{7}P\tau^2 \tag{15}$$

Analysis of the maximum and average hyperfine values using either eqn. (12) or eqn. (15) leads to $\tau^2 = 0.1$. It is upon this result that electron transfer from cobalt(II) to oxygen has been considered more or less complete.

The s electron contribution to the hyperfine structure $(-KP)$ proves troublesome for it leads to $\tau^2 \simeq 0.5$ [60]. The discrepancy between the τ^2 values determined from isotropic and anisotropic hyperfine contributions arises in part from the smaller anisotropy observed for Co-O_2 adducts compared with the corresponding parent compounds.

Experimental hyperfine constants should be corrected for the direct dipole-dipole interaction and this is accounted for in the analysis given later for spin pairing models.

(ii) Spin pairing model

From the ESR point of view, spin pairing models with indirect spin polarization giving rise to cobalt h.f.s., have arisen because of the inconsistencies resulting from O_2^- formulations [60]. In the work of Dickinson and Chien [107], on CoMbO$_2$ it was found that the anisotropic cobalt h.f.s. was due to positive spin density on d_{xz} (their d_{xz}) and negative density on d_{yz} (their d_{xz}). Tovrog, Kitko and Drago [60] reviewed O^{17} h.f. data for Co(bzacen)O$_2$ and found that the total spin density on the two oxygens equalled 1. They were led to postulate a spin polarization mechanism which did not involve spin transfer to cobalt d-orbitals in order to begin to explain the cobalt h.f.s. Their views have been outlined subsequently including some different examples [330–331].

The spin pairing view has been described in simple form by Wayland et al. and [91,334], from a valency bond or Heitler–London viewpoint by Harcourt [92]. Essentially, spin pairing models for Co–O$_2$ systems involve at least three electrons for a description of the key aspects of the electronic structure. Support for these ideas can be found in the results of some molecular orbital calculations [89,93].

The argument regarding O^{17} h.f.s. is summarized as follows [60]. In solution, the ESR due to Co(bzacen)O$_2^{17}$ shows that the two oxygens are equivalent with identical isotropic splittings of 21.6 G. At low temperatures the oxygens are found to be inequivalent with maximum O^{17} h.f. splittings, associated with the O–O direction corresponding to $g_{max}(y_g,\xi)$, of 60 and 88 G, respectively, for middle and terminal oxygens. These splittings lead to estimates of spin densities of 0.4 and 0.6, respectively. Since the total spin density on oxygen is ~ 1 then they argued that the cobalt h.f.s. must arise from an indirect mechanism.

It was noted that in the case, e.g. of Co(acacen)pyO$_2$, comparison of the cobalt h.f. constants with the solution average proves that all three constants must have the *same* sign [60]. They assume all the signs to be negative though that could only be directly confirmed by an ENDOR experiment.

To explain the ideas behind a semi-empirical spin pairing model, we begin with a brief account of the arguments advanced by Tovrog et al. [60]. Their results need to be modified and we also consider a suggestion they made about π-back bonding. In the light of the observations of Dickinson and Chien [101,107], we consider an extended model which includes indirect h.f. coupling from d_{yz} and d_{z^2} and back bonding to d_{xz}.

The spin pairing model [60] may be understood on the basis of the simplified molecular orbital diagram, Fig. 16. One of the oxygen π^* orbitals, $\pi^*(x_g)$, spin pairs with cobalt d_{z^2} to form a σ-bonding orbital, ψ_1, which contains the unpaired electron (ψ_2). (For definitions of x_g and y_g directions

see Fig. 12.) There is an empty antibonding orbital, ψ_3. The orbitals are written in LCAO fashion as

$$\left.\begin{array}{l} \psi_3 = bd_{z^2} - a\pi^*(x_g) \\ \psi_2 = \pi^*(z_g) \\ \psi_1 = ad_{z^2} + b\pi^*(x_g) \end{array}\right\} \tag{16}$$

where

$$b = (1 - a^2)^{1/2} \tag{17}$$

Within this model when $a \doteq 0$ the Co O_2 adduct is formally Co(III)O_2, when $a = b$ it is Co(II) O_2, and when $a = 1$ it is Co(I)O_2^+. The amount of electron transfer which is involved in any of the formal descriptions is dependent on the MO coefficients of the σ-bonding orbital, ψ_1, and is *not* directly dependent upon the unpaired electron in ψ_2. Cobalt h.f.s. can arise as a result of spin polarization of ψ_1 by the unpaired electron in ψ_2. Tovrog et al. [60] modified their analysis initially by including a cobalt $4s$ contribution to ψ_1, writing

$$\psi_1 = \alpha' d_{z^2} + c\,4s + b\pi\left(x_g^*\right) \tag{18}$$

where $\alpha' \neq a$.
Electron transfer within the σ-bonding region is therefore

$$ET = 2(1 - \alpha'^2) - 1 \tag{19}$$
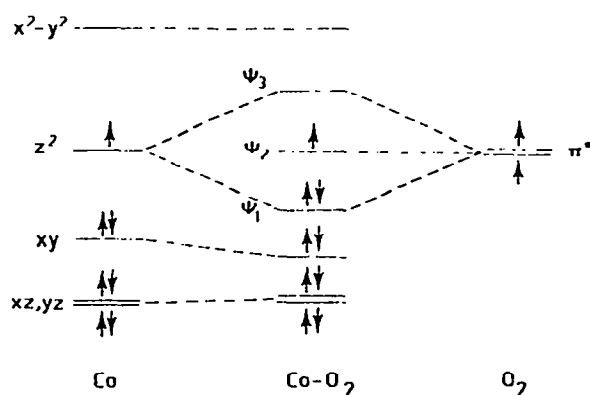

Fig. 16. Simplified schematic representation of molecular orbitals of Co O, complexes. Based upon Tovrog et al. [60] and references therein assuming tetragonal symmetry. Under C_{2v} (v) symmetry, x^2 y^2, yz and z^2 transform as A' while xy and xz transform as A'', e.g. z^2 is augmented with x^2 y^2 and yz. The lowest Co orbitals do not remain degenerate.

Since d_{yz} and d_{z^2} transform according to the same representation of the point group, C_s, appropriate to Fig. 12, one should consider some alteration to the cobalt levels in Fig. 16 and, from the outset, include a d_{yz} contribution to ψ_1.

In a good many of the examples considered by Drago et al. [60,329–332] $A_{max} \approx A_z$ and $A_{min} = A_\perp \simeq A_x \simeq A_y$, but they analyzed them assuming $A_\parallel$ to be along z and *not* along y. The possibility was raised of $g - A$ non-coincidence but, because none of the ESR data considered by them was analyzed according to the model of Fig. 12, or some similar model, one must be cautious about the conclusions they drew regarding the extent of electron transfer.

There is a significant point made by Tovrog et al. [60] concerning the s-electron contribution to the observed cobalt h.f.s. They attempted to analyze the s-electron contribution and found the $4s$ character to range from 20 to 64%, far too high in comparison with parent compounds where the $4s$ character is $\sim 4\%$. Therefore, it was considered more appropriate to concentrate on the anisotropic part of the hyperfine structure. (For a more detailed discussion see [60], especially pp. 5148–5149.)

For an *indirect* spin polarization contribution via d_{z^2}, the anisotropic hyperfine components will be

$$A_{aniso}(d_{z^2}) \propto P\alpha'^2 \left[\begin{array}{ccc} x & y & z \\ \frac{2}{7}, & \frac{2}{7} & -\frac{4}{7} \end{array} \right] \tag{20}$$

where, because of the assumed negative spin density, the signs have all been changed compared with eqn. (10). The experimental data must be corrected for the direct electron(oxygen)–nuclear(cobalt) dipole–dipole interaction before results may be compared with eqn. (20). By analogy with indirect spin polarization in radicals [335], they sought a relationship of the form

$$A_{aniso}(d_{z^2}) = U_{Co-O}\rho_O\alpha'^2 A_{aniso}(3d) \tag{21a}$$

$$= Q\rho_O\alpha'^2 \tag{21b}$$

Here U_{Co-O} is a polarization constant, ρ_O $(= 0.4)$ the spin density on the middle oxygen and $A_{aniso}(3d)$ the hyperfine interaction for the appropriate parent compound, taken to be 0.0098 cm^{-1} along the z direction. Determination of $Q = 0.00609$ cm^{-1} was made from comparison with the aryl nitroso compound $Co(CN)_5(C_6H_2Cl_3)NO$ [336] for which we would have

$$A_{aniso}^{(NO)}(d_{z^2}) = U_{Co-N}\rho_N\alpha_N'^2 A_{aniso}(3d) \tag{22}$$

There it was known that $\rho_N = 0.7$, it was assumed that $U_{Co-N} \approx U_{Co-O}$ and that $\alpha_N'^2$ lay in the range 0.1–0.2. Tovrog et al. [60] mention a parameter, Q, on page 5150 of their paper, but it is nowhere defined. The value of Q quoted above and taken from a later paper [329] is consistent with all of the numerical constants in the earlier work.

Tovrog et al. [60] quite correctly calculated the direct dipolar interaction between both oxygens and cobalt(II) using the coordinates for Co(bzacacen)pyO$_2$ reported by Rodley and Robinson [90, Table 4]. This did not allow for a tilt to the dipolar axes caused by the fact that the cobalt-terminal oxygen direction is not along z, though that would involve only a small correction here. They calculated

$$A_{dip}^{O_2} = \left(\overset{x}{-0.5}, \overset{y}{-0.5}, \overset{z}{1.0} \right) \times 10^{-4} cm^{-1} \qquad (23)$$

using the formulae

$$A_{dip}(x, y) = -\frac{g\beta g_n \beta_n}{r^3} \qquad (24a)$$

and

$$A_{dip}(z) = \frac{2g\beta g_n \beta_n}{r^3} \qquad (24b)$$

The corresponding estimate for the nitroso compound was

$$A_{dip}^{NO} = (-0.66, -0.66, 1.32) \times 10^{-4} cm^{-1} \qquad (25)$$

In correcting for the direct dipolar interaction, Tovrog et al. [60] were at the same time assuming A_{max} to lie along z and not along y. This must alter their estimates of α'^2 and, therefore, the calculated electron transfer values. Furthermore, since d_{z^2} does not have a maximum value along y, we must consider their back bonding argument involving d_{xz}, for which ψ_2 becomes

$$\psi_2 = \varepsilon \pi^* (z_g) + \alpha'' d_{xz} \qquad (26)$$

From eqn. (14) we have, as the *direct* interaction,

$$A_{aniso}(d_{xz}) = P\alpha''^2 \left(\overset{x}{\tfrac{2}{7}}, \overset{y}{-\tfrac{4}{7}}, \overset{z}{\tfrac{2}{7}} \right) \qquad (27)$$

Putting

$$f = Pp_0 U_{Co-O} \alpha'^2 \qquad \text{and} \qquad g = P\alpha''^2 \qquad (28)$$

they examined the equations (29) where the symbol g should not be confused with g-values determined from the ESR spectra

$$\left. \begin{array}{l} a_x = A_x - \langle A \rangle = \tfrac{2}{7}(f + g) \\ a_y = A_y - \langle A \rangle = \tfrac{2}{7}(f - 2g) \\ a_z = A_z - \langle A \rangle = \tfrac{2}{7}(-2f + g) \end{array} \right\} \qquad (29)$$

A_x, A_y and A_z are all corrected for the direct dipolar contribution and are assumed to be negative in the analysis. Since, by definition, f and g are both

positive, then we would expect $a_x > 0$, a_y probably < 0, and a_z to be either positive or negative. If these are the only contributions then, e.g. a negative value of f would seem to imply a direct rather than indirect interaction. Within this framework, we find g is always positive and f sometimes negative, the latter situation arising whenever $|A_x| > |A_z|$ and more especially whenever $A_x \approx \langle A \rangle$. As actually applied, the specific spin polarization model prepared by Tovrog et al. [60] seems to be more appropriate for a linear Co–O–O system. In that case the direct dipolar interaction must be altered because it was based on a Co–O–O angle of 126°. Interestingly, Wayland et al. [91,334] have pointed out that π-back bonding is likely to be greatest for a linear arrangement.

Dickinson and Chien's recent results for $CoMbO_2$ suggest that the negative spin density on d_{yz} (their d_{xz}) must be due to an indirect coupling due to spin polarization [107]. Then ψ_1 must be

$$\psi_1 = \alpha''' d_{yz} + \gamma 4s + \beta \pi^*(x_g) \tag{30}$$

and in place of eqns. (29) one must have

$$
\left.
\begin{aligned}
a_x &= A_x - \langle A \rangle = \tfrac{2}{7}(g + 2h) \\
a_y &= A_y - \langle A \rangle = \tfrac{2}{7}(-2g - h) \\
a_z &= A_z - \langle A \rangle = \tfrac{2}{7}(g - h)
\end{aligned}
\right\} \tag{31}
$$

where

$$h = P\rho_0 U_{Co-O}\alpha'''^2 \tag{32}$$

There is an inconsistency in their analysis relating to the direct dipolar correction. In Table 3 of their paper $A_{dip} = (\overset{y}{-0.7}, \overset{x}{1.4}, \overset{z}{-0.7})$ should be $A_{dip} = (\overset{x}{-0.7}, \overset{y}{-0.7}, \overset{z}{1.4})$. The correction alters the extent of the d_{yz} contribution to anisotropic cobalt h.f.s.

To sum up the various contributions we suggest that the spin pairing model should be modified such that

$$\psi_1 = \alpha' d_{z^2} + \alpha''' d_{yz} + \gamma 4s + b\pi^*(x_g) \tag{33}$$

Since d_{z^2} and d_{yz} transform according to the same representation of C_s (where x is normal to the mirror plane), then we would not expect to be able to separate their individual contributions. A contribution from $d_{x^2-y^2}$ has not been explicitly included in the analysis since it is believed to be smaller than those due to d_{z^2} and d_{yz}. In order to examine the $CoMbO_2$ and Vitamin $B_{12}.O_2$ data, as well as those based on simulations where $\alpha = 0$ (Fig. 12) the following equations should be considered:

$$a_x = \tfrac{2}{7}(f + g + 2h)$$
$$a_y = \tfrac{2}{7}(f - 2g - h)$$
$$a_z = \tfrac{2}{7}(-2f + g - h)$$

(34)

In eqns. (34) f and h represent indirect interactions involving spin polarization of d_{z^2} and d_{yz} respectively, while g represents the direct interaction due to d_{xz}. The parameters f, g and h are defined in eqns. (28) and (32). As a consequence of the transformation properties of d_{z^2} and d_{yz}, the eqns. (34) are linearly dependent. In Tables 19–22 are presented results of calculations based upon eqns. (34) for a range of ESR parameters where the non-coincidence angle, α, is also known. It is, unfortunately, not possible to separate f, g and h. From eqns. (34) we have

$$a_x - a_z = \tfrac{6}{7}(f + h)$$
and
$$a_x - a_y = \tfrac{6}{7}(g + h)$$

(35)

The values of $f + h$ and $g + h$ listed in Tables 19–22 are obtained from eqns.(35) and these are the two quantities expected always to be positive in terms of the model. Except for $CoMbO_2$, the dipolar correction used is that calculated by Tovrog et al. [60]. Variations of the $Co-O_2$ bond angle from $105°$ to $120°$ should not strongly influence the dipolar interaction as it is chiefly variations in the coordinates of the more distant terminal oxygen which would be affected.

It is unfortunate that it is impossible to extract individual values of f, g and h. Therefore we make a few general observations. With one exception, $CoTPP \cdot O_2$, the values of $g + h$ are all positive. The upper limit to the value of g, which represents the direct interaction of the unpaired electron and d_{xz}, will be the values of $g + h$ given by Tables 19–22. For $CoMbO_2$ it is 12.4, for $B_{12r} \cdot O_2$ it is 16.3. For porphyrin-substituted Hb and Mb the value lies in the range $\sim 11–16$. It is smaller for porphyrins $\sim 9–12$ except for $CoTPPS \cdot O_2$ while for Schiff's bases the value is between 12 and 19. In Table 22 which gives results for variations due to addition of different bases, no particular trend is evident but the $g + h$ values are mainly from 10.2 to 13.7. Thus the estimate of α''^2, eqn. (26) from comparison of these values with $P \simeq 0.02$ cm^{-1} suggests that, for the most part, $\alpha''^2 \sim 0.06$. We conclude that an important condition required by Tovrog et al. [60] that back bonding in the model be small, is met through the upper limits implied by $g + h$ values if $h = 0$. If however, as is implied by many of the results for $f + h$ which turn out to be negative, h is actually *not* zero, but negative, then the values of g could possibly be higher. Negative values of $f + h$ are found for most of the Schiff's bases and substituted Mb and Hb and can arise from having either

TABLE 19

Cobalt hyperfine analysis: CoMbO$_2$ and porphyrin substituted Hb, Mb·O$_2$ and B$_{12r}$·O$_2$

	Co(II) porphyrin	Solvent conditions	a_x	a_y	a_z	$f+h$	$g+h$	Ref.	Table
			($\times 10^{-4}$ cm^{-1})						
A. CoMbO$_2$ (centre II)									
Crystal			5.3	−5.3	0.1	6.1	12.4	a	—
B. Apo-protein									
Sperm whale Mb	MeP	H$_2$O	3.8	−9.0	5.3	−1.7	15.6	b	11
	MeP	D$_2$O	3.8	−9.7	5.8	−2.3	15.8	b	11
	PPIX	Phosphate buffer pH 7.0	3.2	−8.8	5.7	−2.9	14.0	b	11
	PPIX		3.5	−7.8	4.2	−0.8	13.2	f	11
Hb Glycera	PPIX	H$_2$O pH 7.0	3.7	−8.8	5.2	−1.7	14.6	b	11
	MeP	H$_2$O	2.8	−6.9	4.1	−1.5	11.3	b	11
Aplysia Mb	MeP	H$_2$O pH 7.0	3.2	−8.7	5.5	−2.7	14.6	c	11
α chain Hb	PPIX	H$_2$O	2.9	−7.0	4.3	−1.6	11.9	d	11
β chain Hb	PPIX	H$_2$O	3.4	−9.2	5.8	−2.8	14.7	d	11
Hb Zürich	PPIX	H$_2$O	3.2	−8.7	5.6	−2.8	14.6	e	11
C. B$_{12r}$·O$_2$	Crystal		5.8	−8.2	2.3	4.1	16.3	8	8

[a] L.C. Dickinson and J.C.W. Chien, Proc. Nat. Acad. Sci. U.S.A., 77 (1980) 1235.

[b] F.J. Kayne and T. Yonetani, Biochim. Biophys. Acta, J. Biol. Chem., 252 (1977) 4882.

[c] M. Ikeda-Saito, M. Brunori, and T. Yonetani, Biochim. Biophys. Acta, 553 (1978) 173.

[d] F.J. Kayne and T. Yonetani, J. Biol. Chem., 252 (1977) 620.

[e] M. Ikeda-Saito, M. Brunori, K.M. Winterhalter and T. Yonetani, Biochim. Biophys. Acta, 580 (1979) 91.

[f] I.M. Ruzic, Ph.D. Thesis, Monash University, 1980.

[g] E. Jörin, A. Schweiger and Hs.H. Günthard, Chem. Phys. Lett., 61 (1979) 228.

TABLE 20

Cobalt hyperfine analysis: Co porphyrins-O_2

	a_x	a_y	a_z	$f+h$	$g+h$	Ref.
	($\times 10^{-4}$ cm^{-1})					
Co$\alpha\beta\gamma\delta$Co TCPP·O_2 in CHCl$_3$/NaOH	3.8	−6.2	2.3	1.7	11.7	a
Co$\alpha\beta\gamma\delta$-Co TCPPO$_2$ in pyridine	4.3	−5.7	1.5	3.3	11.8	a
Co$\alpha\beta\gamma\delta$-p MePPO$_2$ in pyridine	4.2	−5.8	3.7	0.6	11.7	a
CoPPIXDME O$_2$ in pyridine	2.7	−5.5	3.7	−1.2	9.3	a
CoTPP O$_2$	3.5	8.5	−12.0	18.1	−5.8	a
CoTPPS·O$_2$	−0.2	−5.8	6.3	−0.7	2.0	b

[a] R.L. Lancashire, Ph.D. Thesis, Monash University, 1976.
[b] J.A. de Bolfo, T.D. Smith, J.F. Boas and J.R. Pilbrow, J. Chem. Soc., Dalton Trans., (1976) 1495.

TABLE 21

Cobalt hyperfine analysis: cobalt Schiff base·O_2 adducts

	a_x	a_y	a_z	$f+h$	$g+h$	Ref.	Table
	($\times 10^{-4}$ cm^{-1})						
Co(salpdt)O$_2$	3.8	−10.3	6.5	−3.2	16.5	a	8
Co(3-CH$_3$OsalMedpt)O$_2$	2.7	−7.3	−4.7	−2.7	12.0	a	8
Co(α-CH$_3$salMedpt)O$_2$	2.7	−8.7	5.9	−4.3	13.3	a	8
Co(salphdpt)O$_2$	3.4	−9.3	5.9	−2.9	11.8	a	8
Co(5Clsaldape)O$_2$	3.4	−12.9	9.4	−7.0	19.0	a	8
Co(3-CH$_3$OsalMedapp)O$_2$	3.4	−11.3	7.8	−5.1	17.2	a	8
Co(salen)O$_2$(also salpd, salpn)	4.3	−7.2	3.0	1.5	13.4	a	15
Co(α Me salen)O$_2$(also αEt salen)	3.0	−7.5	4.5	−1.8	12.3	b	15
Co(3OMe salen)(also salen)	5.6	−6.4	0.7	5.7	14.0	b	15

[a] Data based on recalculated values outlined by Table 8.
[b] R.L. Lancashire, T.D. Smith and J.R. Pilbrow, J. Chem. Soc., Dalton Trans., (1979) 66.

TABLE 22

Cobalt hyperfine analysis: base variation in cobalt(II) salicylaldazinate·O_2

	a_x	a_y	a_z	$f+h$	$g+h$	Table
	($\times 10^{-4}$ cm^{-1})					
2,4,6-collidine	2.1	−4.2	1.7	0.5	7.4	18
2,4-lutidine [1]	3.1	−8.6	5.4	−2.7	13.7	18
Acridine	2.2	−7.5	5.4	−3.7	11.3	18
Pyridine	1.9	−6.8	5.2	−3.8	10.2	18
2-picoline	2.2	−7.7	5.5	−3.8	11.6	18
2,6-lutidine [1]	3.1	−8.6	5.4	−2.7	13.7	18
DMF	3.0	−7.5	4.5	−1.8	12.3	18

[1] g-values differ slightly. Within fitting errors A-values identical.

both f and h negative or when only either f or h is negative. Negative values imply direct rather than indirect hyperfine coupling.

Inspection of entry A in Table 19 shows that $CoMbO_2$ has $f + h = 6.1$ and $g + h = 12.4$. If we put $f = 0$ to make the results conform to the model of Dickinson and Chien [107], then $f = 6.1$ and $g = 12.4$. These results give different calculated spin densities compared with those reported by Dickinson and Chien [107]. The difference comes about as mentioned earlier from reconsideration of the direct dipolar correction to hyperfine structure. Their general conclusion is correct. The spin density on d_{xz} (their d_{yz}) is positive, involving direct interaction with the unpaired electron whereas the spin density on d_{yz} (their d_{xz}) is negative and therefore due to spin polarization. It is larger than the value they reported.

Positive values of $f + h$ for $CoMbO_2$, $B_{12r}O_2$ and most of the porphyrins (Table 20) confirm the role of indirect spin polarization mechanisms. It is likely that f will be the smaller of the two contributions and thus spin polarization will involve d_{xz} rather than d_{z^2} orbitals.

To estimate the extent of electron transfer within the bond region one now would have, from eqn. (33)

$$ET = 2(1 - \alpha'^2 - \alpha'''^2 - 1)$$ (36)

Using subscripts O and N to distinguish O_2 and NO adducts one may write

$$f_O + h_O = P\rho_O U_{Co-O}\left(\alpha'^2_O + \alpha'''^2_O\right)$$
and
$$f_N + h_N = P\rho_N U_{Co-N}\left(\alpha'^2_N + \alpha'''^2_N\right)$$ (37)

In practice there is a difficulty with the actual nitroxide results [335] used by Tovrog et al. [60] since the correct orientations of the A axes in the molecule are not absolutely clear. Ideally a single crystal nitroxide study would provide a sound basis for comparison. Nevertheless, one should remain a little cautious in view of the molecular orbital calculations already mentioned where electron transfer appears to involve the ligand as well as the cobalt atom. Tovrog et al. [60] qualified their methodology and it seems clear that before their electron transfer results can be used reliably, all the ESR data should be reassessed in terms of a more realistic model of the adducts.

(iii) g-Values of molecular oxygen adducts

Occasionally the g-value expressions derived by Kanzig and Cohen [108] for O_2^- in potassium chloride have been used in attempts to explain observed g-values for $Co-O_2$ adducts and oxygen adsorbed on the surfaces of crystals. The calculations are based on a removal of degeneracy between

the $\pi^*(x_g)$ and $\pi^*(z_g)$ orbitals in first order, and for g_x and g_z, first-order corrections involving promotion of an electron from a filled $2p_{\sigma_g}$ low-lying state to a π^* orbital. In the theory, g_x and g_z are very close to 2 while g_y (along the O–O bond) is given by

$$g_y = 2 + 2\left(\frac{\lambda^2}{\lambda^2 + \Delta^2}\right)^{\frac{1}{2}} \tag{38}$$

where λ is the oxygen spin orbit coupling and Δ the energy separation between $\pi^*(x_g)$ and $\pi^*(v_g)$. For O_2^- in potassium chloride crystals, the two oxygens are equivalent whereas in almost all of the Co–O_2 adducts so far reported the oxygens are inequivalent. Furthermore, in view of the fact that to explain cobalt h.f.s. one may need to alter the cobalt d-orbital energies of Fig. 16, it is possible that the oxygen MO scheme used to obtain the g-values by Kanzig and Cohen may need some reassessment. There does not appear to be any detailed knowledge of the excitations which actually occur.

If eqn. (38) were to be used to cover all cases, it must be remembered that g_y is 2.44 (O_2^-:KCl) [108], ~ 2.08 (Co–O_2) and about 2.02 for peroxy radicals. Biskupič and Valko [94] used the gauge invariant theory developed by Stone [337] to calculate g-values for peroxy radicals. The same approach could presumably be used to derive more generally applicable formulae.

(iv) Concluding remarks

For Co–O_2 adducts, a good deal of the reported ESR data presently in the literature needs to be re-evaluated in terms of a more realistic model of the Co–O–O geometry. Unfortunately it seems inappropriate to take present estimates of electron transfer from hyperfine analysis as being the final values in view of the need for data reported by Tovrog et al [60,330–333] to be reinterpreted. In trying to assess the consistency of the arguments advanced here relating to direct and indirect hyperfine coupling effects, we note that several examples do not fit the scheme proposed (underlined in Tables 16–18). We have no immediate solution to this problem.

It is interesting to reflect upon the fact that in spite of the evident popularity of O_2^- formulations to describe the ESR of oxygen combined by a variety of systems, a formidable amount of evidence now points to a spin pairing model. Drago et al. [60,330 – 333] have shown clearly the implications of a spin pairing model in relation to formal descriptions of the Co–O_2 system and attempts to interpret indirect effects in hyperfine structure. It is a pity that their numerical calculations did not deal with more appropriate geometry. Nevertheless, the general features of their argument remain valid and point the way to a more complete picture. Examples of oxygen bound to III–V semiconductors such as reported by Miller and

Haneman [111] are believed by the authors to fit into the same general theoretical framework. Spin pairing of $\pi^*(z_g)$ to an $Al(p_z)$ orbital would most likely occur and provide an explanation for the resolved Al h.f.s. observed. The spin pairing models need not be restricted to d-orbitals.

There remain a number of puzzles. Although the broad features of $CoMbO_2$ are similar to most of the other cobalt O_2 adducts, the $g - A$ non-coincidence is different from that observed for Vitamin $B_{12r} \cdot O_2$ and occurs somewhat differently. The differences may be associated with the possible histidine binding in the former. Nor is it clear why the isoelectronic centres formed in γ-irradiated Mb and Hb should have such different g-values and principal g-directions from the analogous $Co-O_2$ systems.

We suggest that there is room for further work involving related series of compounds, preferably experiments on single crystals. ENDOR experiments on suitable cases would settle the question of the signs of the hyperfine constants which were assumed to be negative in the hyperfine analysis. To quote from the paper by Dickinson and Chien [107] in connection with $CoMbO_2$: "the dioxygen has two unpaired electrons before ligation and retains most of its second electron unpaired after bonding the Co."

NOTE ADDED IN PROOF

Hori, Ikeda-Saito and Yonetassi (Nature, 288 (1980) 501) have reported a single crystal study of $CoMbO_2$ at ambient temperatures and find evidence for only one O_2 centre in agreement with X-ray data [170].

REFERENCES

1   M. Dole, Oxygen, in Proceedings of a Symposium sponsored by the New York Heart Association. Little, Brown and Company, Boston, 1965, p. 5 (supplement to the J. Gen. Physiol., 49, 1965, No. 1, part 2).
2   L.V. Berkner and L.C. Marshall, Discuss. Faraday Soc., 37 (1964) 122.
3   G.I. Renger, in Topics in Current Chemistry (Springer-Verlag), 69 (1977) 39.
4   G.M. Cheniae, Rev. Plant Physiol., 21 (1970) 467.
5   L.H. Vogt, H.M. Faigenbaum and S.E. Wiberty, Chem. Rev., 63 (1963) 269.

6   J.A. O'Connor and E.A.V. Ebsworth, Adv. Inorg. Chem. Radiochem., 6 (1964) 279.

7   E. Bayer and P. Stretzmann, Struct. Bonding (Berlin), 2 (1967) 181.

8   S. Fallab, Angew. Chem. Int. Ed. Engl., 6 (1967) 496.

9   L. Vaska, Acc. Chem. Res., 1 (1968) 335.

10   A.G. Sykes and J.H. Weil, Prog. Inorg. Chem., 13 (1970) 1.

11   R.G. Wilkins, Adv. Chem. Ser., No. 100 (1971) 111.

12   V.J. Choy and C.J. O'Connor, Coord. Chem. Rev., 19 (1972/73) 145.

13   J.S. Valentine, Chem. Rev., 73 (1973) 235.

14   L. Kieran, J. Peone and S.K. Madan, J. Chem. Educ., 50 (1973) 670.

15   F. Basolo, J. Indian Chem. Soc., 51 (1974) 1.

16   G. Henrici-Olivé and S. Olivé, Angew. Chem. Int. Ed. Engl., 13 (1974) 29.

17   F. Basolo, B.M. Hoffman and J.A. Ibers, Acc. Chem. Res., 8 (1975) 384.

18   V. Savitsky and V.I. Nelyubia, Russ. Chem. Rev., 44 (1975) 110.

19   E. Ochiai, J. Inorg. Nucl. Chem., 37 (1975) 1503.

20   R.W. Erskine and B.O. Field, Struct. Bonding (Berlin), 9 (1976) 1.

21   G. McLendon and A.E. Martell, Coord Chem. Rev., 19 (1976) 1.

22   L. Vaska, Acc. Chem. Res., 9 (1976) 175.

23   J.P. Collman, Acc. Chem. Res., 10 (1977) 265.

24   G. Speier, Magy. Kem. Lapja, 32 (1977) 381.

25   Y. Moriguchi, Dojin Nyusu, 7 (1977) 1.

26   A. Nishinaga, in O. Hayaishi and K. Asada (Eds.), Biochemical and Medical Aspects of Activation of Oxygen, Univ. Park Press, Baltimore, MD, 1977, p. 13.

27   T. Eishun, Kagaku Sosetsu, 20 (1978) 30.

28   F. Basolo, Chem. Aust., 45 (1978) 127.

29   A.B.P. Lever and H.B. Gray, Acc. Chem. Res., 11 (1978) 348.

30   R.D. Jones, D.A. Summerville and F. Basolo, Chem. Rev., 79 (1979) 139.

31   D.A. Summerville, R.D. Jones, B.M. Hoffman and F. Basolo, J. Chem. Educ., 56 (1979) 157.

32   R.S. Drago, J.R. Stahlbush, D.J. Kitko and J. Breese, J. Am. Chem. Soc., 102 (1980) 1884.

33   R.W. Hay, P.R. Norman and F. McLaren, Inorg. Chim. Acta, 44 (1980) L125.

34   V.V. Zelentsov, A.P. Bogdanov, I.L. Zatsny and Yu. I. Bratushko, Russ. J. Inorg. Chem., 22 (1977) 880.

35   Y. Suguira, Biochem. Biophys. Res. Commun., 88 (1979) 913; J. Am. Chem. Soc., 102 (1980) 5208, 5216.

36   Chu. Y. Ng, A.E. Martell and R.J. Motekaitis, J. Coord. Chem., 9 (1979) 255.

37   M. Calvin, R.H. Bailes and W.K. Wilmarth, J. Am. Chem. Soc., 68 (1946) 2254.

38   C.H. Barkelew and M. Calvin, J. Am. Chem. Soc., 68 (1946) 22.

39   W.K. Wilmarth, S. Aranoff and M. Calvin, J. Am. Chem. Soc., 68 (1946) 2263.

40   M. Calvin and C.H. Barkelew, J. Am. Chem. Soc., 68 (1946) 2267.

41   E.W. Hughes, W.K. Wilmarth and M. Calvin, J. Am. Chem. Soc., 68 (1946) 2273.

42   O.L. Harle and M. Calvin, J. Am. Chem. Soc., 68 (1946) 2612.

43   R.H. Bailes and M. Calvin, J. Am. Chem. Soc., 69 (1947) 1886.

44   H. Diehl, Iowa State Coll. J. Sci., 21 (1947) 271.

45   H. Diehl, C.C. Hach, G.C. Harrison and L.M. Liggett, Iowa State Coll. J. Sci., 21 (1947) 278.

46   H. Diehl, G.C. Harrison, C.C. Hach and L.M. Liggett, Iowa State Coll. J. Sci., 21 (1947) 287.

47   H. Diehl and L.M. Liggett, Iowa State Coll. J. Sci., 21 (1947) 326.

48   H. Diehl, R.J. Brouns, G.C. Harrison and L.M. Liggett, Iowa State Coll. J. Sci., 21 (1947) 335.

49   H. Diehl, L.M. Liggett, G.C. Harrison, C.C. Hach and R. Curtis, Iowa State Coll. J. Sci., 22 (1948) 91.

50   H. Diehl, L.M. Liggett, G.C. Harrison, L. Henselmeier, R. Schwardt and J. Matthews, Iowa State Coll. J. Sci., 22 (1948) 110.

51   H. Diehl and T.S. Chas, Iowa State Coll. J. Sci., 22 (1948) 126.

52   H. Diehl, R.J. Brouns, G.C. Harrison and L.M. Liggett, Iowa State Coll. J. Sci., 22 (1948) 129.

53   H. Diehl, C.C. Hach, G.C. Harrison, L.M. Liggett and R.J. Brouns, Iowa State Coll. J. Sci., 22 (1948) 150.

54   H. Diehl and J. Henn, Iowa State Coll. J. Sci., 23 (1949) 273.

55   P. Pfeiffer, E. Breith, E. Lübbe and T. Tsumaki, Justus Liebigs Ann. Chem., 502 (1933) 84.

56   T. Tsumaki, Bull. Chem. Soc. Jpn., 13 (1938) 252.

57   D.J. Aymes, B. Bollotte and R. Pâris, J. Mol. Catal., 7 (1980) 289.

58   A. Lapidot and C.S. Irving, in O. Hayaishi (Ed.), Molecular Oxygen in Biology, North Holland Publishing Co., 1974.

59   K. Kubokura, H. Okawa and S. Kida, Bull. Chem. Soc. Jpn., 51 (1978) 2036.

60   B.S. Tovrog, D.J. Kitko and R.S. Drago, J. Am. Chem. Soc., 98 (1976) 5144.

61   M.J. Carter, D.P. Rillema and F. Basolo, J. Am. Chem. Soc., 96 (1974) 392.

62   T.J. Beugelsdijk and R.S. Drago, J. Am. Chem. Soc., 97 (1975) 6466.

63   F. Ann Walker, J. Am. Chem. Soc., 95 (1973) 1154.

64   M.J. Carter, L.M. Engelhardt, D.P. Rillema and F. Basolo, J. Chem. Soc., Chem. Commun., (1973) 810.

65   D.V. Stynes, H.C. Stynes, B.R. James and J.A. Ibers, J. Am. Chem. Soc., 95 (1973) 1796.

66   V. Subramanian, K. Seff and T. Ottersen, J. Am. Chem. Soc., 100 (1978) 2911.

67   S. Abramowitz and N. Acquista, Chem. Phys. Lett., 50 (1977) 423.

68   Y. Seno and J. Otsuka, Adv. Biophys., 11 (1978) 13.

69   J. Otsuka, Y. Seno, N. Fuchikami and O. Matsuoka, in P. Pullman and N. Goldblum (Eds.), Metal–Ligand Interactions in Organic Chemistry and Biochemistry , Reidel, Dordrecht, Part 2, 1977, p. 59.

70   D.A. Case, B.H. Huynth and M. Karplus, J. Am. Chem. Soc., 101 (1979) 4433.

71   W.A. Eaton, L.K. Hanson, P.J. Stephens, J.C. Sutherland and J.B.R. Dunn, J. Am. Chem. Soc., 100 (1978) 4991.

72   M. Cerdonio, A. Congin-Costellano, F. Mogno, B. Pispisa, G.L. Romani and S. Vitale, Proc. Natl. Acad. Sci., U.S.A., 74 (1977) 398.

73   Z.S. Herman and G.H. Loen, J. Am. Chem. Soc., 102 (1980) 1885.

74   H. Brunner, Naturwissenschaften, 61 (1974) 129.

75   W.S. Caughey, U.H. Barlow, J.C. Maxwell, J.A. Volpe and W.J. Wallace, Ann. N.Y. Acad. Sci., 244 (1975) 1.

76   M.W. Makinen, A.K. Churg and H.A. Glick, Proc. Natl. Acad. Sci., U.S.A., 75 (1978) 2291.

77   Y. Maeda, Adv. Biophys., 11 (1978) 199.

78   H. Ficher and A. Trautwein, J. Chem. Phys., 50 (1969) 2540.

79   B.M. Kincaid, P. Eisenberger, K.O. Hodgson and S. Doniach, Proc. Natl. Acad. Sci., U.S.A., 72 (1975) 2340.

80   M. Weissbluth, Stanford University, private communication, 1980.

81   A. Dedieu, M.-M. Rohmer and A. Veillard in B. Pullman and N. Goldblum (Eds.), Metal–Ligand Interactions in Organic Chemistry and Biochemistry, Reidel, Dordrecht, Part 2, 1977, p. 101.

82   A. Syamal, E.F. Cavey and L.J. Theriot, Inorg. Chem., 12 (1973) 245.

83   J.H. Burness, J.G. Dillard and L.T. Taylor, J. Am. Chem. Soc., 97 (1975) 6080.

84   B.M. Hoffman, D.L. Diemente and F. Basolo, J. Am. Chem. Soc., 92 (1970) 61.

85   T. Szymanski, T.W. Cape, R.P. Van Duyne and F. Basolo, J. Chem. Soc., Chem. Commun., (1979) 5.

86   R.D. Jones, J.R. Budge, P.E. Ellis, J.E. Linard, D.A. Summerville and F. Basolo, J. Organomet. Chem., 181 (1979) 151.

87   J. Ellis, J.M. Pratt and M. Green, J. Chem. Soc., Chem. Commun., (1973) 781.

88   H.A.O. Hill, D.R. Turner and G. Pellizer, Biochem. Biophys. Res. Commun., 56 (1974) 739.

89   P. Fantucci and V. Valenti, J. Am. Chem. Soc., 98 (1976) 3832.

90   G.A. Rodley and W.T. Robinson, Nature (London), 235 (1972) 438.

91   B.B. Wayland, J.V. Minkiewicz and M.E. Abd-Elmageed, J. Am. Chem. Soc., 96 (1974) 2975.

92   R.D. Harcourt, Int. J. Quant. Chem., 4 (1977) 143 and references cited therein.

93   A. Dedieu, M.-M. Rohmer and A. Veillard, J. Am. Chem. Soc., 98 (1976) 5789.

94   S. Biskupič and L. Valko, J. Mol. Struct., 27 (1975) 97.

95   S.C. Abraham, Q. Rev., Chem. Soc., 10 (1956) 407.

96   R.J. Celotta, R.A. Bennett, J.R. Hall, M.W. Siegel and J. Levini, Phys. Rev., A, 6 (1972) 631.

97   M. Krauss, D. Newmann, A.C. Wahl, G. Das and W. Zenke, Phys. Rev. A., 7 (1973) 69; W. Zenke, G. Das and A.C. Wahl, Chem. Phys. Lett., 14 (1972) 310.

98   B.M. Hoffman, D.L. Diemente and F. Basolo, J. Am. Chem. Soc., 92 (1970) 61.

99   B.M. Hoffman and D.H. Petering, Proc. Natl. Acad. Sci., U.S.A., 67 (1970) 637.

100   D.L. Diemente, B.M. Hoffman and F. Basolo, Chem. Commun., (1970) 467.

101   J.C.W. Chien and L.C. Dickinson, Proc. Natl. Acad. Sci., U.S.A., 69 (1972) 2783.

102   T. Yonetani, H. Yamamoto and T. Iizuka, J. Biol. Chem., 249 (1974) 2168.

103   R.J. Gupta. A.S. Mildvan. T. Yonetani and T.S. Srivastava, Biochem. Biophys. Res. Commun., 67 (1975) 1005.

104   J.A. de Bolfo, T.D. Smith, J.F. Boas and J.R. Pilbrow, J. Chem. Soc., Dalton Trans., (1976) 1495.

105   M.F. Corrigan, K.S. Murray, B.O. West, P.R. Hicks and J.R. Pilbrow, J. Chem. Soc., Dalton Trans., (1977) 1478.

106   R.L. Lancashire, T.D. Smith and J.R. Pilbrow, J. Chem. Soc., Dalton Trans., (1979) 66.

107   L.C. Dickinson and J.C.W. Chien, Proc. Natl. Acad. Sci., U.S.A., 77 (1980) 1235.

108   W. Känzig and M.H. Cohen, Phys. Rev. Lett., 3 (1959) 509.

109   E. Jörin, A. Schweiger and Hs. H. Günthard, Chem. Phys. Lett., 61 (1979) 228.

110   J.R. Pilbrow and M.R. Lowrey, Rep. Prog. Phys., 43 (1980) 433.

111   D.J. Miller and D. Haneman, Phys. Rev. B, 3 (1972) 2918.

112(a) J.R. Pilbrow and M.E. Winfield, Mol. Phys., 25 (1973) 1073.

112(b) J.R. Pilbrow, Mol. Phys., 16 (1969) 307.

113   R. Aasa and T. Vänngård, J. Magn. Res., 19 (1975) 308.

114   C.P. Keijzers, G.F.M. Paulussen and E. de Boer, Mol. Phys., 29 (1975) 973.

115   W.G. Waller and M.T. Rogers, J. Magn. Res., 9 (1973) 92 and references cited therein.

116   R.H. Niswander and L.T. Taylor, J. Magn. Res., 26 (1977) 491.

378

117   M.J. Lin and J.H. Lunsford, J. Phys. Chem., 80 (1976) 2015.
118   R.M. Morris, R.A. Kaba, T.G. Groshens, K.J. Klabunde, R.J. Baltisberger, N.F. Woolsey and V.I. Sternberg, J. Am. Chem. Soc., 102 (1980) 3419.
119   A.J. Tench and P. Holroyd, J. Chem. Soc., Chem. Commun., (1968) 471.
120   A.J. Tench and T. Lawson, Chem. Phys. Lett., 8 (1971) 177.
121   C. Naccache, P. Meriaudeau, M. Che and A.J. Tench, Trans. Faraday Soc., 67 (1971) 506.
122   J.H. Lunsford, Catal. Rev., 8 (1973) 135.
123   M.C.R. Symons, Chemical and Biochemical Aspects of Electron-Spin Resonance Spectroscopy. Van Nostrand Reinhold, London, 1978, p. 13.
124   A.D. McLachlan, M.C.R. Symons and M.G. Towsend, J. Chem. Soc., (1959) 952.
125   P.W. Atkins, J.A. Brivati, N. Keen, M.C.R. Symons and P.A. Trevalion, J. Chem. Soc., (1962) 4785.
126   R.S. Eachus, P.R. Edwards, S. Subramanian and M.C.R. Symons, J. Chem. Soc. (A), (1968) 1704.
127   K. Tayaya and N.Takeshi, J. Phys. Soc. Jpn., 23 (1967) 70.
128   T. Anderson, J.R. Byberg and K.J. Olsen, J.Phys. Chem., 71 (1967) 4129.
129   F.T. Gamble, J. Chem. Phys., 47 (1967) 1193.
130   M.M. Cosgrove and M.A. Collins, J. Chem. Phys., 52 (1970) 989.
131   A.J. Tench and T. Lawson, Chem. Phys. Lett., 7 (1970) 459.
132   W.B. Williamson, J.H. Lunsford and C. Naccache, Chem. Phys. Lett., 9 (1971) 33.
133   C.L. Gardner and E.J. Casey, Can. J. Chem., 49 (1971) 1782.
134   S. Sehlick, Chem. Phys. Lett., 4 (1969) 421.
135   P. Gravelle, F. Juillet, P. Meriaudeau and S.J. Teichner, Discuss. Faraday Soc., No. 52 (1971) 140.
136   R.B. Clarkson and A.C. Cirillo, J. Vac. Sci. Technol., 9 (1973) 1073.
137   N. Shimizu, K. Shimokoshi and I. Yusumori, Bull. Soc. Chem. Jpn., 46 (1973) 2929.
138   R. Clarkson and A.C. Cirillo, J. Catal., 33 (1974) 392.
139   S. Tanaka and T. Yamashima, J. Catal., 40 (1975) 140.
140   M. Akimoto and E. Echigoya, Bull. Chem. Soc. Jpn., 51 (1978) 3061.
141   J.S. Valentine and A.B. Curtis, J. Am. Chem. Soc., 97 (1975) 224.
142   J.S. Valentine, Y. Tatsumo and M. Nappa, J. Am. Chem. Soc., 99 (1977) 3522.
143   E. McCandish, A.R. Mikszstal, M. Nappa, A.D. Sprenger, J.S. Valentine, J.D. Strong and T.G. Spiro, J. Am. Chem. Soc., 102 (1980) 4268.
144   I. Tyuma, in H. Yo Shikawa and S.M. Rapoport (Eds.), Cellular and Molecular Biology of Erythrocytes, University Park Press, Baltimore, MD, 1974, p. 279.
145   R. Valdes and G.K. Ackers, Proc. Natl. Acad. Sci., U.S.A., 75 (1978) 311.
146   F.C. Mills and G.K. Ackers, Proc. Natl. Acad. Sci., U.S.A., 76 (1979) 273.
147   R. Bansil, J. Herzfeld and H.E. Stanley, J. Mol. Biol., 103 (1976) 89.
148   Y.A. Ilan, A. Samumi, M. Chevion and G. Czapski, J. Biol. Chem., 253 (1978) 82.
149   M. Weissbluth, in A. Kleinzeller, G.F. Springer and H.G. Wittman (Eds.), Molecular Biology, Biochemistry and Biophysics, 15 Hemoglobin, 1974, Springer-Verlag, Berlin.
150   J.M. Baldwin, Prog. Biophys. Mol. Biol., 29 (1975) 227.
151   M.F. Perutz, Annu. Rev. Biochem., 48 (1979) 327.
152   M.F. Perutz, Proc. R. Soc. London, Ser. B, 208 (1980) 135.
153   M.F. Perutz, Br. Med. Bull., 32 (1976) 195.
154   G. Weber, Biochemistry, 11 (1972) 864.
155   J.R. Lakowicz and G. Weber, Biochemistry, 12 (1973) 4171.
156   A.G. Marshall and K.M. Lee, J. Am. Chem. Soc., 102 (1980) 1460.

157   B. Alpert and L. Lindquist, Science, 187 (1975) 836.
158   R.H. Austin, K.W. Beeson, L. Fisenstein, H. Frauenfelder and I.C. Gunsalus, Biochemistry, 14 (1975) 5355.
159   M. Coppey, H. Tourbez, P. Valat and B. Alpert, Nature (London), 284 (1980) 568.
160   P. Eisenberger, R.G. Schulman, B.M. Kincaid, G.S. Brown and S. Ogawa, Nature (London), 274 (1978) 30.
161   J.J. Hopfield, J. Mol. Biol., 77 (1973) 207.
162   S. Ogawa and R.G. Shulman, J. Mol. Biol., 70 (1972) 315.
163   M. Seno, P.D. Smith, J.A. McCray and T. Asakura, J. Biol. Chem., 251 (1976) 1418.
164   L.W.-M. Fung, A.P. Minton, T.R. Lindstrom, A.V. Prisciotta and C. Ho, Biochemistry, 16 (1977) 1452.
165   R.J. Wiechelman, J. Fox, P.R. McCurdy and C. Ho, Biochemistry, 17 (1978) 1791.
166   G. Geraci, A. Tada and C. Cirotto, Eur. J. Biochem., 77 (1977) 555.
167   J.A. Shelnutt, D.L. Rousseau, J.M. Friedman and S.R. Simon, Proc. Natl. Acad. Sci., U.S.A., 76 (1979) 4409.
168   K. Imai, T. Yonetani and M. Ikeda-Saito, J. Mol. Biol., 109 (1977) 83.
169   P.S. Guzelian and D.M. Bissell, J. Biol. Chem., 251 (1976) 4421.
170   G.A. Petsko, D. Rose, D. Tsernoglou, M. Ikeda-Saito and T. Yonetani, in P.L. Dutton, J.S. Leigh and A. Scarpa (Eds.), Frontiers in Bioenergetics,Academic Press, New York, 1978, p. 1011.
171   I. Yamazaki, T. Araiso, Y. Hayashi, H. Yamada and R. Makino, Adv. Biophys., 11 (1978) 249.
172   M.Y.R. Wang, B.M. Hoffman and P.F. Hollenberg, J. Biol. Chem., 252 (1977) 6268.
173   D.R. Paulson, A.W. Addison, D. Dolphin and B.R. James, J. Biol. Chem., 254 (1979) 7002.
174   M.C.R. Symons and R.L. Peterson, Proc. R. Soc., London Ser. B, 201 (1978) 285.
175   M.C.R. Symons and R.L. Peterson, Biochim. Biophys. Acta, 535 (1978) 241.
176   J. Bayston, N.K. King, F.D. Looney and M.E. Winfield, J. Am. Chem. Soc., 91 (1969) 2775.
177   S.A. Cockle, H.A.O. Hill and R.J.P. Williams, Inorg. Nucl. Chem. Lett., 6 (1970) 131.
178   G.N. Schrauzer and L.P. Lee, J. Am. Chem. Soc., 92 (1970) 1551.
179   H.R. Allcock, P.P. Greigger, J.E. Gardner and J.L. Schmutz, J. Am. Chem. Soc., 101 (1979) 606.
180   D.E. Hultquist and G. Parson, Nature, New Biol., 229 (1971) 252.
181   D.E. Hultquist, R.H. Douglas and R.T. Dean, in G.L. Brewer (Ed.), Erythrocyte Structure and Function, Liss, New York, 1975, p. 297.
182   I.A. Cohen and W.S. Caughey, Biochemistry, 7 (1968) 636.
183   C.K. Chang, D. Powell and T.G. Traylor, Croat. Chem. Acta, 49 (1977) 295.
184   D.H. Chin, J. Del Gaudio, G.N. La Mar and A. Balch, J. Am. Chem. Soc., 99 (1977) 5486.
185   D.H. Chin, A.L. Balch and G.N. La Mar, J. Am. Chem. Soc., 102 (1980) 1448.
186   O.H.W. Kao and J.H. Wang, Biochemistry, 4 (1965) 342.
187   M.M.L. Chu, C.E. Castro and G.M. Hathaway, Biochemistry, 17 (1978) 481.
188   J. Emert, W. Pietro and R. Ambrose, J. Am. Chem. Soc., 102 (1980) 4912.
189   Der-Hang Chin, G.N. La Mar and A.L. Balch, J. Am. Chem. Soc., 102 (1980) 4344.
190   M.R. Green, H.A.O. Hill and D.R. Turner, FEBS Lett., 103 (1979) 176.
191   D.M. Stanbury, D. Haas and H. Taube, Inorg. Chem., 19 (1980) 518.
192   A.R. Battersby and A.D. Hamilton, J. Chem. Soc., Chem. Commun., (1980) 117.
193   M. Momenteau and B. Loock, J. Mol. Catal., 7 (1980) 315.

380

194   M. Momenteau, B. Loock, J. Mispeltes and E. Bisagni, Nouveau J. Chim., 3 (1979) 77.
195   A.R. Battersby, D.G. Buckley, S.G. Hartley and M.D. Turnbull, J. Chem. Soc., Chem. Commun., (1976) 879.
196   A.R. Battersby, S.G. Hartley and M.D. Turnbull, Tetrahedron Lett., (1978) 3169.
197   J.M. Burke, J.R. Kincaid, S. Peters, R.R. Cagné, J.P. Collman and T.G. Spiro, J. Am. Chem. Soc., 100 (1978) 6083.
198   H. Brunner, Naturwissenschaften, 61 (1974) 129.
199   J.P. Collman, J.I. Brauman, K.M. Doxsee, T.R. Habbert and K.S. Suslick, Proc. Natl. Acad. Sci.,, U.S.A., 75 (1978) 564.
200   D.K. White, J.B. Cannon and T.G. Traylor, J. Am. Chem. Soc., 101 (1979) 2443.
201   H. Goff, J. Am. Chem. Soc., 102 (1980) 3252.
202   T.G. Traylor, C.K. Chang, J. Geibel, A. Berzinis, T. Mincey and J. Cannon, J. Am. Chem. Soc., 101 (1979) 6716.
203   T.G. Traylor and A.P. Berzinis, Proc. Natl. Acad. Sci., U.S.A., 77 (1980) 3171.
204   M-Y.R. Wang, B.M. Hoffman, S.J. Shire and F.R.N. Gurd, J. Am. Chem. Soc., 101 (1979) 7394.
205   L. Eales, Y. Grosser and G. Sears, Ann. N.Y. Acad. Sci., 244 (1975) 481.
206   A.G. Greenberg, R. Hayashi, I. Siefert, H. Reese and G.W. Peskin, Surgery (St. Louis), 86 (1979) 13.
207   F. De Venuto, H.I. Friedman, J.R. Neville and C.C. Peck, Surg. Gynecol. Obstet., 149 (1979) 417.
208   L. Schindel, Side Eff. Drugs Annu., 3 (1979) 270.
209   J.G. Riess and M. Le Blanc, Angew. Chem., 90 (1978) 654.
210   C.A. Hall and M.E. Rappazzo, Purg. Clin. Biol. Res., 19 (1977) 41.
211   R. Pabst, Med. Klin., 72 (1977) 1555.
212   G.W. Peskin, J. Surg. Res., 26 (1979) 185.
213   D.D. Lawson, J. Moacanin, K.V. Scherev, T.F. Terranova and J.D. Ingham, J. Fluorine Chem., 12 (1978) 221.
214   W. Lautsch, W. Broser, W. Beiderman, U. Doering and H. Zoschki, Kolloid. Z., 125 (1952) 72.
215   J.H. Wang, J. Am. Chem. Soc., 80 (1958) 3168.
216   J.H. Wang, Acc. Chem. Res., 3 (1970) 90.
217   E. Tsuchida, Kagaku Sosetsu, 20 (1978) 41.
218   T. Sasaki and F. Matsumaga, Bull. Chem. Soc. Jpn., 41 (1968) 2440.
219   G.C. Wagner and R.J. Kassner, J. Am. Chem. Soc., 96 (1974) 5593.
220   G.N. La Mar and F.A. Walker, J. Am. Chem. Soc., 95 (1973) 1790.
221   W.R. Scheidt and J.A. Ramanuja, Inorg. Chem., 14 (1975) 2643.
222   W.R. Scheidt and J.L. Hoard, J. Am. Chem. Soc., 95 (1973) 8281.
223   R.G. Little and J.A. Ibers, J. Am. Chem. Soc., 96 (1974) 4452.
224   F.A. Walker, J. Mag. Res., 15 (1974) 201.
225   B.B. Wayland, J.V. Minkiewicz and M.E. Abd-Elmageed, J.Am. Chem. Soc., 96 (1974) 2795.
226   B.B. Wayland and M.E. Abd-Elmageed, J. Am. Chem. Soc., 96 (1974) 4809.
227   D.V. Stynes, H.C. Stynes, B.R. James and J.A. Ibers, J. Am. Chem. Soc., 95 (1973) 1796.
228   J.A. Ibers, D.V. Stynes, H.C. Stynes and B.R. James, J. Am. Chem. Soc., 96 (1974) 1358.
229   D.V. Stynes, H.C. Stynes, J.A. Ibers and B.R. James, J. Am. Chem. Soc., 95 (1973) 1142.

230 B.R. James, A.W. Addison, M. Caoins, D.Dolphin, N.F. Farrell, D.R. Paulson and S.Walker, Fundamental Rev. Homogenous Catal., 3 (1979) 751.
231 L.C. Dickinson and J.C.W. Chien, Inorg. Chem., 15 (1976) 1111.
232 A. Pezeshk, P.E. Davison and F.T. Greenaway, Inorg. Nucl. Chem. Lett., 16 (1980) 105.
233 R.C. Haushalter and R.W. Rudolph, J. Am. Chem. Soc., 101 (1979) 7080.
234 J.A. de Bolfo, T.D. Smith, J.F. Boas and J.R. Pilbrow, J. Chem. Soc., Dalton Trans., (1976) 1495.
235 W.C. Lin and P.W. Lau, J. Am. Chem. Soc., 98 (1976) 1447.
236 C. Daul, C.W. Schläpfer and A. von Zelewsky, Struct. Bonding, 36 (1979) 129.
237 R.L. Lancashire, T.D. Smith and J.R. Pilbrow, J. Chem. Soc., Dalton Trans., (1979) 66.
238 S.R. Tirant, M.Sc. Thesis, Monash University, 1979.
239 B.B. Wayland, J.V. Minkewicz and M.E. Abd-Elmageed, J.Am. Chem. Soc., 96 (1974) 2795.
240 R.H. Niswander, A.K. St.Clair, S.R. Edmondson and L.T. Taylor, Inorg. Chem., 14 (1975) 478.
241 R.H. Niswander and L.T. Taylor, Inorg. Nucl. Chem. Lett., 12 (1976) 339.
242 M. Sakarada, Y. Sasaki, M. Matsui and T. Shigematsu, Bull. Inst. Chem. Rev., Kyoto Univ., 55 (1977) 466.
243 M. Kodama and E. Kimura, J. Chem. Soc., Dalton Trans., (1980) 327.
244 W.R. Harris, J.H. Timmons and A.E. Martell, J. Coord. Chem., 8 (1979) 251.
245 S.R. Pickens and A.E. Martell, Inorg. Chem., 19 (1980) 15.
246 W.R. Harris, G.L. McLendon, A.E. Martell, R.C. Bess and M.Mason, Inorg. Chem., 19 (1980) 21.
247 G. McLendon and W.F. Mooney, Inorg. Chem., 19 (1980) 12.
248 G.A. Lawrance and P.A. Lay, J. Inorg. Nucl. Chem., 41 (1979) 301.
249 K. Ishizu, J. Hirai, M. Kodama and E. Kimura, Chem. Lett., (1979) 1045.
250 V.L. Goedken, N.K. Kildahl and D.H. Busch, Coord. Chem., 7 (1977) 89.
251 V. Gottfried, A. Weiss and Z. Dori, J. Am. Chem. Soc., 102 (1980) 3948.
252 C.-L. Wong, J.A. Switzer, K.P. Balakrishman and J.F. Endicott, J. Am. Chem. Soc., 102 (1980) 5511.
253 J.C. Stevens, P.J. Jackson, W.P. Schammel, G.G. Christoph and D.H. Busch, J. Am. Chem. Soc., 102 (1980) 3283.
254 J.C. Stevens and D.H. Busch, J. Am. Chem. Soc., 102 ('980) 3285.
255 Y. Yamada, Bull. Chem. Soc. Jpn., 45 (1972) 60.
256 Y. Yamada, Bull. Chem. Soc. Jpn., 45 (1972) 64.
257 J.H. Lunsford, Catal. Rev., Sci. Eng., 12 (1975) 137.
258 W. Dewilde and J.H. Lunsford, Inorg. Chim. Acta, 34 (1979) L229.
259 E.F. Vansant, in D. Delman and G. James (Eds.), Catalysis, Heterogeneous and Homogeneous, Elsevier, Amsterdam, 1975, p. 171.
260 R.F. Howe and J.H. Lunsford, J. Am. Chem. Soc., 97 (1975) 5157.
261 K.A. Windhorst and J.H. Lunsford, J. Am. Chem. Soc., 97 (1975) 1407.
262 R. Kellerman, P.J. Hatta and K. Klier, J. Am. Chem. Soc., 96 (1974) 5946.
263 S.M. Davis, R.F. Howe and J.H. Lunsford, J. Inorg. Nucl. Chem., 39 (1977) 1069.
264 T. Matsuura, Tetrahedron, 33 (1977) 2869.
265 J.E. Lyons, in R. Ugo (Ed.), Aspects Homogeneous Catalysis, Reidel, Dordrecht, 3 (1977) 3.
266 A. Nishinaga, H. Tomita, T. Shimizu and T. Matsuura, in Y. Ishii and M. Tsutsui (Eds.) Fundamental Research in Homogeneous Catalysis, Plenum Press, London and New York, 2 (1978) 241.

382

267   M.M. Tagui Khan and A.E. Martell, Homogeneous Catalysis by Metal Catalysts, Academic Press, New York and London, Vol. 1 (1974) 79.
268   A. Nishinaga and H. Tomita, J. Mol. Catal., 7 (1980) 179.
269   A. Bielanski and J. Haber, Catal. Rev., Sci. Eng., 19 (1979) 1.
270   R.A. Sheldon and J.K. Kochi, Oxid. Combust. Rev., 5 (1973) 135.
271   M. Tezuka, O. Sekiguchi, Y. Ohkatsu and T. Osa, Bull. Chem. Soc. Jpn., 49 (1976) 2765.
272   Y. Ohkatsu and T. Osa, Bull. Chem. Soc. Jpn., 50 (1977) 2945.
273   M. Ohkatsu, T. Hara and T. Osa, Bull. Chem. Soc. Jpn., 50 (1977) 696.
274   Y. Ohkatsu, O. Sekiguchi and T.Osa, Bull. Chem. Soc. Jpn., 50 (1977) 701.
275   Y. Ohkatsu and T. Tsuruta, Bull. Chem. Soc. Jpn., 51 (1978) 188.
276   H. Sakamoto, T. Funabiki, S. Yoshida and K.Tarama, Bull. Chem. Soc. Jpn., 52 (1979) 2760.
277   M. Costantini, A. Dromard, M. Jouffret, B. Brossard and J. Varaguat, J. Mol. Catal., 7 (1980) 89.
278   J.-H. Fuhrhop, M. Baccouche, H. Grabow and H. Azoumanian, J. Mol. Catal., 7 (1980) 245.
279   J.H. Fuhrhop, M. Baccouche and G. Penzlin, J. Mol. Catal., 7 (1980) 257.
280   M.N. Dufour, A.L. Crumbliss, G. Johnston and A. Gaudemer, J. Mol. Catal., 7 (1980) 277.
281   J. Simon and J. Le Moigne, J. Mol. Catal., 7 (1980) 137.
282   C.M. Wagnerorá, E.Schwertnerová and J. Vepřek-Šiška, Coll. Czech. Chem. Commun., 39 (1974) 3036.
283   D.M. Wagnerová, J. Blanck, G. Smettan, J. Vepřek-Šiška, Coll. Czech. Chem. Commun., 43 (1978) 2105.
284   D.M. Wagnerová, E. Schwertnerová and J. Vepřek-Šiška, Coll. Czech. Chem. Commun., 39 (1974) 3036.
285   D.J. Cookson, T.D. Smith, J.F. Boas, P.R. Hicks and J.R. Pilbrow, J. Chem. Soc., Dalton Trans., (1977) 109.
286   E.W. Abel, J.M. Pratt and R. Whelan, J. Chem. Soc., Chem. Commun., (1971) 449.
287   F. Cariati, D. Galizzioli, F. Morazzoni and C. Busetto, J. Chem. Soc., Dalton Trans., (1975) 556.
288   D.H.J. Carlson and J.R. Deering, U.S. Pat., 4, 168, 245, Chem. Abstr., 92 (1980) 8745.
289   R.R. Frame, U.S. Pat., 4,159,964, Chem. Abstr., 91 (1979) 177928p.
290   R.R. Frame, U.S. Pat. 4,157,312, Chem. Abstr., 91 (1979) 160195z.
291   D.H.J. Carlson, U.S. Pat. 4,098,681, Chem. Abstr., 89 (1978) 200208y.
292   J.H. Schatten and P.Piet, Makromol. Chem., 180 (1979) 2341.
293   F. Steinbach and H.H. Schmidt, J. Catal., 52 (1978) 302.
294   J. Swart and J.H.M.C. Van Wolput, J. Mol. Catal., 5 (1979) 235.
295   J.H. Schutten and J. Swart, J. Mol. Catal., 5 (1979) 109.
296   E. Tsuchida and H. Nishide, Adv. Polym. Sci., Springer-Verlag, Berlin, No. 24, 1977, p. 1.
297   J.C. Bailar, Catal. Rev., 10 (1974) 17.
298   A.A. Berlin and A.I. Sherle, Russ. Chem. Rev., 48 (1979) 1125.
299   B.S. Tovrog, S.E. Diamond and F. Marcs, J. Am. Chem. Soc., 101 (1979) 272.
300   W.P. Schaefer, R. Waltzman and B.T. Huie, J. Am. Chem. Soc., 100 (1978) 5063.
301   J.J. Pignatello and F.R. Jensen, J. Am. Chem. Soc., 101 (1979) 5929.
302   B.S. Tovrog, S.E. Diamond and F. Marcs, J. Am. Chem. Soc., 101 (1979) 5067.
303   P.S. Drago, J. Gaul, A. Zombeck and D.K. Straub, J. Am. Chem. Soc., 102 (1980) 1033.

304 S. Németh, Z. Szeverényi and L.I. Simandi, Inorg. Chim. Acta, 44 (1980) 107.
305 Y. Nishida, N. Oishi and S. Kida, Inorg. Chim. Acta, 44 (1980) L169.
306 H. Jahnke, M. Schönborn and G. Zimmermann, Topics Current Chem., 61 (1976) 133.
307 M.R. Tarasevich, R.A. Radyushkina and S. Andruseva, Bioelectrochem. Bioenerg., 4 (1977) 18.
308 J.P. Raudin, Electrochim. Acta, 19 (1974) 83.
309 J. Ulstrap, J. Electroanal. Chem. Interfac. Electrochem., 79 (1977) 191.
310 F. Beck, J. Appl. Electrochem., 7 (1977) 239.
311 D.T. Sawyer, M.J. Gibian, M.M. Morrison and E.T. Seo, J. Am. Chem. Soc., 100 (1978) 628.
312 D.T. Sawyer and E.T. Seo, Inorg. Chem., 16 (1977) 501.
313 H. Meier, U. Tshirwitz, E. Zimmerhacki, W. Albrecht and G. Zeitier, J. Phys. Chem., 81 (1977) 712.
314 J. Kuwana, M. Fujihira, K. Sunakawa and T. Osa, J. Electroanal. Chem. Interfac. Electrochem., 88 (1978) 299.
315 C. Kretzschmar, K. Wiesener, M. Musilora, J. Mrha and R. Dabrowski, J.Power Sources, 2 (1978) 351.
316 H. Böhm, J. Power Sources, 1 (1977) 177.
317 L. Mueller and H. Moritz, Z. Phys. Chem. (Leipzig), 259 (1978) 331.
318 A.S. Erokhin, Yu. S. Schumov and S. Borisenkova, Vestu. Mosk. Univ. Ser. 2, Khim, 19 (1978) 370 (Chem. Abstr. 89 137584a).
319 N. Kobayashi, M. Fujihira, S. Sunakawa and T. Osa, J. Electroanal. Chem. Interfac. Electrochem., 101 (1979) 269.
320 V.E. Kazarinov, M.R. Tarasevich, K.A. Radyushkina and V.N. Andreev, J. Electrochem. Interfac. Electrochem., 100 (1979) 225.
321 S. Maroie, M. Savy and J.J. Verbist, Inorg. Chem., 18 (1979) 2560.
322 J. Manassen, Cat. Rev., 9 (1974) 223.
323 N. Kobayashi, M. Fujihira, K. Sunakawa and T. Osa, J. Electroanal. Chem. Interfac. Electrochem., 101 (1979) 269.
324 B.Z. Nikolii, R.R. Adzii E.B. Yeager, J. Electroanal. Chem. Interfac. Electrochem., 103 (1979) 281.
325 N. Kobayashi, M. Fujihira, K. Sunakawa and T. Osa, J. Electroanal. Chem. Interfac. Electrochem., 101 (1979) 269.
326 V.E. Kazarinov, M.R. Tarasevich, K.A. Radyushkina and V.N. Andreev, J. Electroanal. Chem. Interfac. Electrochem., 100 (1979) 225.
327 M. Brezina, W. Khalil, J. Koryta and M. Musilova, J. Electroanal. Chem. Interfac. Electrochem., 77 (1977) 237.
328 Y. Umezawa and T. Yamamura, J. Chem. Soc., Chem. Commun., (1978) 1106.
329 R.K. Sen, J. Segal and E. Yeager, Inorg. Chem., 16 (1977) 3380.
330 R.S. Drago, T. Beugelsdijk, J.A. Breese and J.P. Cannady, J. Am. Chem. Soc., 100 (1978) 5374.
331 R.S. Drago, in I. Bertini and R.S. Drago (Eds.), ESR and NMR of Paramagnetic Species in Biological and Related Systems, D. Reidel Publishing Co., 1970, p. 51.
332 R.S. Drago and B.B. Corden, Acc. Chem. Res., 13 (1980) 353.
333 R.S. Drago, Coord. Chem. Rev., 32 (1980) 97.
334 B.B. Wayland and A.R. Newman, in F.R. Longo (Ed.), Porphyrin Chemistry Advances, Ann Arbor Science, 1979, p. 245.
335 T.F. Hunter and M.C.R. Symons, J. Chem. Soc. (A), (1967) 1770.
336 M.C.R. Symons and J.G. Wilkinson, J. Chem. Soc. Faraday II, 68 (1972) 1265.
337 A.J. Stone, Proc. R. Soc., A271 (1963) 424.